AD NUMBER: AD0462033

LIMITATION CHANGES

TO:

Approved for public release; distribution is unlimited.

FROM:

Distribution authorized to US Government Agencies and their Contractors; Administrative/Operational Use; 12 Mar 1965. Other requests shall be referred to US Naval Weapons Lab, Dahlgren, VA, 22448.

AUTHORITY

Per USNWL ltr dtd 9 Aug 1965

FOR ERRATA

AD 462033

THE FOLLOWING PAGES ARE CHANGES

TO BASIC DOCUMENT

diagrams to identify the appropriate instruments.

The three-voltmeter method of impedance measurement used for previous studies from 100 cps to 500 kc could not be used. The SGS in this frequency range has an input impedance equivalent to a very small capacitor. The power capacity of available signal sources and sensitivity of detectors were inadequate to provide quantitative data. However, the impedance data can be extrapolated from the adjacent higher frequency range with reasonable accuracy.

A General Radio RF Impedance bridge was used successfully from 800 kc to 40 mc for complex input impedance measurements. Accurate readings could not be obtained with this bridge from 400 kc through 700 kc for the reasons given above.

In the frequency range from 40 mc to 300 mc, a General Radio UHF admittance meter was used with good accuracy for direct measurement of admittance, from which impedance was calculated. This instrument was used in accordance with the manufacturer's published instructions; however, the special technique illustrated in Figure 2 was employed in order to eliminate the admittance transformation caused by the electrical distance from the detector probe to the squib input terminal.

In the frequency range from 300 mc to 10 gc, the standing wave analysis method was used for complex impedance measurements. This method is described in detail in Genistron Special Technical Report 2400-5754-1, revised 4 June, 1965, and is derived in Electromagnetic Waves and Radiating Systems, by E. C. Jordan, Prentice-Hall Book Co., Section 8.07, 1958. Briefly, this method requires determination, by use of a slotted line or adjustable-length transmission line, of the voltage standing wave ratio on a transmission line terminated in the unknown impedance, and of the wave-length in the transmission line. From this date the unknown impedance is calculated in complex form as described in the references given above.

1.2 RF Power Input Measurements

During an early phase of this program, theoretical analysis indicated that the reflectometer method of power measurement illustrated in Figure 3 would not be suitable for most protective devices and RF-insensitive squibs, because of typically high VSWR values. The reflectometer method requires that the incident and reflected power be measured separately and simultaneously in the transmission line. A dual directional coupler equipped with bolometers senses the incident and reflected power separately for measurement at two power meters or at a

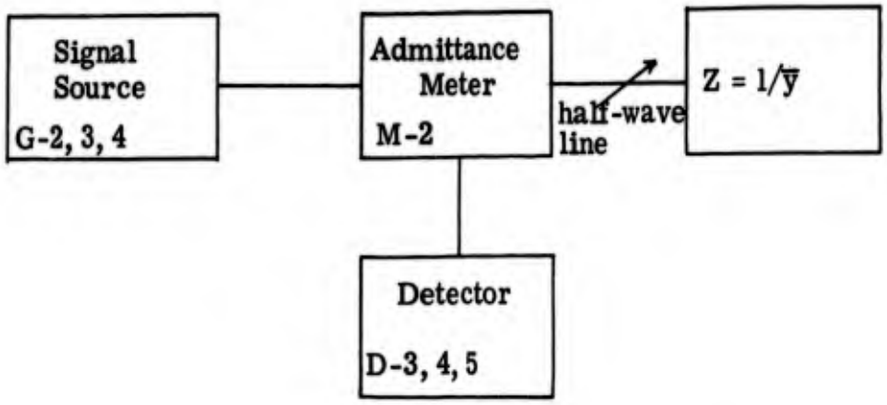

Figure 2. Impedance measurement with UHF Admittance Meter.

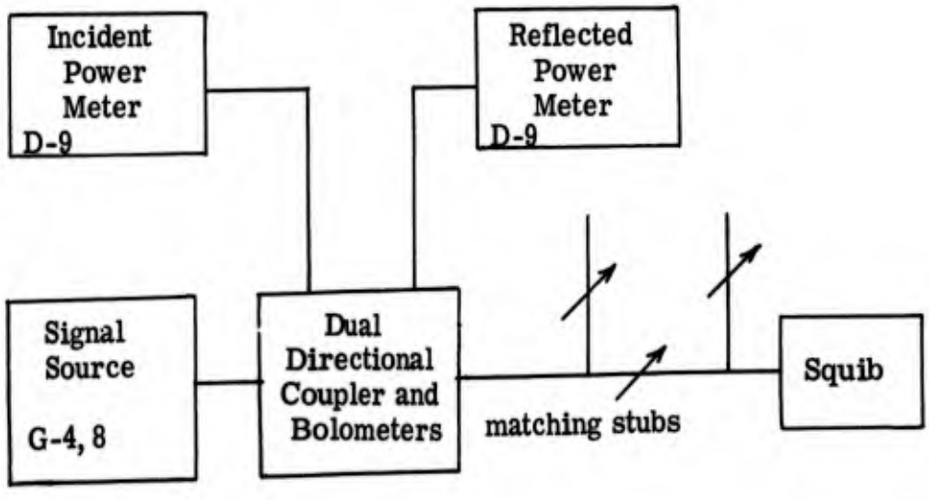

Figure 3. RF Power Measurement, Reflectometer Method.

END CHANGE PAGES

Genistron
INCORPORATED

APPLIED RESEARCH DIVISION
7100 Baltimore Avenue, College Park, Maryland

462033

DETERMINATION OF RESPONSES OF PROTECTED AND UNPROTECTED ELECTRIC INITIATORS TO ELECTRICAL STIMULI

SPECIAL TECHNICAL REPORT ON

SPARK GAP SQUIBS

REPORT NO. 2400-5754-4

CONTRACT N178-8290
U.S. NAVAL WEAPONS LABORATORY, DAHLGREN, VIRGINIA

A RESEARCH AND DEVELOPMENT PROJECT
CONDUCTED BY
GENISTRON, INCORPORATED
LOS ANGELES, CALIFORNIA
12 MARCH 1965

Genistron
INCORPORATED
APPLIED RESEARCH DIVISION
7100 Baltimore Avenue, College Park, Maryland

DETERMINATION OF RESPONSES OF PROTECTED AND UNPROTECTED ELECTRIC INITIATORS TO ELECTRICAL STIMULI

SPECIAL TECHNICAL REPORT ON

SPARK GAP SQUIBS

REPORT NO. 2400-5754-4

CONTRACT N178-8290
U. S. NAVAL WEAPONS LABORATORY, DAHLGREN, VIRGINIA

A RESEARCH AND DEVELOPMENT PROJECT
CONDUCTED BY
GENISTRON, INCORPORATED
LOS ANGELES, CALIFORNIA
12 MARCH 1965

PREPARED BY V P Musil
V. P. MUSIL - SENIOR PROJECT ENGINEER

REVISED AND APPROVED BY J C Senn
J. C. SENN - MANAGER, APPLIED RESEARCH

TABLE OF CONTENTS

ILLUSTRATIONS

TABLE OF CONTENTS
(continued)

TABLE OF CONTENTS
(concluded)

ABSTRACT

The effectiveness of Spark Gap Squibs (SGS) against radio frequency electromagnetic fields was studied over the frequency range 100 cps to 10 gc. The data obtained on effectiveness is limited in accuracy by difficulties in power measurement imposed by the squib construction, and by lack of availability of RF power sources of sufficient capacity over the desired frequency range. However, qualitative results are encouraging, indicating a high degree of immunity for the SGS against RF electromagnetic fields.

1.0 INTRODUCTION

This is the fourth in a series of Special Technical Reports prepared by Genistron, Inc., under U.S. Naval Weapons Laboratory Contract N178-8290. The objective of this report is to present data collected during evaluation testing of Bendix Spark Gap Squibs (SGS).

The Spark Gap Squib is a special "RF-insensitive" squib design intended to reduce the hazard of unintentional detonation or dudding by stray RF electromagnetic fields without the necessity of a separate in-line protective device.

The results reported here include detailed impedance measurements on ten SGS samples, data on input conductance and Q, and data on RF power sensitivity of 29 SGS samples. Qualitative data on power sensitivity and qualitative conclusions on effectiveness are presented. Accurate quantitative data could not be obtained because of lack of RF power sources of adequate capacity and inherent difficulties in power measurements imposed by the squib design.

1.1 Description of Spark Gap Squibs (SGS)

Figure 1 is a simplified diagram of the Bendix Scintilla Spark Gap Squib. The device comprises two open electrodes bridged by a semi-conducting material contained in a small sealed spark chamber. A voltage of sufficient amplitude applied to the electrodes will cause a spark to appear. If this spark has sufficient energy, it will increase the chamber pressure, rupture the diaphragm, and ignite the pyrotechnic mixture. The ignited mixture then ruptures the end seal and initiates the desired pyrotechnic action. Any energy of insufficient level to cause a high-energy spark is theoretically dissipated by leakage across the spark gap or through the semi-conductor bridge.

2.0 MEASUREMENT METHODS AND INSTRUMENTATION.

Characteristics which were measured directly were as follows:

(a) Complex input impedance, $\overline{Z_i} = R_i + jX_i$.
(b) Input RF power, P_i.
(c) Temperature rise at the base of the squib.

2.1 Impedance Measurements

Table I lists all instrumentation used for the measurements reported here. The letter-number code for each item in Table I appears in the test

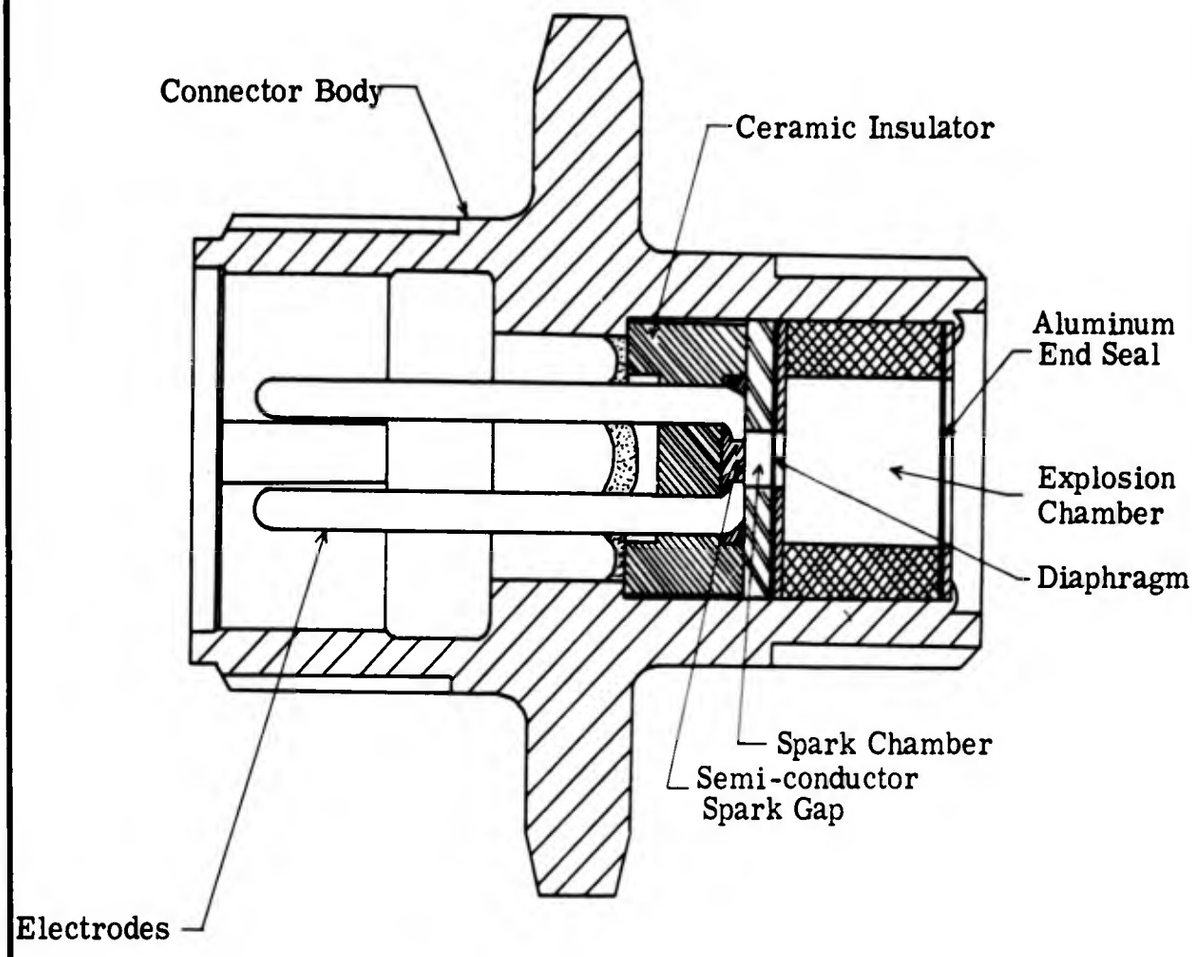

Figure 1. Cross-section View, Bendix Scintilla Spark Gap Squib. (No scale.)

TABLE 1. LIST OF INSTRUMENTS USED

Signal Sources

G1 Hewlett-Packard 606A Signal Generator (50 kc - 65 mc)

G2 Hewlett-Packard 608C Signal Generator (10 mc - 480 mc)

G3 Hewlett-Packard 612A Signal Generator (450 mc - 1230 mc)

G4 Maxson 1241AB Power Oscillator (200 mc - 2500 mc)

G5 Waveforms 512 Audio Oscillator (1 cps - 500 kc)

G6 Borg-Warner Model 20 Signal Generator (85 kc - 40 mc)

G7 Boonton 230 A RF Power Amplifier (10 mc - 500 mc)

G8 Government Supplied Model SLT-3 Microwave Source (1 gc - 10 gc)

G9 General Radio 1001-A Signal Generator (5 kc - 50 mc)

G10 Polarad Field Intensity Meter, Oscillator Section (1 gc - 10 gc)

Detectors

D1 Stoddart NM-10A Field Intensity Meter (14 kc - 250 kc)

D2 Stoddart NM-22A Field Intensity Meter (150 kc - 25 mc)

D3 Stoddart NM-30A Field Intensity Meter (20 mc - 400 mc)

D4 Stoddart NM-50A Field Intensity Meter (375 mc - 1000 mc)

D5 Polarad Field Intensity Meter, Detector Section (1 gc - 10 gc)

D6 Boonton 91 D Precision RF Voltmeter (10 kc - 1.2 gc)

D7 Hewlett-Packard 400 HR Vacuum Tube Voltmeters (10 cps - 4 mc)

D8 Hewlett-Packard 403A Vacuum Tube Voltmeter (1 cps - 1 mc)

D9 Hewlett-Packard 430C Microwave Power Meter (10 mc - 10 gc)

TABLE 1. Concluded

Miscellaneous Instruments

M1 Tektronix 555 Oscilloscope

M2 General Radio 1602B Admittance Meter

M3 General Radio 1606A RF Bridge

M4 General Radio 900 LB Precision Slotted Line (.3 - 9 gc)

M5 General Radio 874 LTL Adjustable Line (dc - 2 gc)

M6 Hewlett-Packard 809B/806B slotted line (3 gc - 10 gc)

M7 General Radio 1607-A Transfer Function and Immitance Bridge (25 mc - 1.5 gc)

M8 Genistron Coaxial Current Probe, Low Frequency (0.1 kc - 30 mc)

M9 Genistron Coaxial Current Probe, High Frequency (10 mc - 0.5 gc)

M10 Genistron Coaxial Current Voltage Probe, Microwave (0.5 - 10 gc)

M11 Alnor Type 1200-8 Thermocouple Pyrometer (0-400°F)

diagrams to identify the appropriate instruments.

The three-voltmeter method of impedance measurement used for previous studies from 100 cps to 500 kc could not be used. The SGS in this frequency range has an input impedance equivalent to a very small capacitor. The power capacity of available signal sources and sensitivity of detectors were inadequate to provide quantitative data. However, the impedance data can be extrapolated from the adjacent higher frequency range with reasonable accuracy.

A General Radio RF Impedance bridge was used successfully from 800 kc to 40 mc for complex input impedance measurements. Accurate readings could not be obtained with this bridge from 400 kc through 700 kc for the reasons given above.

In the frequency range from 40 mc to 300 mc, a General Radio UHF admittance meter was used with good accuracy for direct measurement of admittance, from which impedance was calculated. This instrument was used in accordance with the manufacturer's published instructions; however, the special technique illustrated in Figure 2 was employed in order to eliminate the admittance transformation caused by the electrical distance from the detector probe to the squib input terminal.

In the frequency range from 300 mc to 10 gc, the standing wave analysis method was used for complex impedance measurements. This method is described in detail in Genistron Special Technical Report 2400-5754-1, dated 22 January 1965, and is derived in Electromagnetic Waves and Radiating Systems, by E. C. Jordan, Prentice-Hall Book Co., Section 8.07, 1958. Briefly, this method requires determination, by use of a slotted line or adjustable-length transmission line, of the voltage standing wave ratio on a transmission line terminated in the unknown impedance, and of the wavelength in the transmission line. From this data the unknown impedance is calculated in complex form as described in the references given above.

2.2 RF Power Input Measurements

During an early phase of this program, theoretical analysis indicated that the reflectometer method of power measurement illustrated in Figure 3 would not be suitable for most protective devices and RF-insensitive squibs, because of typically high VSWR values. The reflectometer method requires that the incident and reflected power be measured separately and simultaneously in the transmission line. A dual directional coupler equipped with bolometers senses the incident and reflected power separately for measurement at two power meters or at a

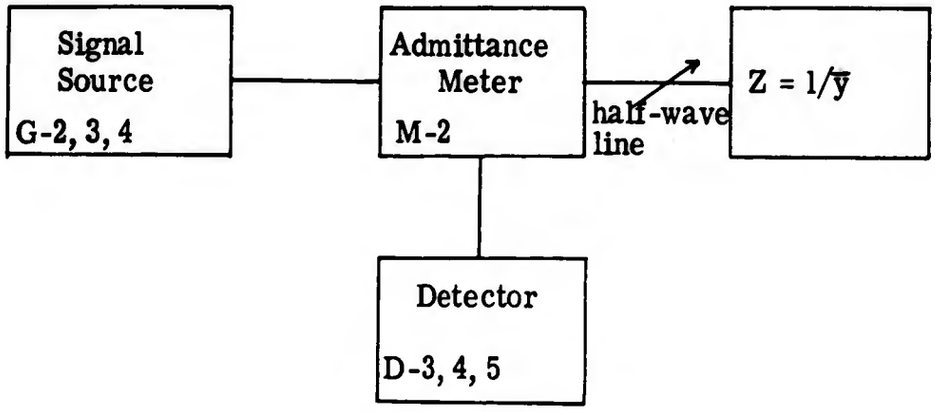

Figure 2. Impedance measurement with UHF Admittance Meter.

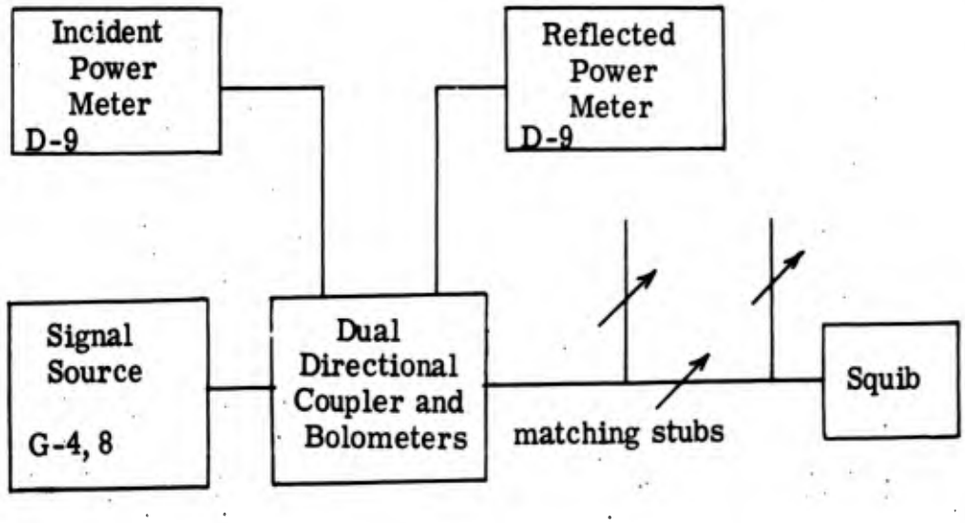

Figure 3. RF Power Measurement, Reflectometer Method.

differential power meter. The power absorbed by the device under test is then the difference between incident and reflected power. Several difficulties were anticipated, and were confirmed by experiment during preliminary testing on Spark Gap Squibs.

The basic difficulty arises because the SGS input impedance at most frequencies has a large reactive component and its magnitude is much larger or smaller than the standard 50 ohms of the generators and transmission line characteristic impedance. The resulting large voltage standing wave ratio leads to several sources of gross error and difficulties of measurement. These are described briefly as follows:

(a) Most of the available power is reflected back to the source, making it extremely difficult to deliver enough power to the squib to determine the firing sensitivity.

(b) Dual directional couplers must be terminated in a load of reasonably low VSWR to insure adequate isolation of incident and reflected fields and to maintain the coupling factor calibration. This condition was violated by the SGS, with the result that the apparent reflected power in some measurements exceeded the incident power.

(c) The incident and reflected power are so nearly equal in such a mis-matched system that the absorbed power can be a smaller percentage of either reading than the minimum percentage error in the power meters. The meter error, taken as a percentage of absorbed power is extremely large, and in some cases, indeterminate.

(d) Carefully adjusted tuning stubs between the dual directional coupler and the SGS made more power available to the SGS and also reduced the error in the absorbed power as seen by the coupler. However, a large and indeterminate fraction of the measured power was actually dissipated in the tuning stubs. This was made painfully obvious by the rapid heating of the stubs, which damaged two of them sufficiently to require replacement of insulating beads.

Because of the difficulties described above, the RF input power measurements reported here were obtained indirectly by the method described in the following paragraph, when VSWR was large.

2.2.1 RF Power from Voltage and Conductance Measurements

The power absorbed by the load (squib) can be calculated from the relationship

$$P = V_i^2 G_i,$$

in which V_i and G_i are the load terminal voltage and input conductance, respectively. The input voltage can be monitored with good accuracy by means of a calibrated non-directional coupler and RF detector. The input conductance is calculated from complex impedance measurements or measured directly as the real part of complex admittance.

Figure 4 illustrates this power measurement method. In actual use, a tuned half-wavelength transmission line section is inserted between the squib and the point of voltage measurement to eliminate the effects of voltage transformation by the small length of line required to insert the coupler. The three variations in test setup shown in Figure 4 were used to maximize the power input by matching the squib impedance to the source impedance. This method eliminates the error caused by losses in the tuning stubs, since the measurements were taken at the load side of the stubs. However, some error is still experienced because of power losses near the voltage null (current maximum) appearing between the coupler and the squib. This loss was sometimes large enough to cause sensible heating.

A second source of error appeared because of unpredictable slow variations and occasional rapid variations in the measured voltage during exposure. It was suspected that this might be caused by arcing in the spark chamber section of the squib. The end seal, powder, and diaphragm were removed from 4 samples, and the samples were energized at a high level. No arcing could be detected by visual observation in a darkened room for these samples, although they were heated to approximately 120°C by the RF input.

During preliminary testing, it was found that rubber inserts in the adaptors used to mount the squibs heated very rapidly at certain frequencies. This heating was serious enough to destroy the inserts. New inserts made of silicone rubber were installed. This greatly reduced, but did not completely eliminate, power losses in the inserts.

The fluctuations in voltage probably can be attributed to one or both of the following:

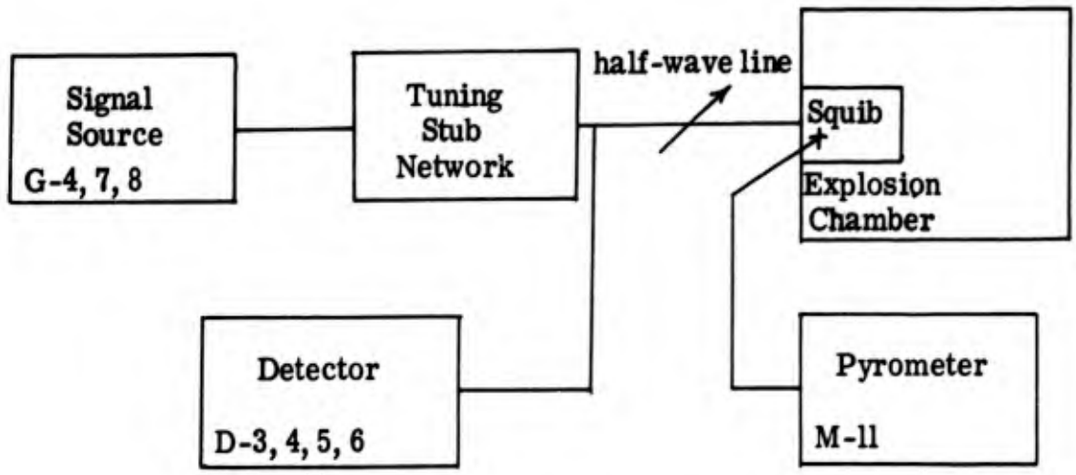

(a) General test setup.

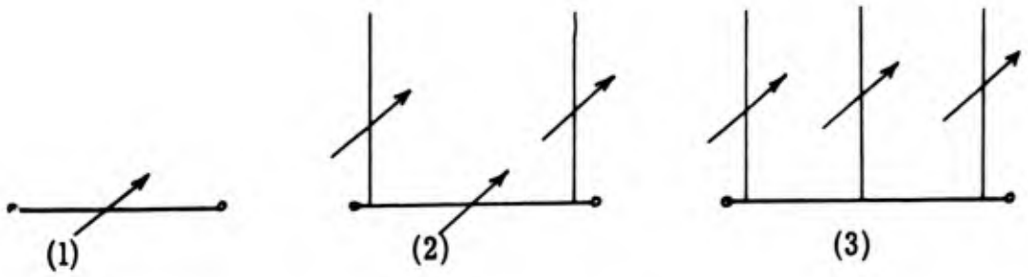

(b) Variations of tuning stub network shown in (a).

Figure 4. RF Power from Voltage Measurement and Known Conductance.

(a) Localized momentary breakdown of adaptor insulation or spark gap semi-conductor bridge as evidenced by sensible heating.

(b) Localized arc discharges in the transmission line and coupler due to field gradients caused by minute mechanical discontinuities.

2.2.2 Squib Test Connections

Figure 5 illustrates the four variations in the manner of RF excitation of squib test samples. The two configurations in which the squib case is grounded simulate the conditions of exposure most likely to occur in an actual installation.

3.0 TEST RESULTS

Figures 6 through 67 show in graphic form the results of input impedance measurements performed on ten spark gap squibs. Graphs are organized in groups of 6 for each squib serial number. Each set contains the following information, plotted against frequency:

(a) Input impedance components R and X.
(b) Input conductance, G.
(c) Input reactance factor, Q.

Each of the above is given for the lead-to-case and lead-to-lead configuration. Both impedance and conductance are plotted as logarithmic functions because of the extremely large range of values measured.

One additional curve is given for each of the two configurations showing the average of all input conductance values.

Tables 2 and 3 show the results of RF exposure tests on a series of squibs identified by serial number. Table 2 covers all squibs exposed to the maximum output of generators of "medium" power capacity, all at 1 kmc or less except for a series of pulsed and square-wave modulated outputs.

Table 3 covers squibs exposed to the maximum available output of the Navy SLT-3 microwave power source at 1 to 10 gc.

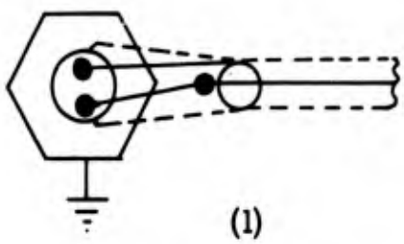

(1)

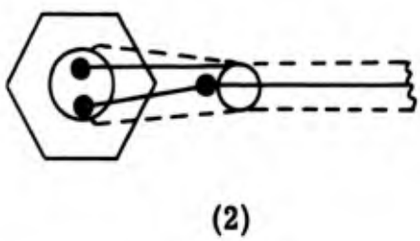

(2)

(1) Lead-to-lead, case ground.

(2) Lead-to-lead, case isolated.

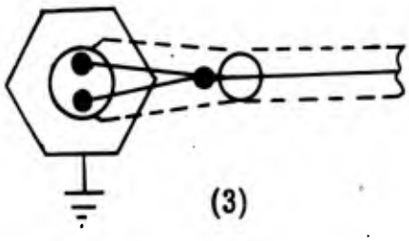

(3)

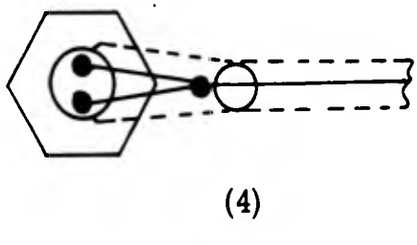

(4)

(3) Lead-to-case, case grounded.

(4) Lead-to-case, case isolated.

Figure 5. Configurations Used for RF Exposure of Squibs.

The third column of Tables 2 and 3 shows the configuration in which the squibs were exposed. The numbers in this column refer to the configuration diagrams of Figure 5. The "Firing Data" column indicates whether the squib fired or dudded during RF testing, or whether the squib fired normally after RF exposure, using the Bendix squib-firing circuit. An "X" indicates that the squib fired during RF exposure, or fired on the first attempt in the Bendix firing unit after RF exposure.

3.1 Impedance Variations

It was apparent from the large variations of voltage during RF exposure that the input impedance exhibited large changes, both erratic fluctuations and steady variations. However, a series of input impedance measurements on four samples at elevated temperatures did not reveal any measurable change from the room temperature measurements. Since it is known from data taken by Bendix that the dc resistance changes appreciably over this temperature range, it is probable that the reactance component of impedance masked the resistance change caused by temperature alone.

The fluctuating nature of the power input indicates the possibility of localized arcing and/or voltage-sensitive impedance characteristics of the semi-conductor bridge across the spark gap. Four squib samples were unloaded and tested to investigate for the presence of arcing under high RF voltage.

The arcing test was performed by viewing the spark gap in a darkened room with maximum available RF voltage applied. Although the RF input was sufficient to raise the squib temperature to 120°C, no visible arcing could be detected. However, these particular samples did not exhibit rapid fluctuations in input voltage. Arcing at the spark gap has been observed on other samples according to a report issued by Bendix.

4.0 CONCLUSIONS

The following conclusions can be drawn from the test results reported here:

(a) The Bendix Scintilla Spark Gap Squibs are for all practical purposes immune to radio frequency electromagnetic fields.

(b) A quantitative conclusion as to the degree of immunity cannot be drawn at this time because of lack of sufficient RF power

Form 30 A.P.

TABLE 2. SUMMARY OF RF POWER TESTS, MEDIUM POWER SOURCES

Squib Number	Frequency MC	Configuration (Figure 5)	Power, Watts	Time, Minutes	Temp. Rise C°	Firing Data		Notes
						RF	Post-RF	
193	200	2	0.75	5	0			
	220	2	0.75	5	0			
	330	2	0.75	5	0			
	345	2	0.90	5	0			
	350	2	0.75	5	0			
	353	2	6.4	15	11			
	335	2	9.0	20	50			
	340	2	10	20	63		X	
265	0.25	1	0.003	5	0			
	0.25	1	0.015	5	0			
	0.25	3	0.0001	5	0			
	0.25	3	0.0006	5	0			
	0.25	4	0.00009	5	0			
	2.0	2	0.01	5	0			
	2.0	4	0.002	5	0			
	20	2	0.002	5	0			
	20	4	0.00001	5	0			
	200	1	0.32	5	0			
	200	2	0.68	5	0			
	200	3	0.50	5	0			
	200	4	0.58	5	0			
	1000	1	1.0	5	0			Note 1. RF source - maxson generator.
	1000	2	1.2	5	0			Note 1.
	1000	3	1.2	5	0			Note 1.
	1000	4	1.2	5	0			Note 1.
							Note 2.	Note 2. Squib 265 was later exposed at 4.8 gc. See Table 3.

Form 36 A.P.

TABLE 2. (Continued)

Squib Number	Frequency MC	Configuration (Figure 5)	Power, Watts	Time, Minutes	Temp. Rise C°	Firing Data		Notes
						RF	Post-RF	
171	500	1	.041	5	0			
	500	2	.044	5	0			
	500	3	.050	5	0			
	500	4	.050	5	0		Note 3	Note 3. Squib 171 was later exposed at 9.5 and 9.96 gc. See Table 3.
129	1000	1	1.5	5	0			
	1000	2	1.6	5	0			
	1000	3	1.0	5	0			
	1000	4	1.9	5	0		X	
184	9000	1	470 peak 0.47ave	5	0			Note 4. Pulsed source. Power is maximum estimated available at squib.
	500	1	0.8peak 0.4ave	5	0		X	Note 5. Square-wave modulated source. Power is maximum estimated available at squib.
135	600	1	0.8peak 0.4ave	5	0		X	Note 5.
186	800	1	0.8peak 0.4 ave	5	0		X	Note 5.
177	900	1	0.8peak 0.4ave	5	0		X	Note 5.

Form 30 A.P.

TABLE 2. (Concluded)

Squib Number	Frequency MC	Configuration (Figure 5)	Power, Watts	Time, Minutes	Temp. Rise C^{O}	Firing Data		Notes
						RF	Post-RF	
190	1000	1	0.8peak 0.4ave	5	0		X	Note 5.

Form 30 A.P.

TABLE 3. SUMMARY OF RF POWER TESTS. HIGH POWER SOURCE.

Squib Number	Frequency GC	Configuration (Figure 5)	Power, Watts	Time, Minutes	Temp. Rise C°	Firing Data		Notes
						RF	Post-RF	
206	1.0 1.0	1 3	60 44	5 5	28 14		X	Note 1. Power is initial level. Rapid fluctuations required continual adjustment of tuning in both configurations.
151	1.0 1.0	3 4	78 102	5 5	11 36		X	Note 1. Note 2. Large proportion of power was dissipated in transmission line heating, both configurations.
261	1.0	4	10	4	121	DUD	DUD	Note 3. Aluminum end seal fell off during RF test, spilling part of powder charge. Silicone rubber adapter insert was charred on end next to squib. Heavy smoke was released. Squib could not be fired (diaphragm would not puncture) from Bendix firing unit. Note 4. Power is initial level. Power input increased as squib heated.
230	1.0 1.0 1.0	4 4 4	8.0 8.0 9.7-39	30 30 approx. 5	124 70 80	X		Note 5. Power increased to 9.7 watts. During adjustment of matching stubs, voltage suddenly became erratic and squib fired. Power approximately 39 watts at firing.

Form 30 A.P.

TABLE 2. (Concluded)

Squib Number	Frequency MC	Configuration (Figure 5)	Power, Watts	Time, Minutes	Temp. Rise C°	Firing Data		Notes
						RF	Post-RF	
190	1000	1	0.8peak 0.4ave	5	0		X	Note 5.

Form 30 A.P.

TABLE 3. SUMMARY OF RF POWER TESTS. HIGH POWER SOURCE.

Squib Number	Frequency GC	Configuration (Figure 5)	Power, Watts	Time, Minutes	Temp. Rise C°	Firing Data		Notes
						RF	Post-RF	
206	1.0	1	60	5	28			Note 1. Power is initial level. Rapid fluctuations required continual adjustment of tuning in both configurations.
	1.0	3	44	5	14		X	
151	1.0	3	78	5	11			Note 1. Note 2. Large proportion of power was dissipated in transmission line heating, both configurations.
	1.0	4	102	5	36		X	
261	1.0	4	10	4	121	DUD	DUD	Note 3. Aluminum end seal fell off during RF test, spilling part of powder charge. Silicone rubber adapter insert was charred on end next to squib. Heavy smoke was released. Squib could not be fired (diaphragm would not puncture) from Bendix firing unit. Note 4. Power is initial level. Power input increased as squib heated.
230	1.0	4	8.0	30	124			
	1.0	4	8.0	30	70			
	1.0	4	9.7-39	approx. 5	80	X		Note 5. Power increased to 9.7 watts. During adjustment of matching stubs, voltage suddenly became erratic and squib fired. Power approximately 39 watts at firing.

TABLE 3. (Continued)

Squib Number	Frequency GC	Configuration (Figure 5)	Power, Watts	Time, Minutes	Temp. Rise C°	Firing Data		Notes
						RF	Post-RF	
228	1.0	4	10.4	20	142			
	1.0	4	10.4	20	152		X	
154	3.0	4	71.8	20	120		X	Notes 1 and 2.
232	3.0	4	91.3	20	134		X	Notes 1 and 2.
165	3.0	4	71.0	20	112		X	Notes 1 and 2.
215	3.0	4	71.0	20	114		X	Notes 1 and 2.
192	4.8	1	3.7	5	30			
	4.8	3	7.0	5	33		X	Note 1. (Configuration 3 only.)
204	4.8	2	8.8	5	22			Note 1.
	4.8	4	10.0	5	44		X	
265	4.8	2	14.4	0.5	40		X	Note 6. This was first high-power microwave test using rubber adapter inserts. The insert was destroyed in 30 seconds. This type of insert was not used for other tests. Squib fired normally after this RF test. Note 7. This squib was previously exposed at lower frequencies. See Table 2.

Form 36 A.P.

TABLE 3. (Continued)

Squib Number	Frequency GC	Configuration (Figure 5)	Power, Watts	Time, Minutes	Temp. Rise C°	Firing Data		Notes
						RF	Post-RF	
121	5.0	1	16	20	89		X	Notes 1 and 2.
167	5.0	1	62	20	122		X	Notes 1 and 2.
176	5.0	1	53	20	142		X	Notes 1 and 2.
166	5.0	1	67	20	120		X	Notes 1 and 2.
171	9.5	1	1.3	5	5.6			Note 7. This squib was previously exposed at lower frequencies. See Table 2.
	9.5	2	1.0	5	9.5			
	9.5	3	1.2	5	6.7			
	9.5	4	1.2	5	4.5			
	9.96	2	2.6	5	6.1			
	9.96	4	2.0	5	3.3		X	
155	9.96	1	2.1	5	2.2			
	9.96	3	2.0	5	2.1		X	

TABLE 3. (Concluded)

Squib Number	Frequency GC	Configuration (Figure 5)	Power Watts	Time, Minutes	Temp. Rise C°	Firing Data		Notes
						RF	Post-RF	
268	10	1	22	20	48	note 8	note 8	Note 8. Squib was desensitized. It fired on third attempt from the Bendix firing unit.
149	10	1	14	20	50		X	
188	10	1	11	20	54	note 8	note 8	Note 8. (Desensitized.)
159	10	1	16	20	49		X	

capability to determine threshold sensitivity, and lack of accurate measurement methods for determining power input at most frequencies.

(c) The effectiveness of the SGS can probably be attributed to (1) the extremely large input impedance at most frequencies which makes impedance matching to any practical RF source very difficult, (2) the large input resistance which limits the power that can be absorbed, and (3) the ability of the semiconductor bridge to dissipate large quantities of power without damage or detonation of the powder charge.

Of the entire lot of squibs exposed to maximum available RF power, only one was detonated. This occurred at an RF input power level of approximately 39 watts at 1.0 gc, after having been twice previously exposed for 30 minutes at 1.0 gc at 8 watts. Two squibs were apparently desensitized after 20-minute exposures to 11 and 22 watts, respectively, at 10 gc. However, the sample of six units tested at or very near this frequency is not statistically meaningful. Two samples given similar exposures at the same frequency (at 14 and 16 watts) fired normally, after exposure. It is quite possible that the two "desensitized" units were less sensitive before RF exposure.

5.0 RECOMMENDATIONS

Since completion of these tests, an investigation of improved methods of RF power measurement on high-VSWR loads has been carried out, and new high-power capacity slotted lines have been obtained which are suitable for use in these measurements. One promising method requires measurement only of the maximum and minimum RF voltage, using a slotted line and RF detector. The slotted line can be inserted between the high-VSWR load and the matching stubs, thus eliminating the large unknown power loss in the stubs from the measured power. The slotted line can be adjusted to follow steady changes in input impedance, although it would not be able to follow erratic changes because of arcing.

It is recommended that the remaining squib samples be subjected in the future to additional microwave RF exposures using a slotted line technique of power measurement.

Frequencies for these tests can be selected from a study of the impedance versus frequency characteristics of the squibs. Thus, the test frequencies can be limited to those most likely to cause detonation, and a statistically-meaningful sample may be obtained.

ACKNOWLEDGEMENT

We wish to acknowledge gratefully the extremely valuable assistance and technical direction provided on this study by Messrs. Lyde Pruett, Ralph Hagar, and Rodney Schmidt of the U. S. Naval Weapons Laboratory, Dahlgren, Virginia.

Genistron personnel who participated in measurements, data analysis and reduction, and preparation of this report include the following:

Thomas Boykin, Electronics Technician
Robert B. Cowdell, Senior Research Engineer
Victor P. Musil, Senior Project Engineer
David R. Harrell, Electronics Technician
Hiram H. Ohta, Project Engineer
James C. Senn, Manager, Applied Research
Jerrald C. Shifman, Research Engineer

Genistron
INCORPORATED

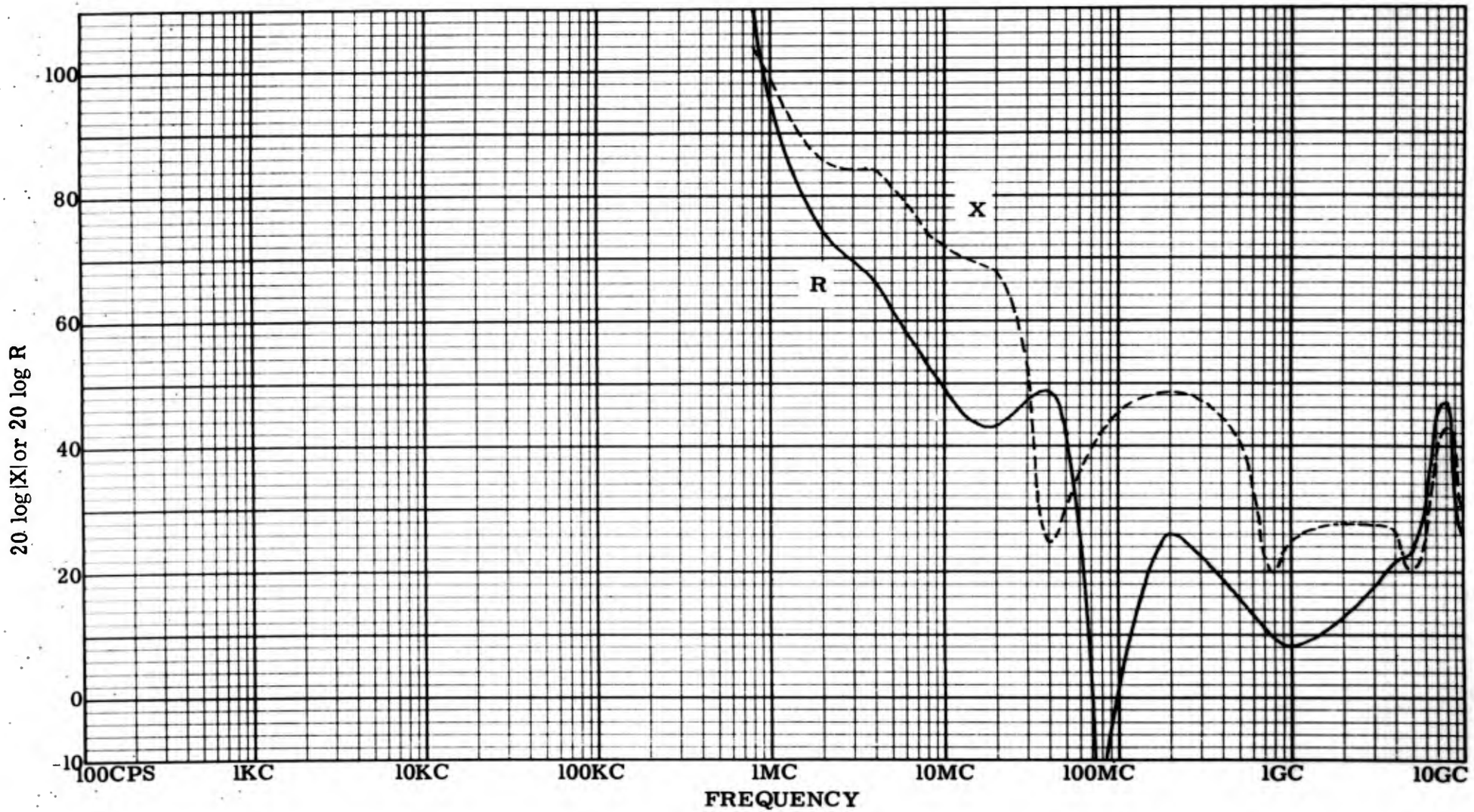

Figure 6: Input resistance and reactance, lead-to-lead, Serial #193

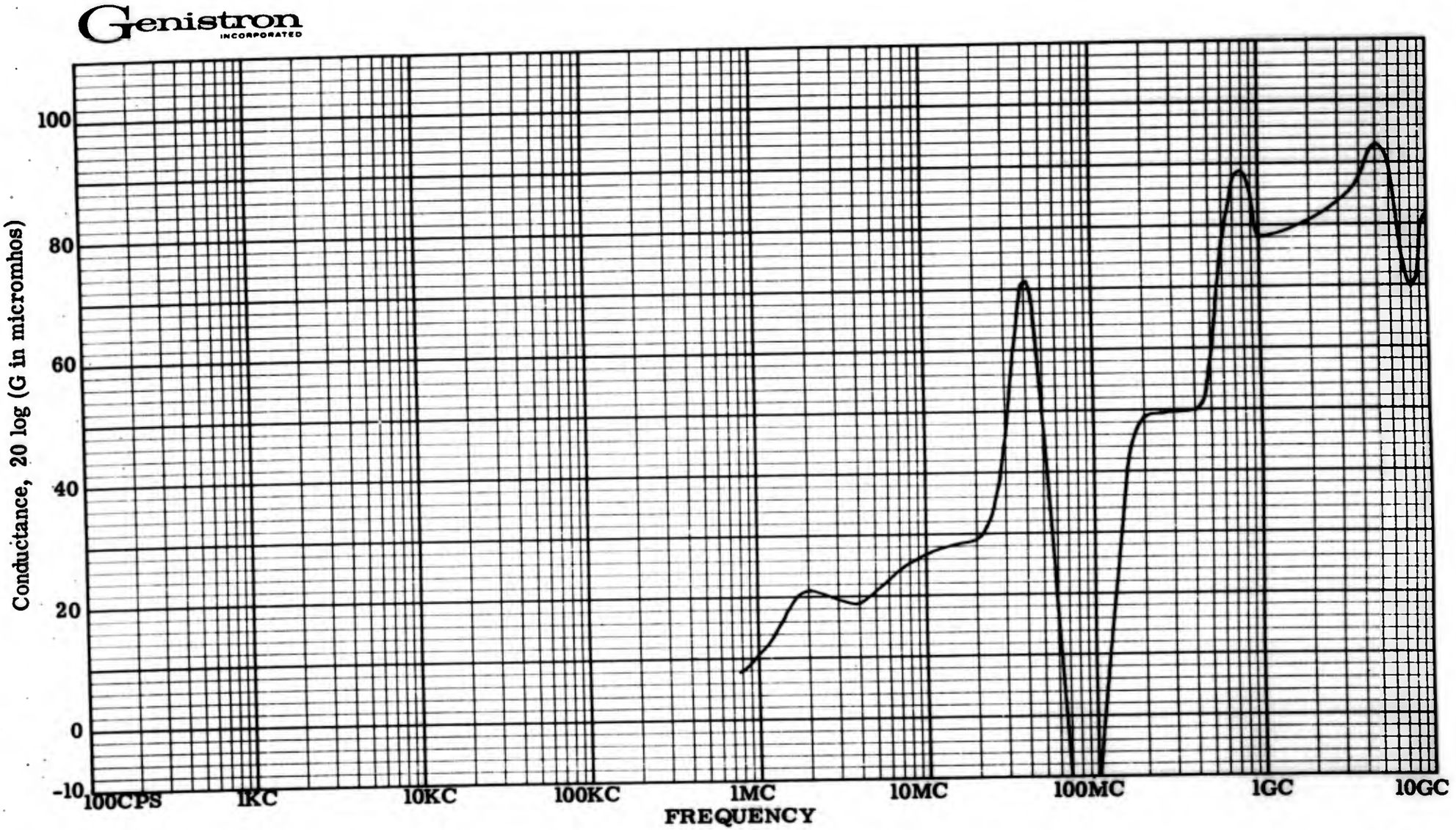

Figure 7: Input conductance, lead-to-lead, Serial #193.

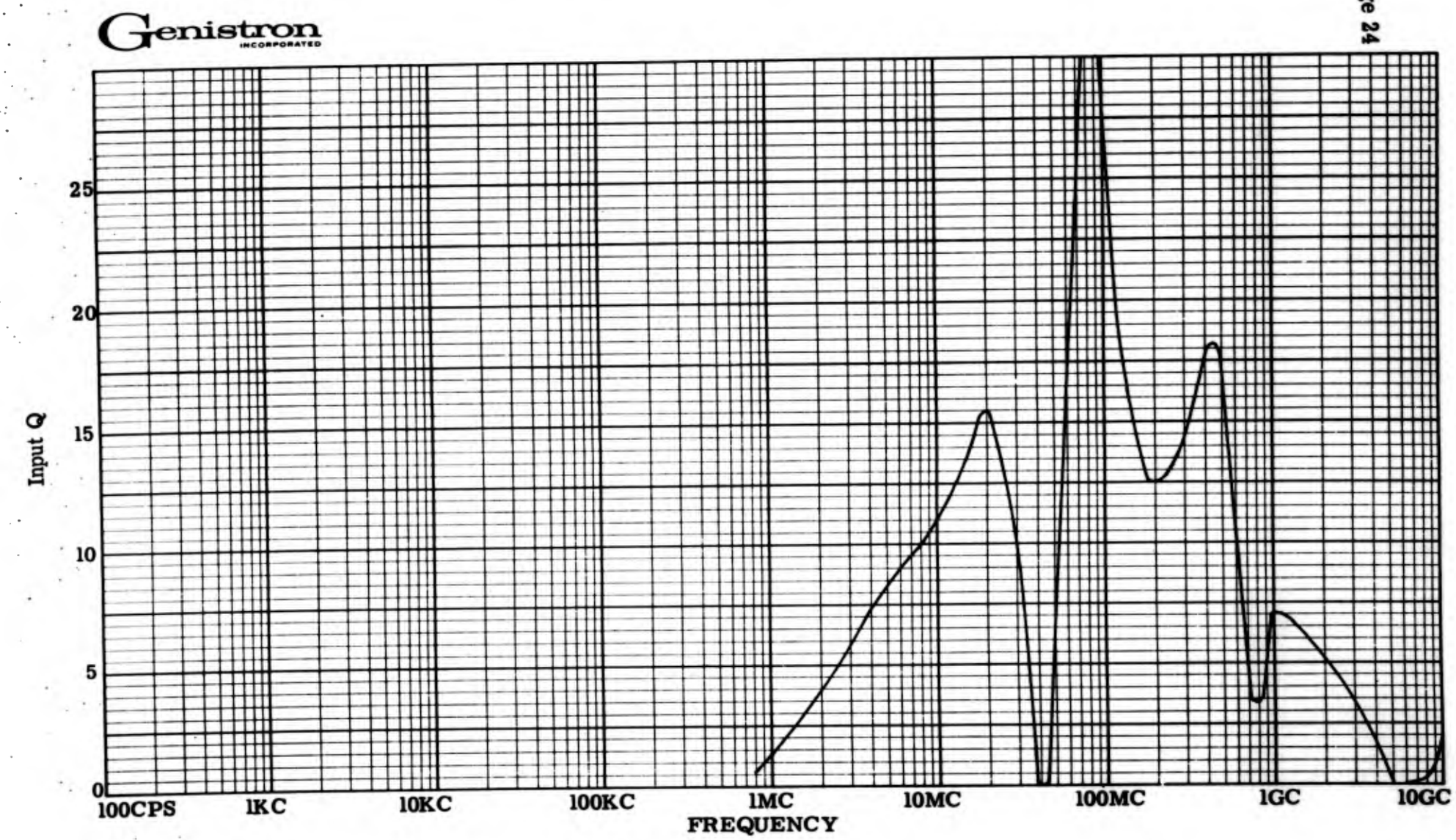

Figure 8: Input Q, lead-to-lead, Serial #193.

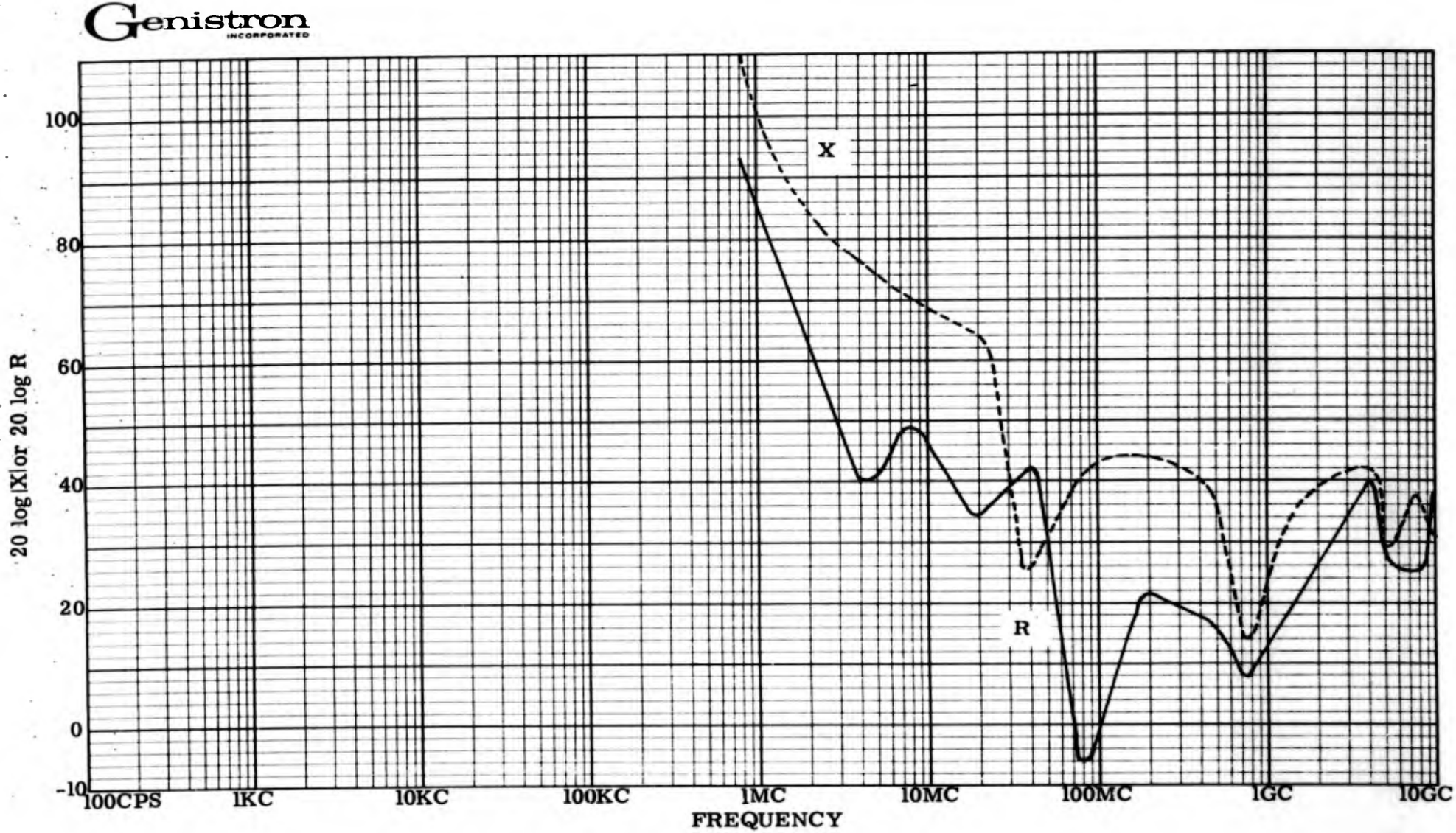

Figure 9: Input resistance and reactance, lead-to-case, Serial #193.

Genistron
INCORPORATED

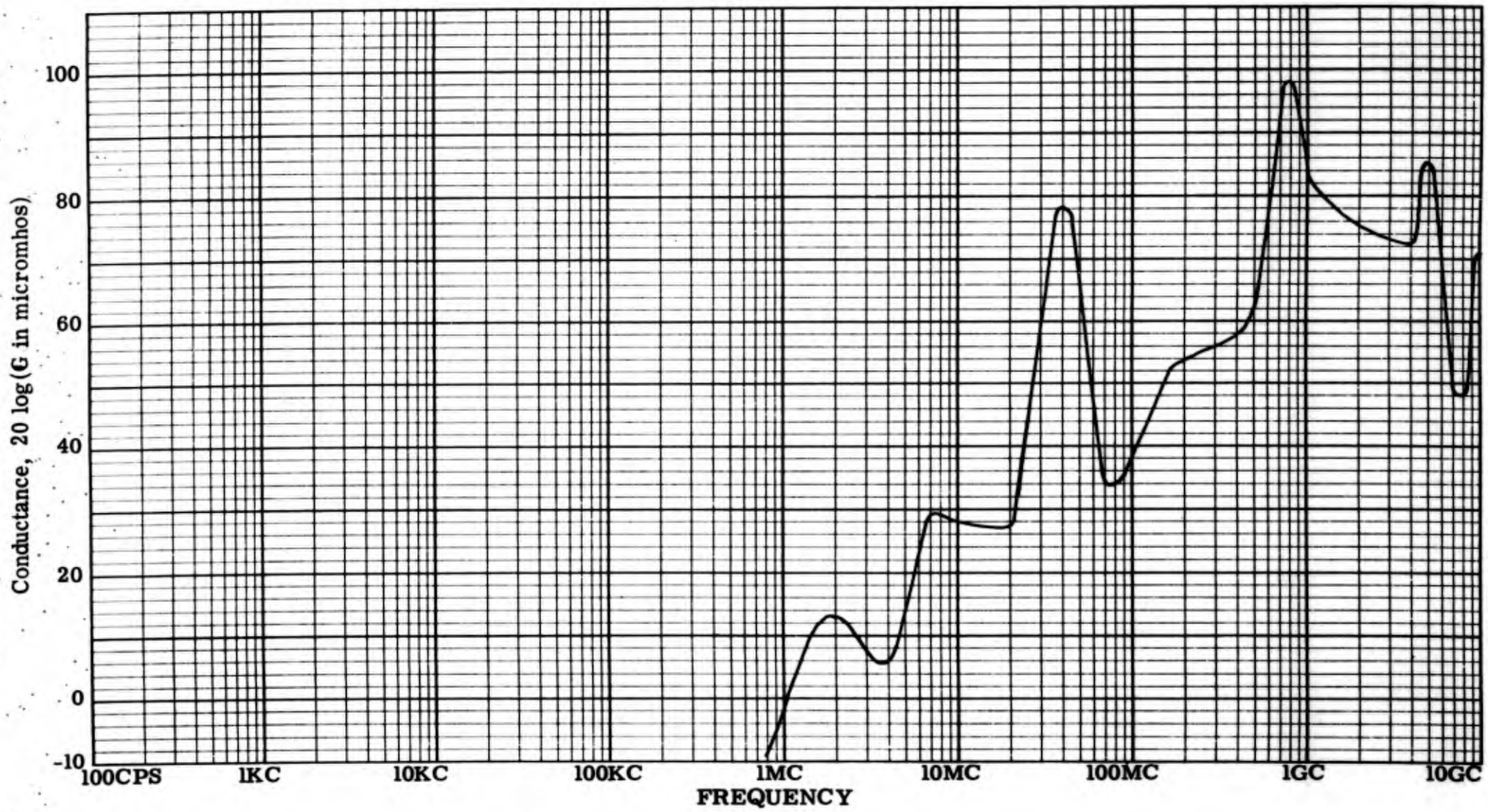

Figure 10: Input conductance, lead-to-case, Serial #193.

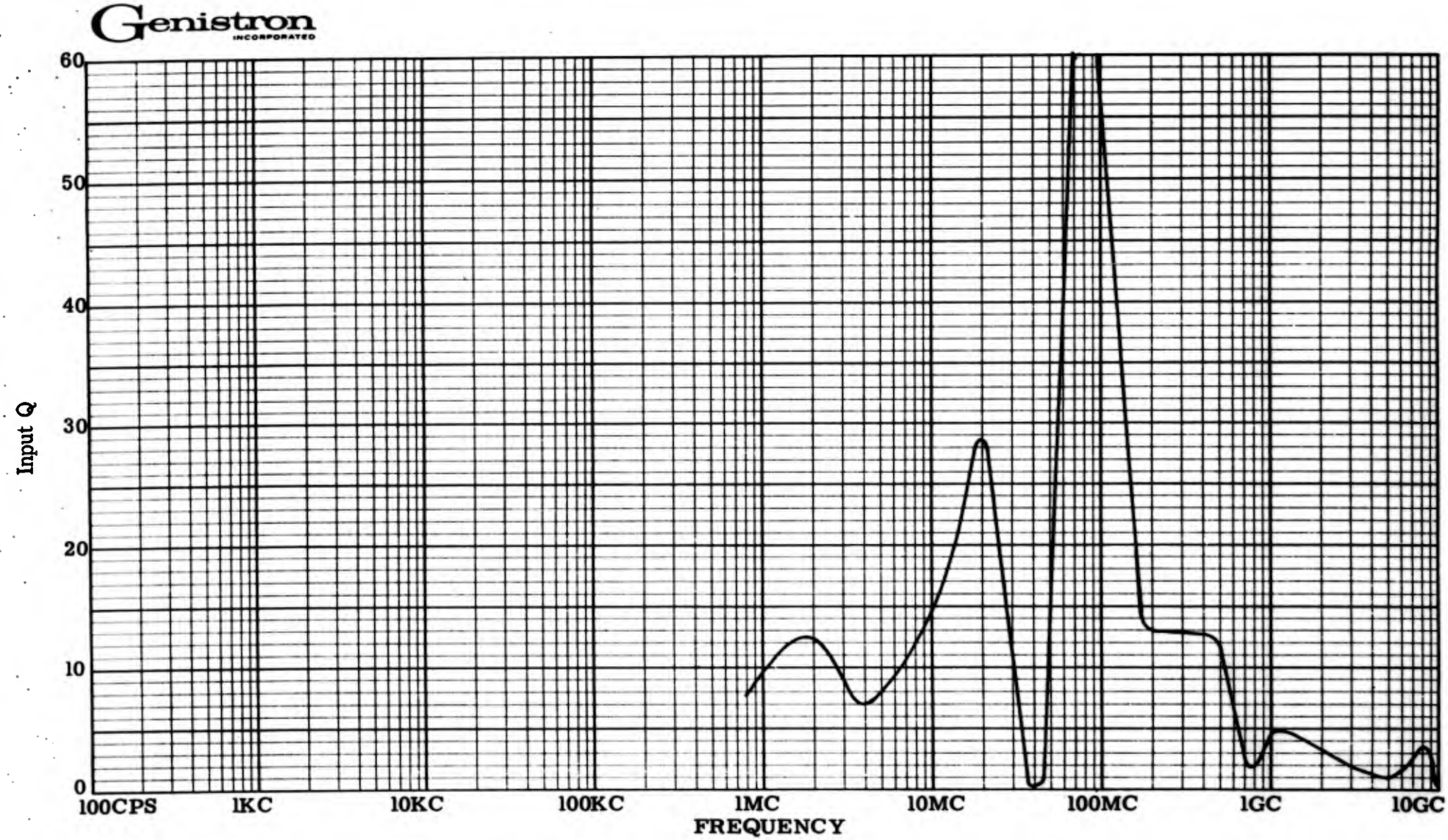

Figure 11: Input Q, lead-to-case, Serial #193.

Genistron INCORPORATED

Figure 12: Input resistance and reactance, lead-to-lead, Serial #228.

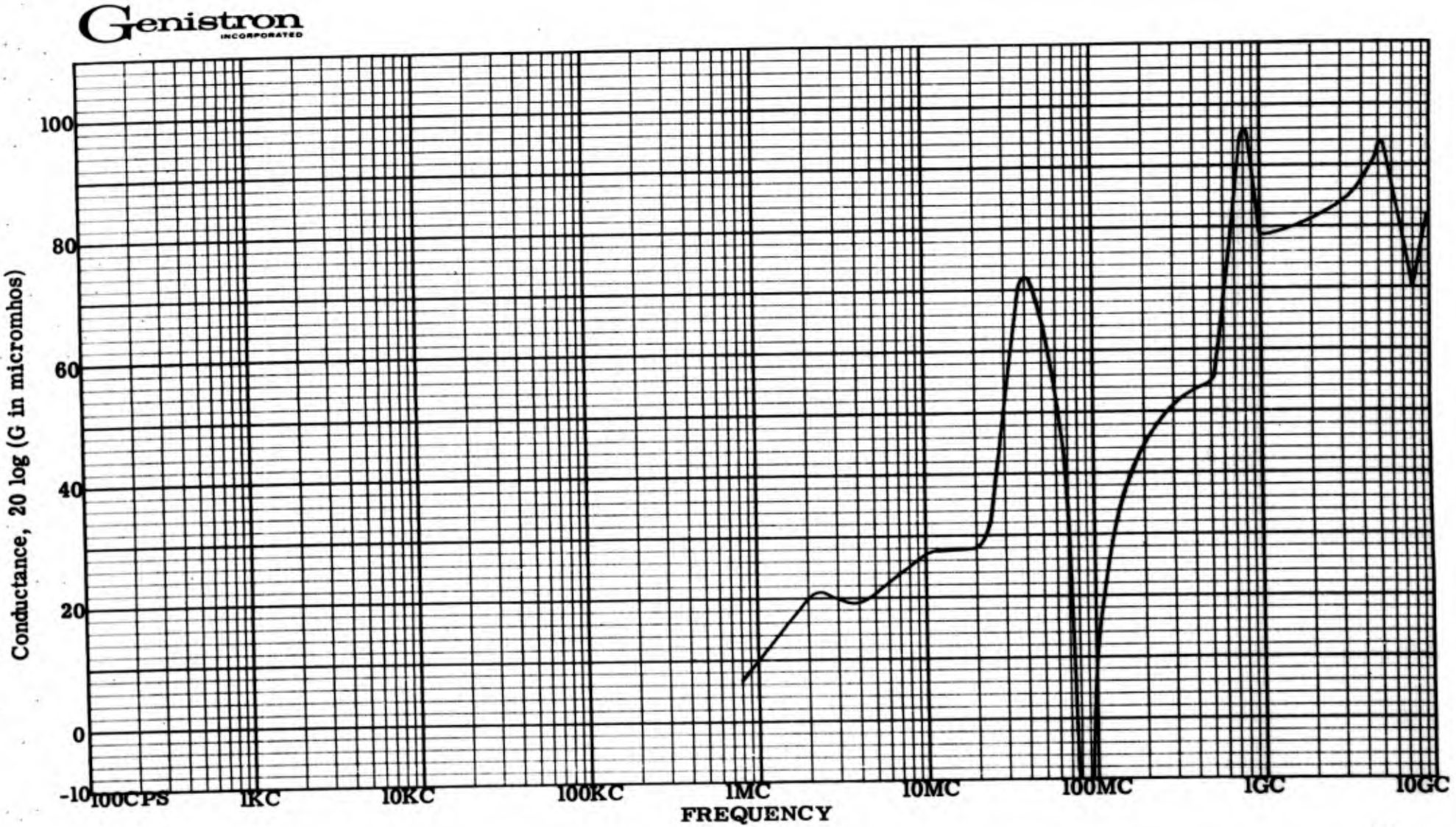

Figure 13. Input conductance, lead-to-lead, Serial #228.

Genistron
INCORPORATED

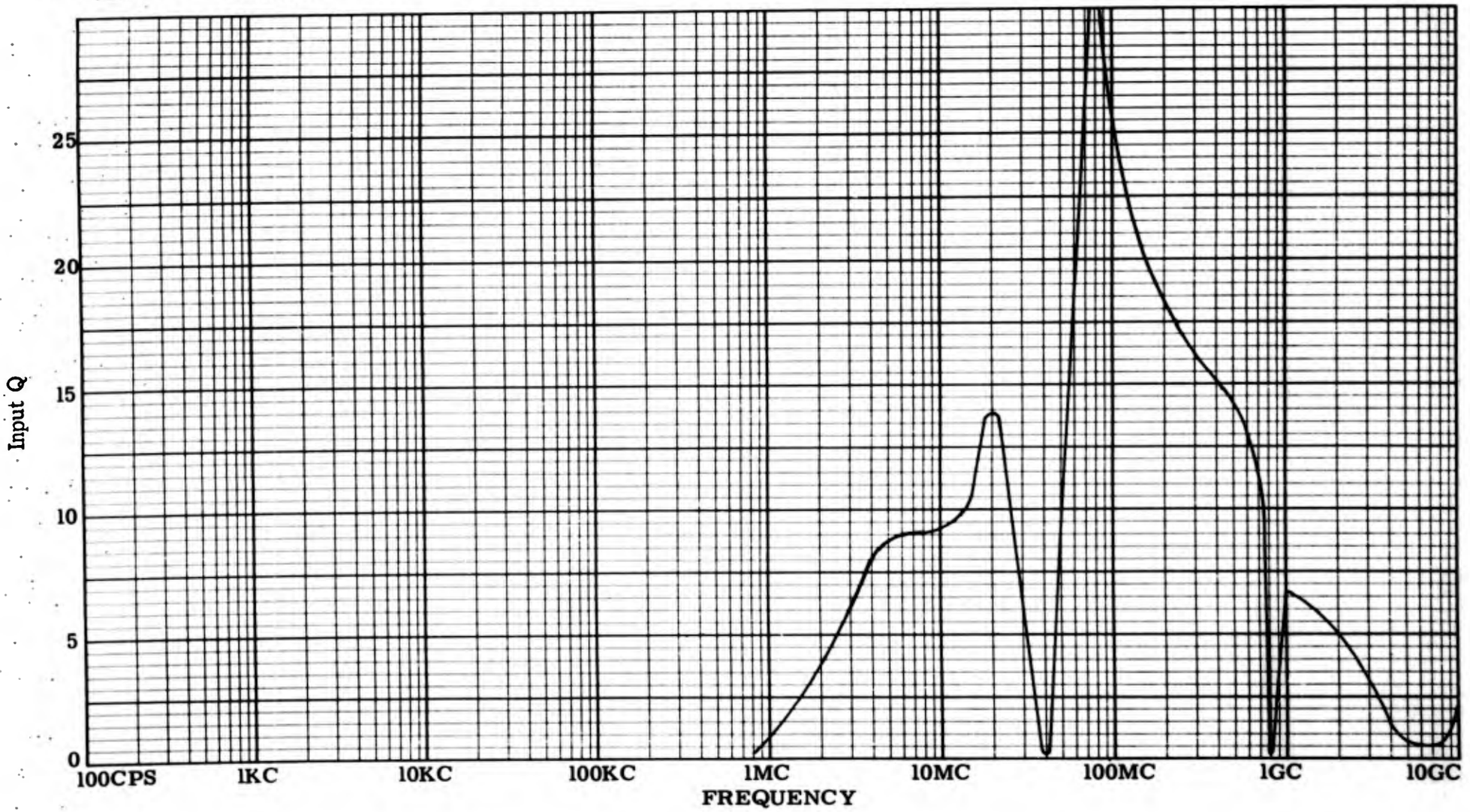

Figure 14: Input Q, lead-to-lead, Serial #228.

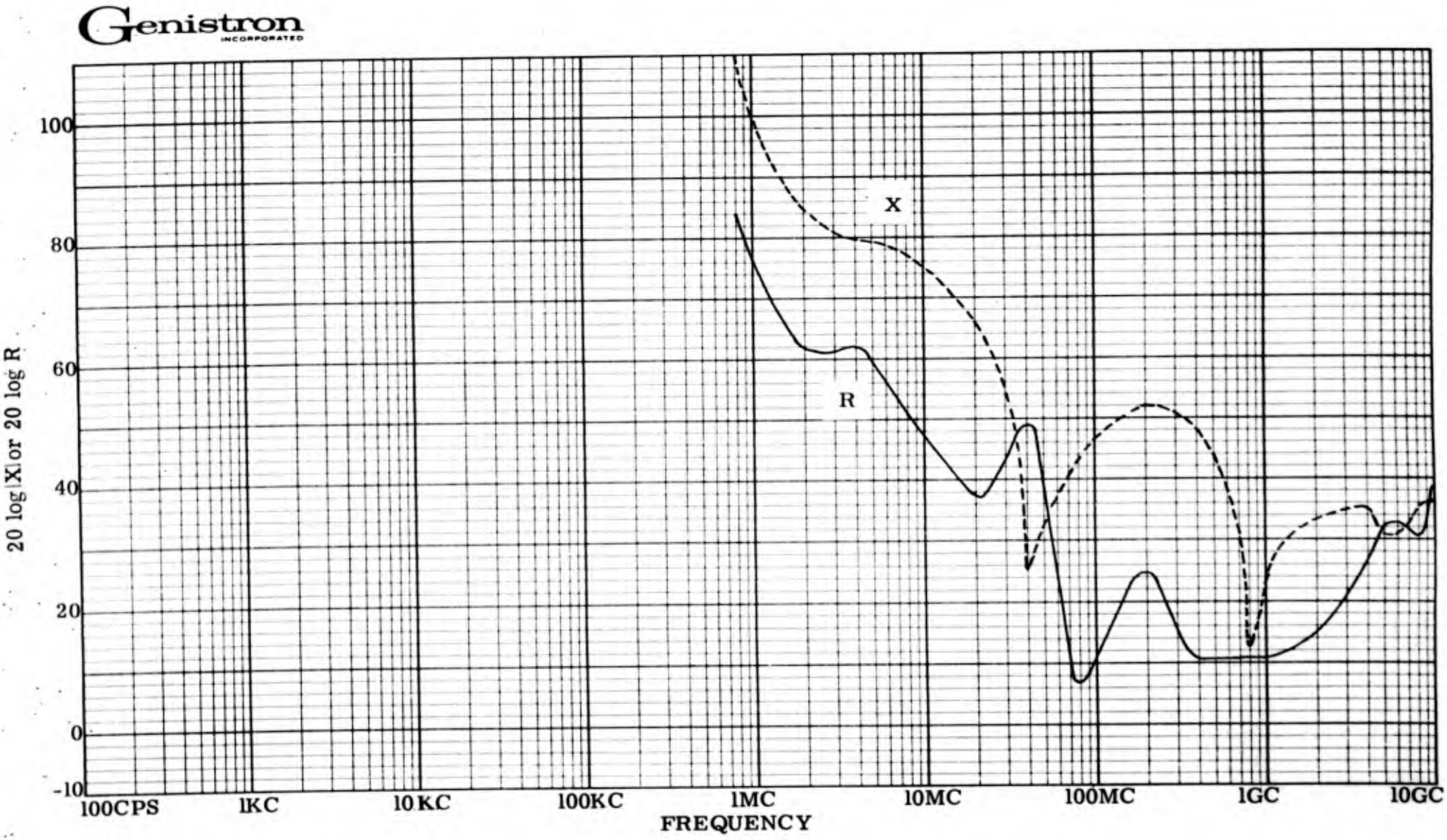

Figure 15: Input resistance and reactance, lead-to-case, Serial #228.

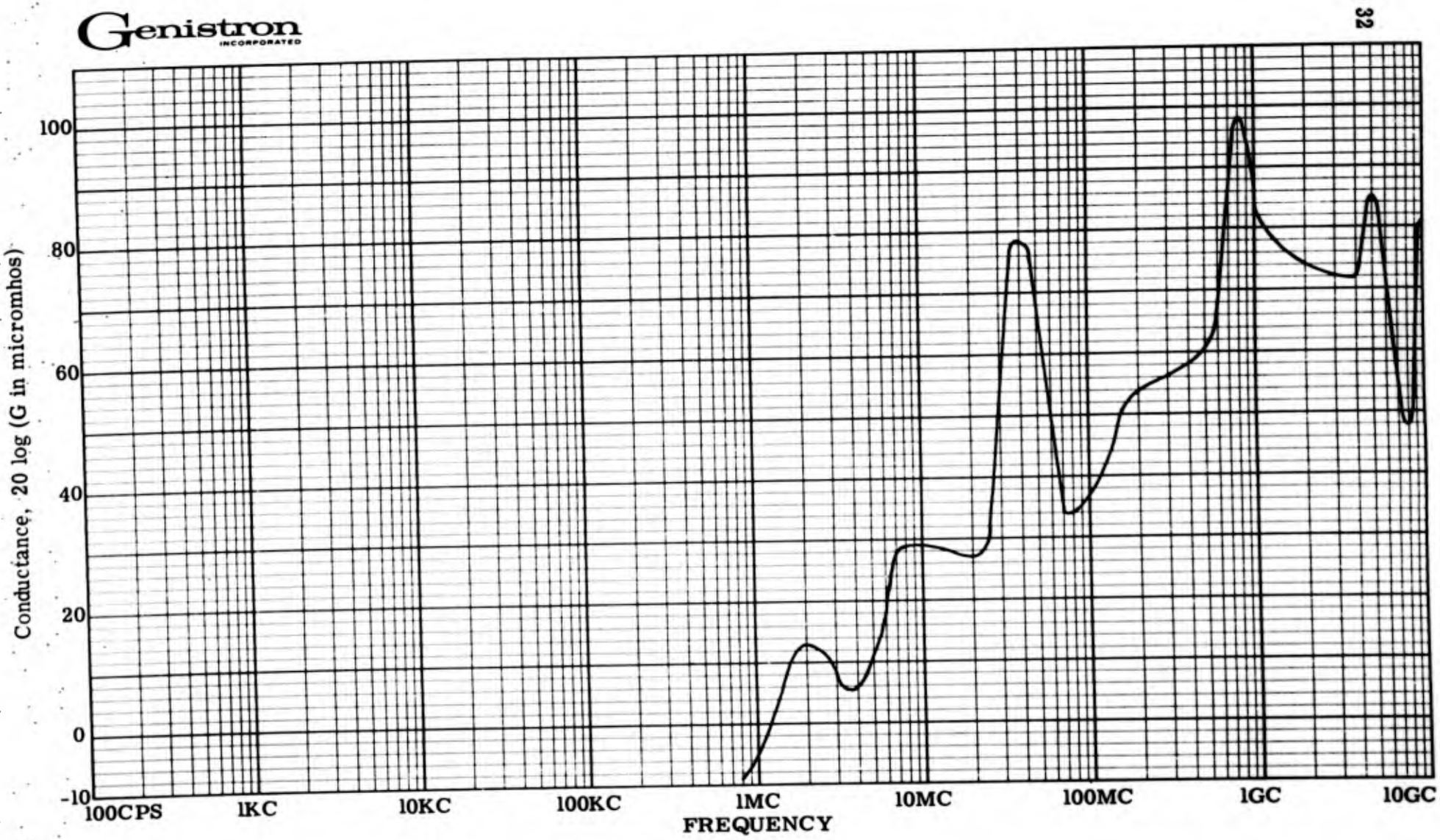

Figure 16: Input conductance, lead-to-case, Serial #228.

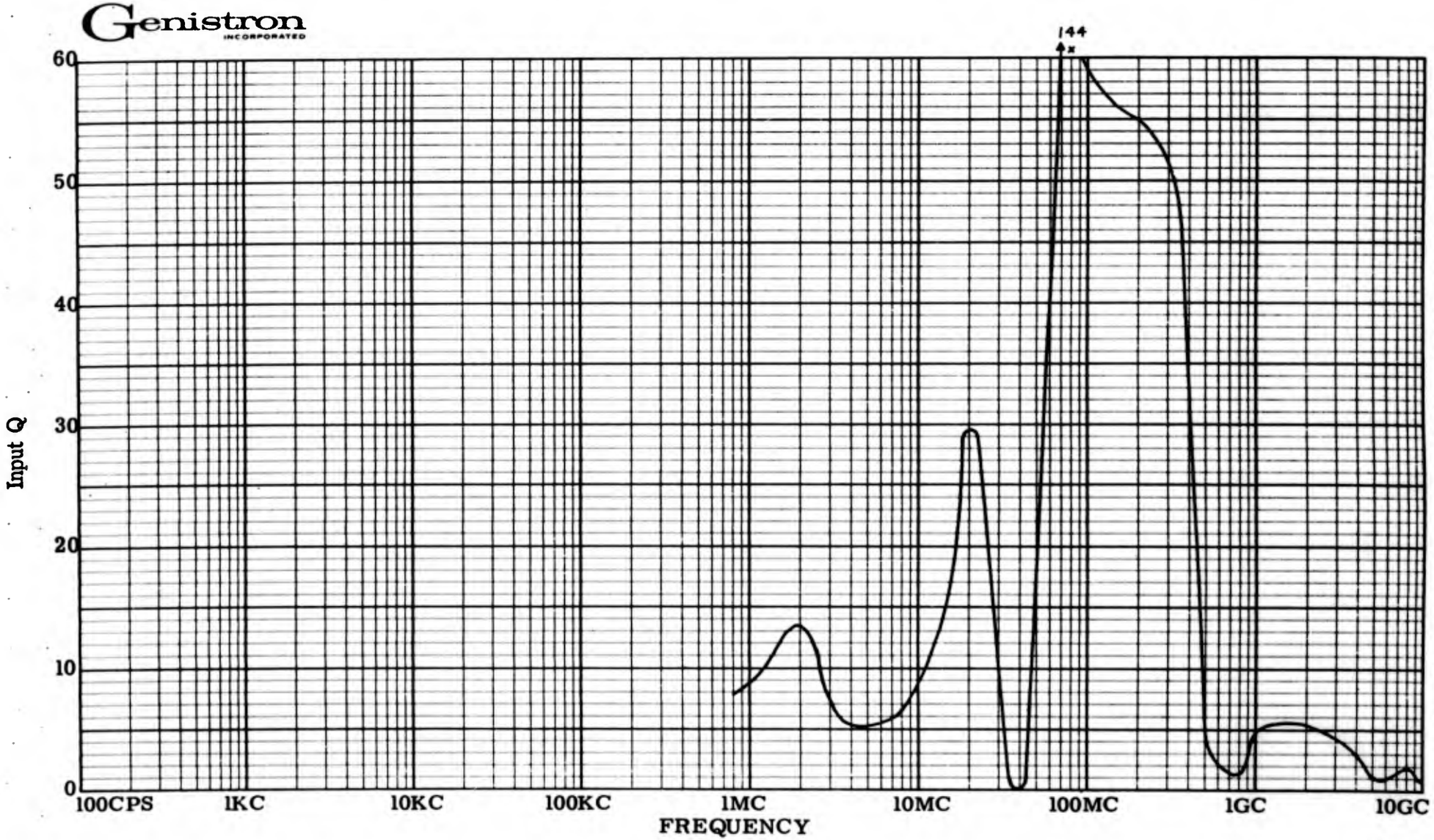

Figure 17: Input Q, lead-to-case, Serial #228.

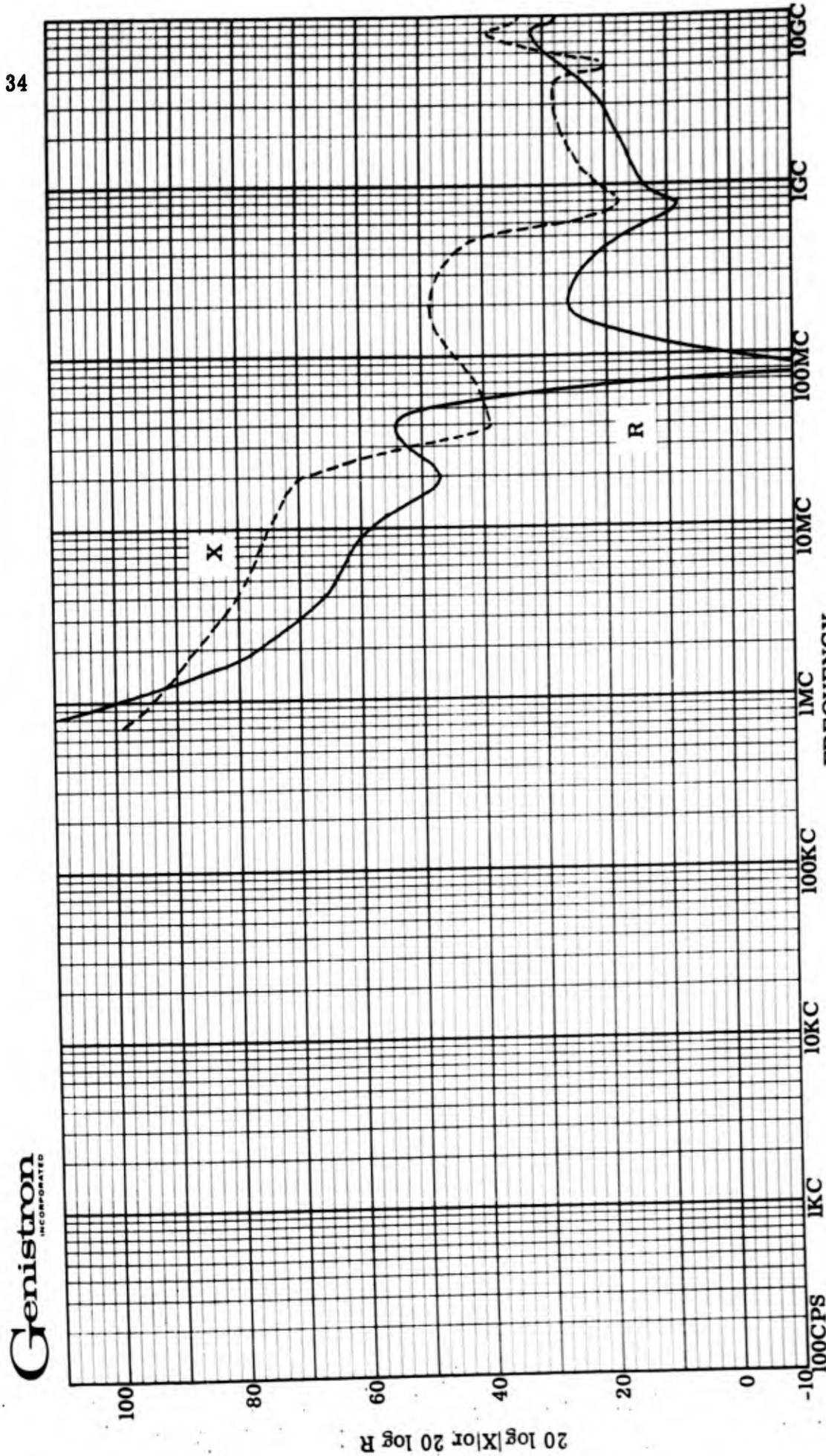

Figure 18: Input resistance and reactance, lead-to-lead, Serial #230.

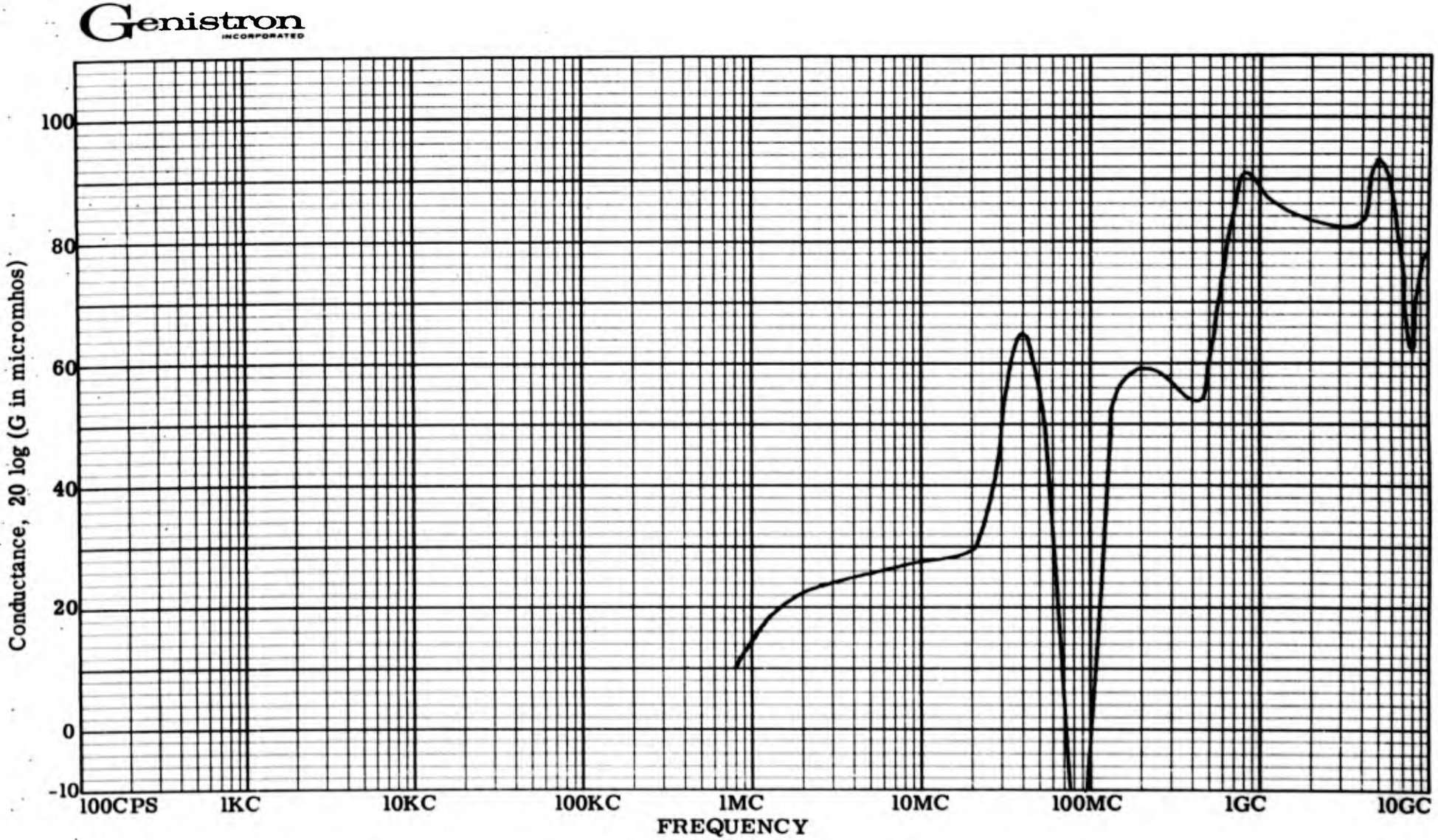

Figure 19: Input conductance, lead-to-lead, Serial #230.

Genistron
INCORPORATED

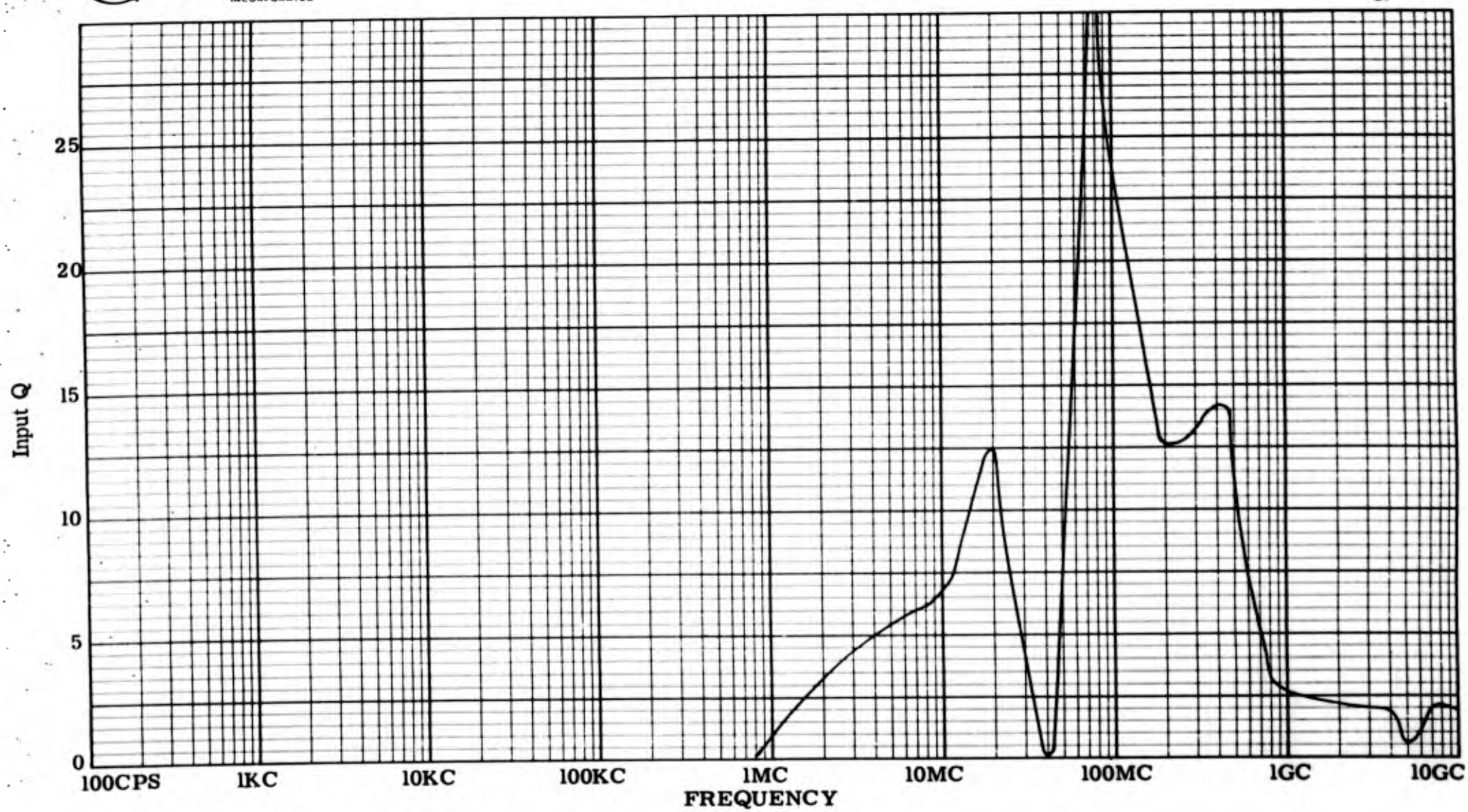

Figure 20: Input Q, lead-to-lead, Serial 230.

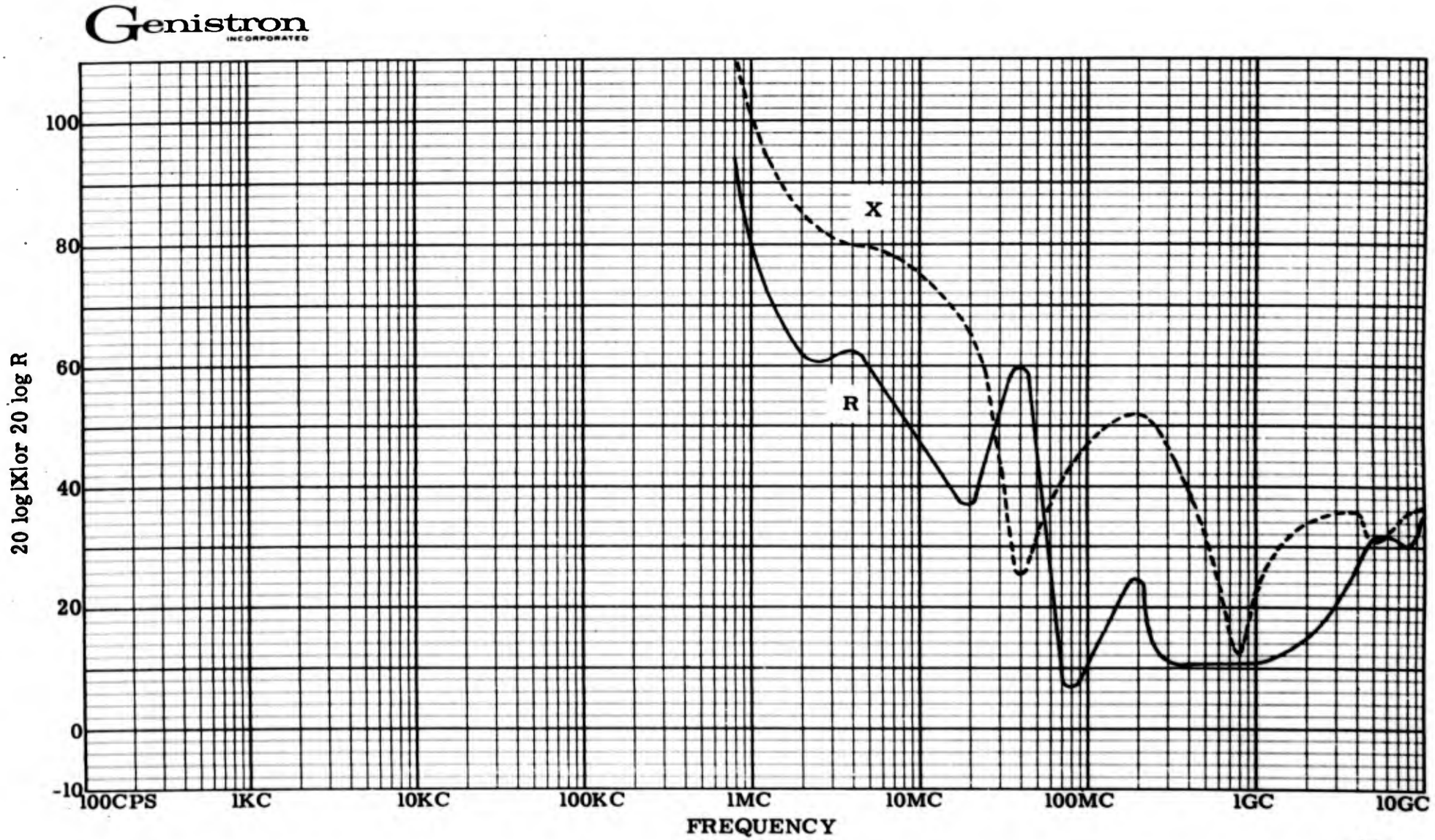

Figure 21: Input resistance and reactance, lead-to-case, Serial #230.

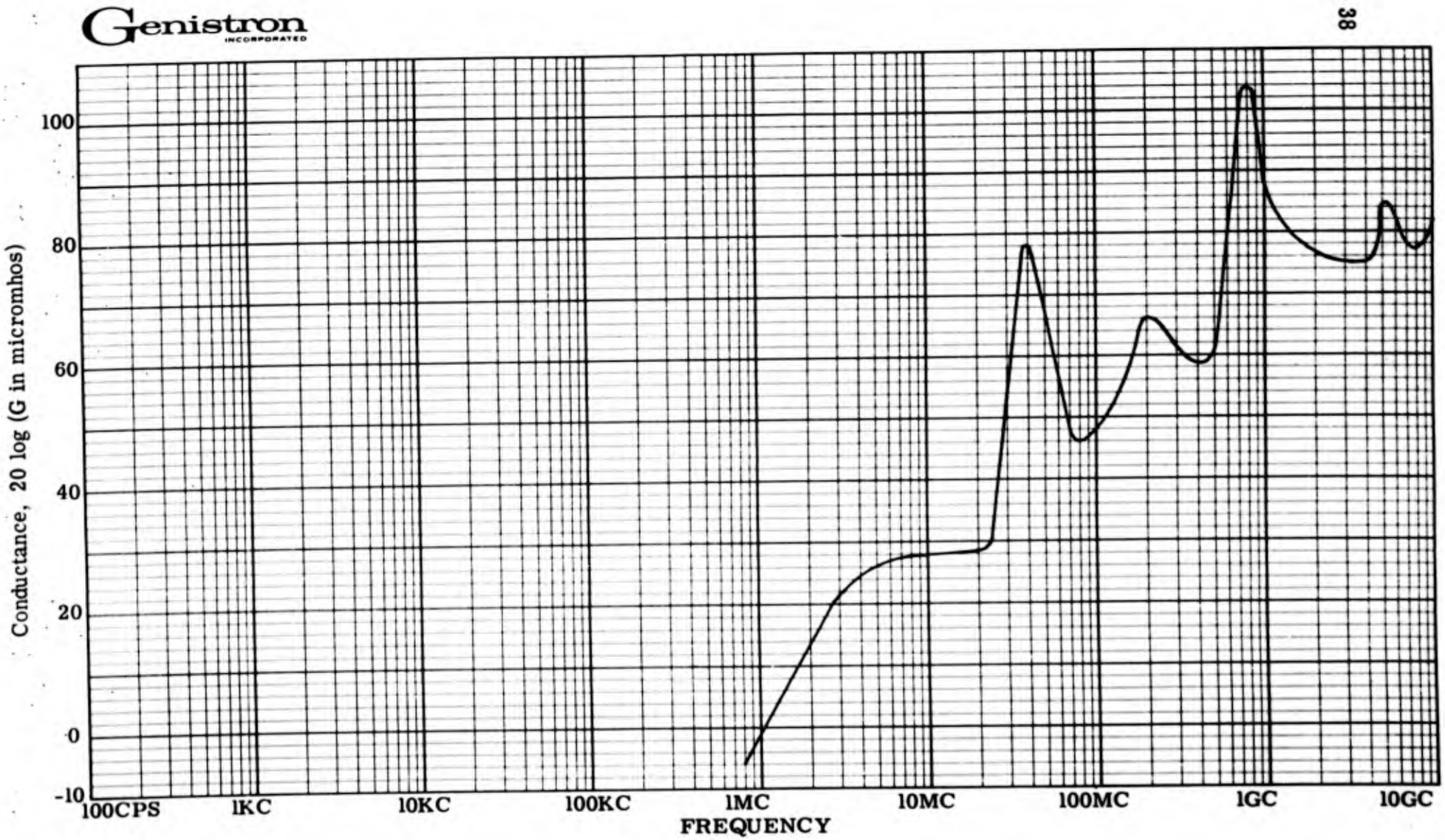

Figure 22: Input conductance, lead-to-case, Serial #230.

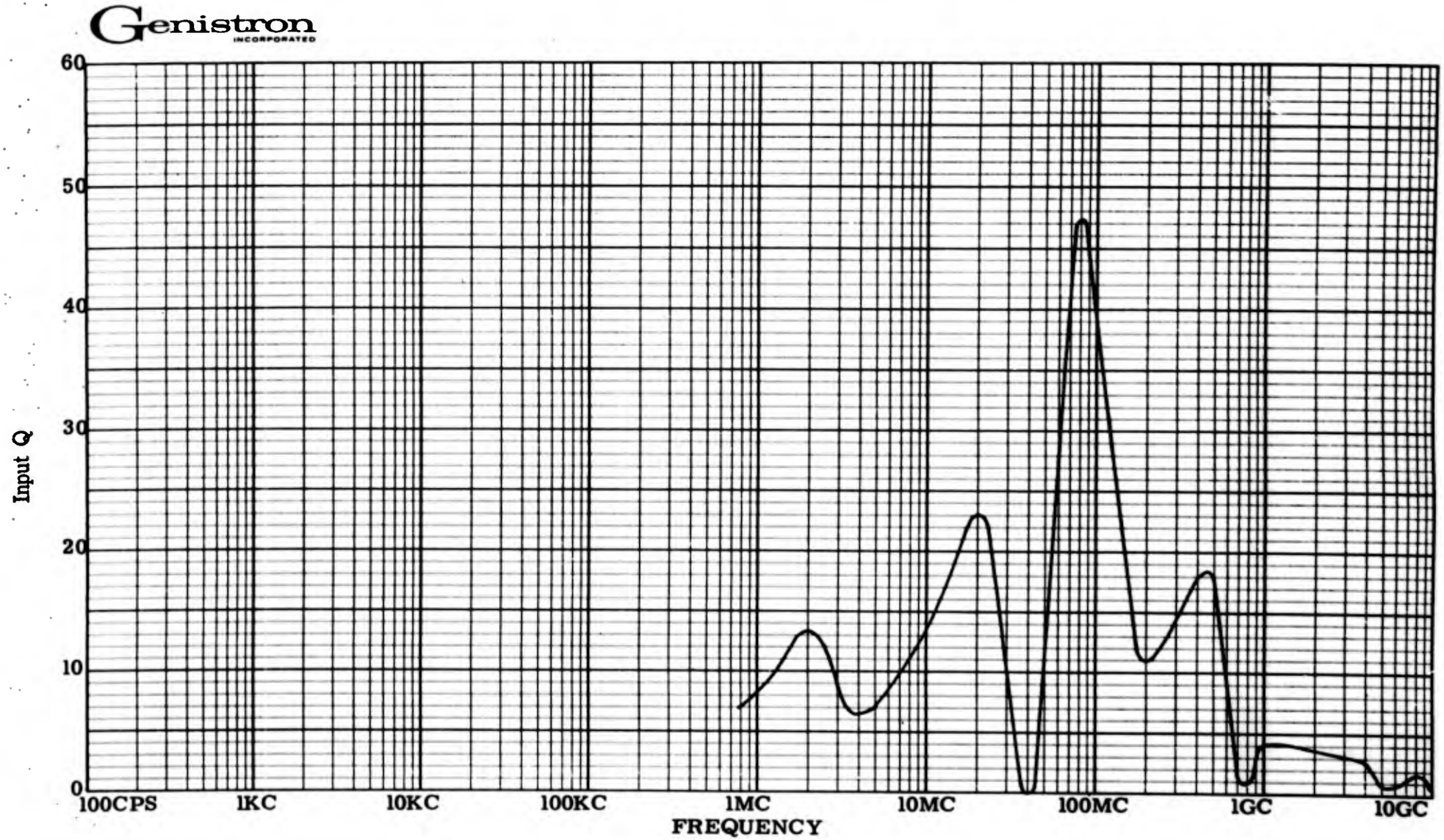

Figure 23: Input Q, lead-to-case, Serial #230.

Genistron
INCORPORATED

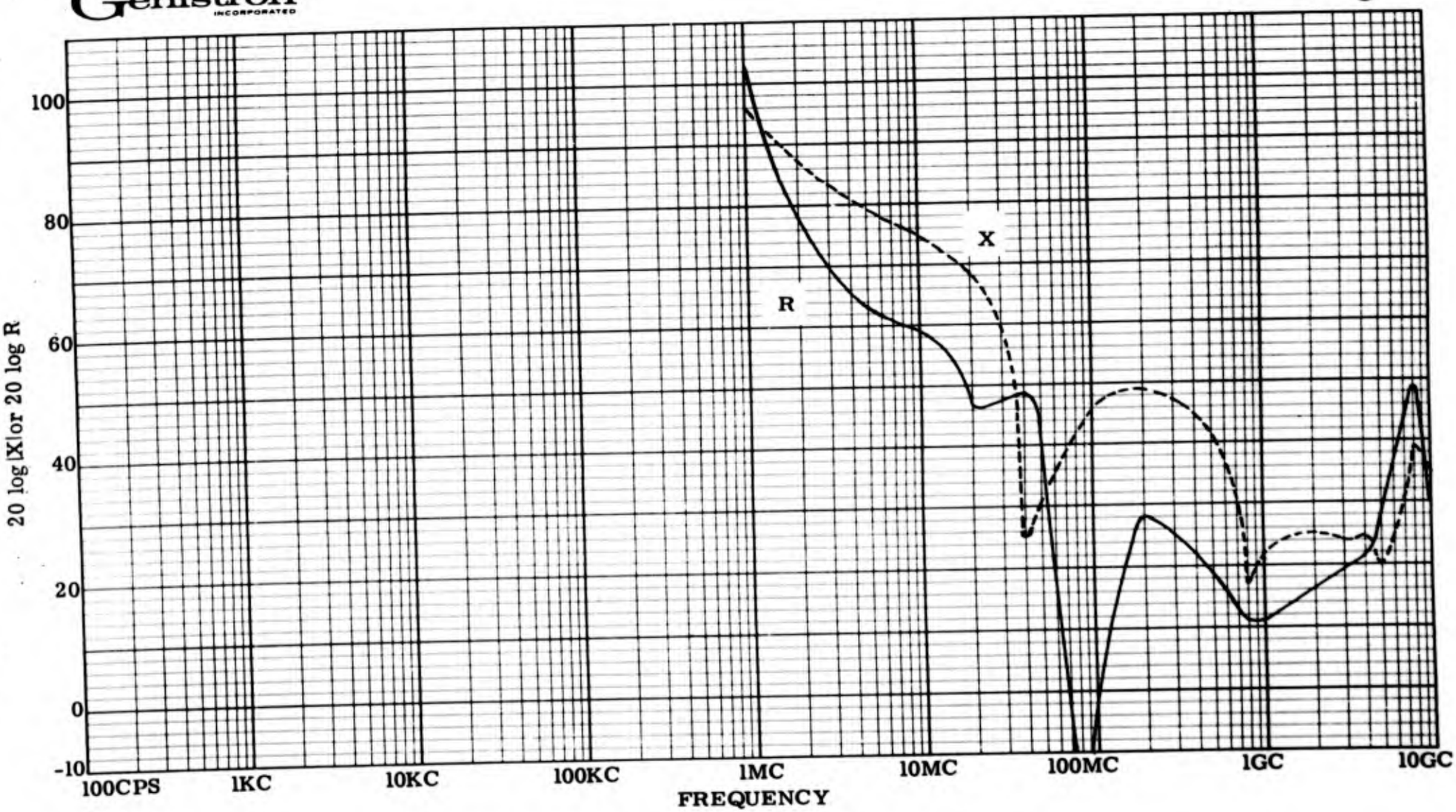

Figure 24: Input resistance and reactance, lead-to-lead, Serial #239.

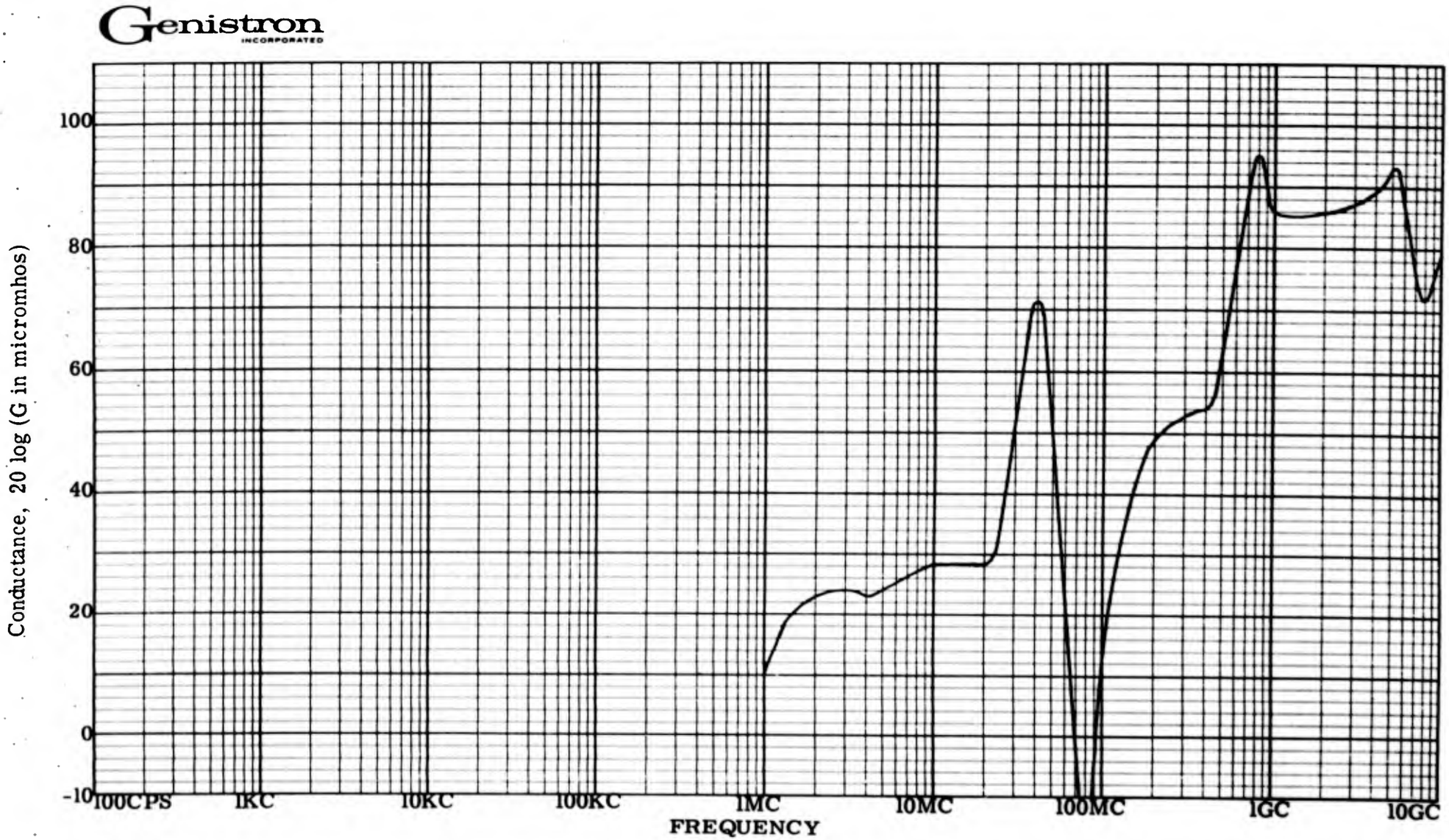

Figure 25: Input conductance, lead-to-lead, Serial #239.

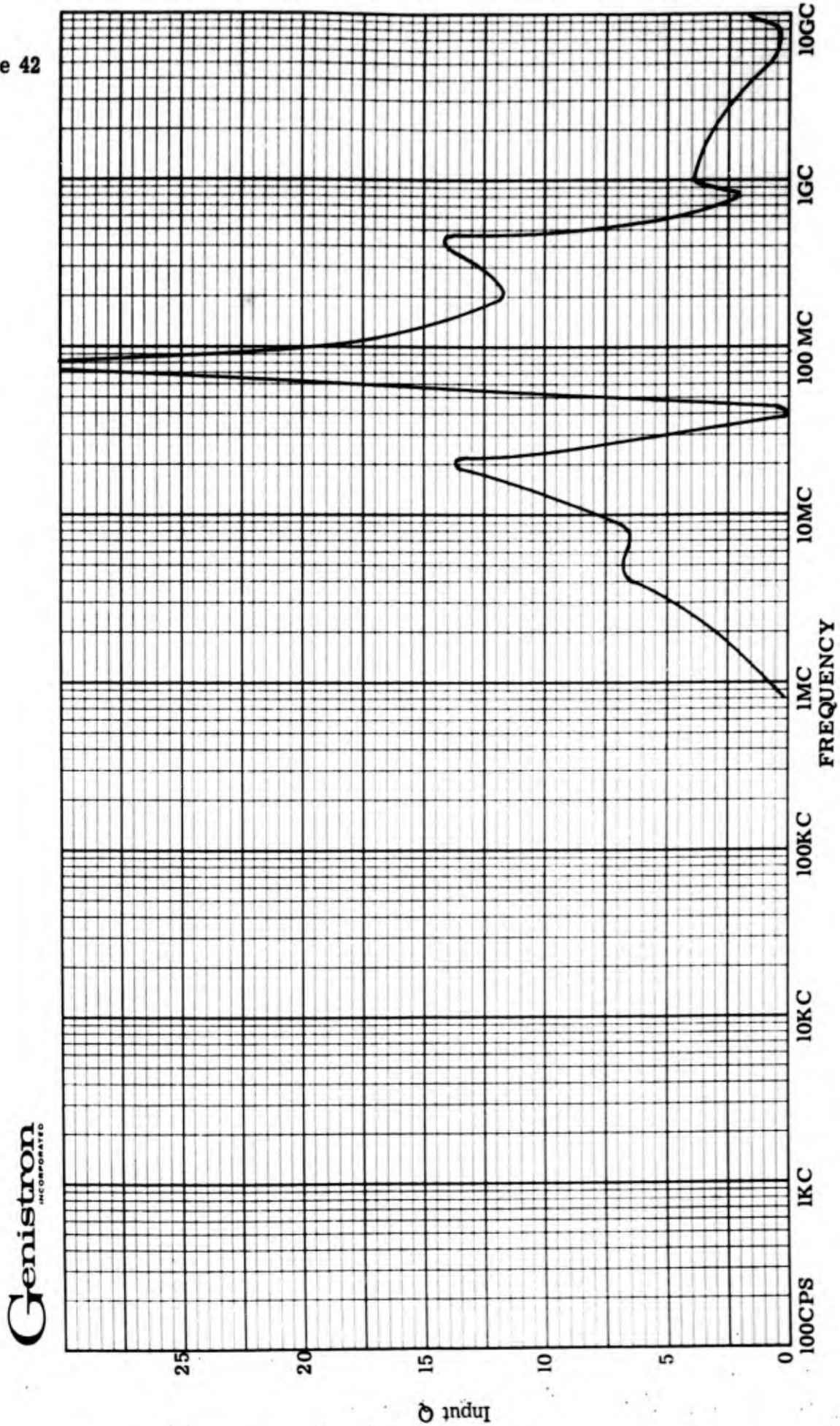

Figure 26: Input Q, lead-to-lead, Serial #239.

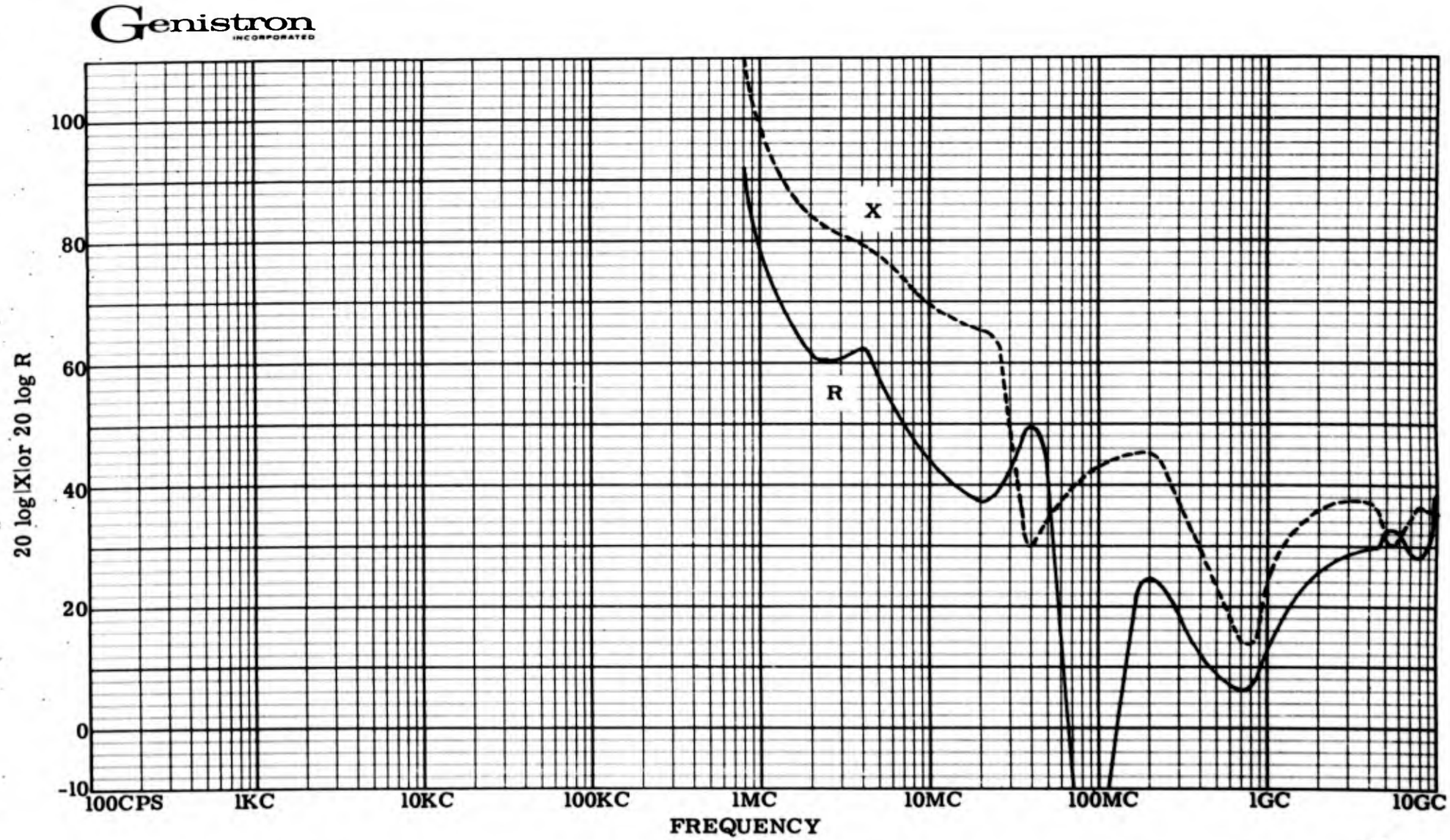

Figure 27: Input resistance and reactance, lead-to-case, Serial #239.

Genistron
INCORPORATED

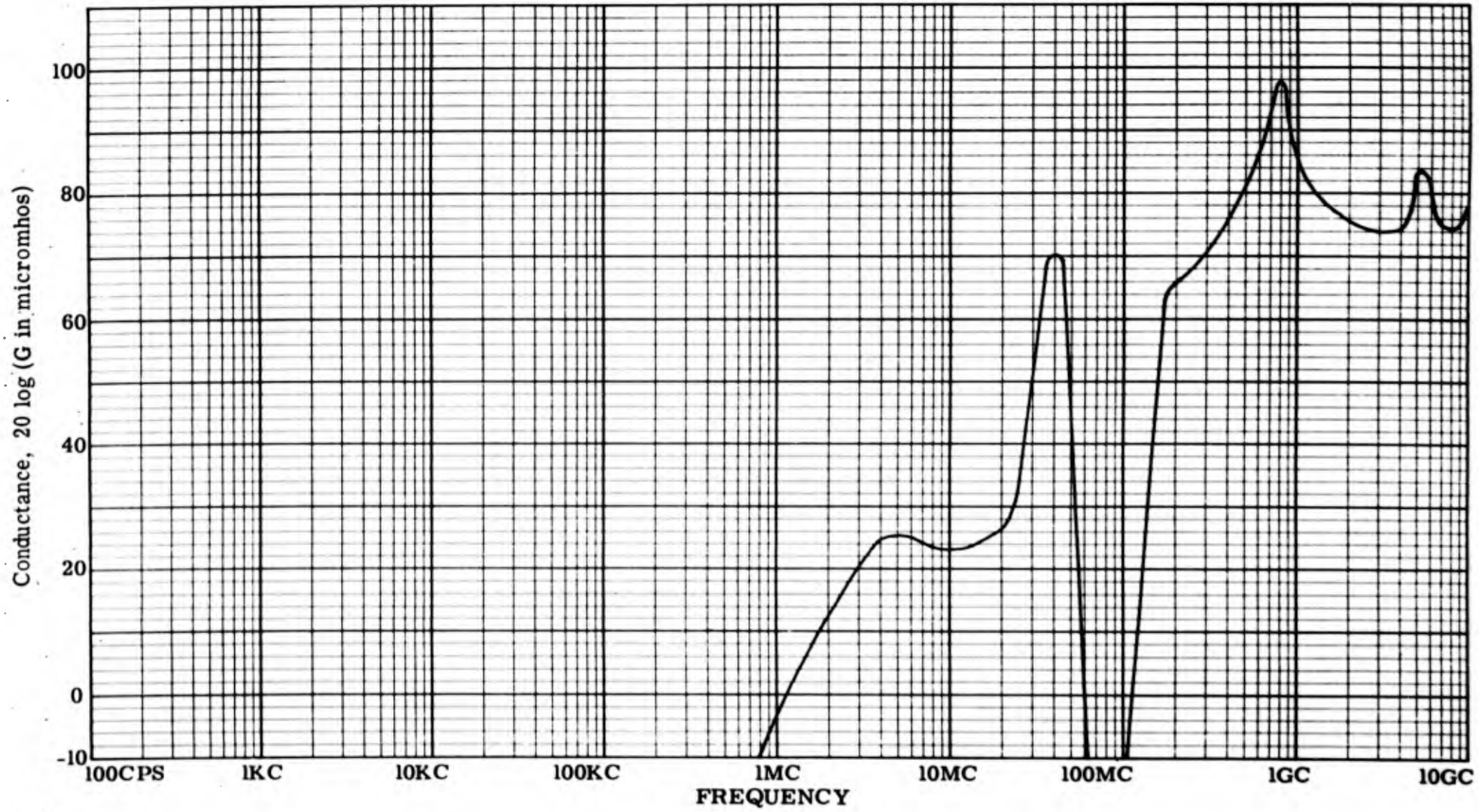

Figure 28: Input conductance, lead-to-case, Serial #239.

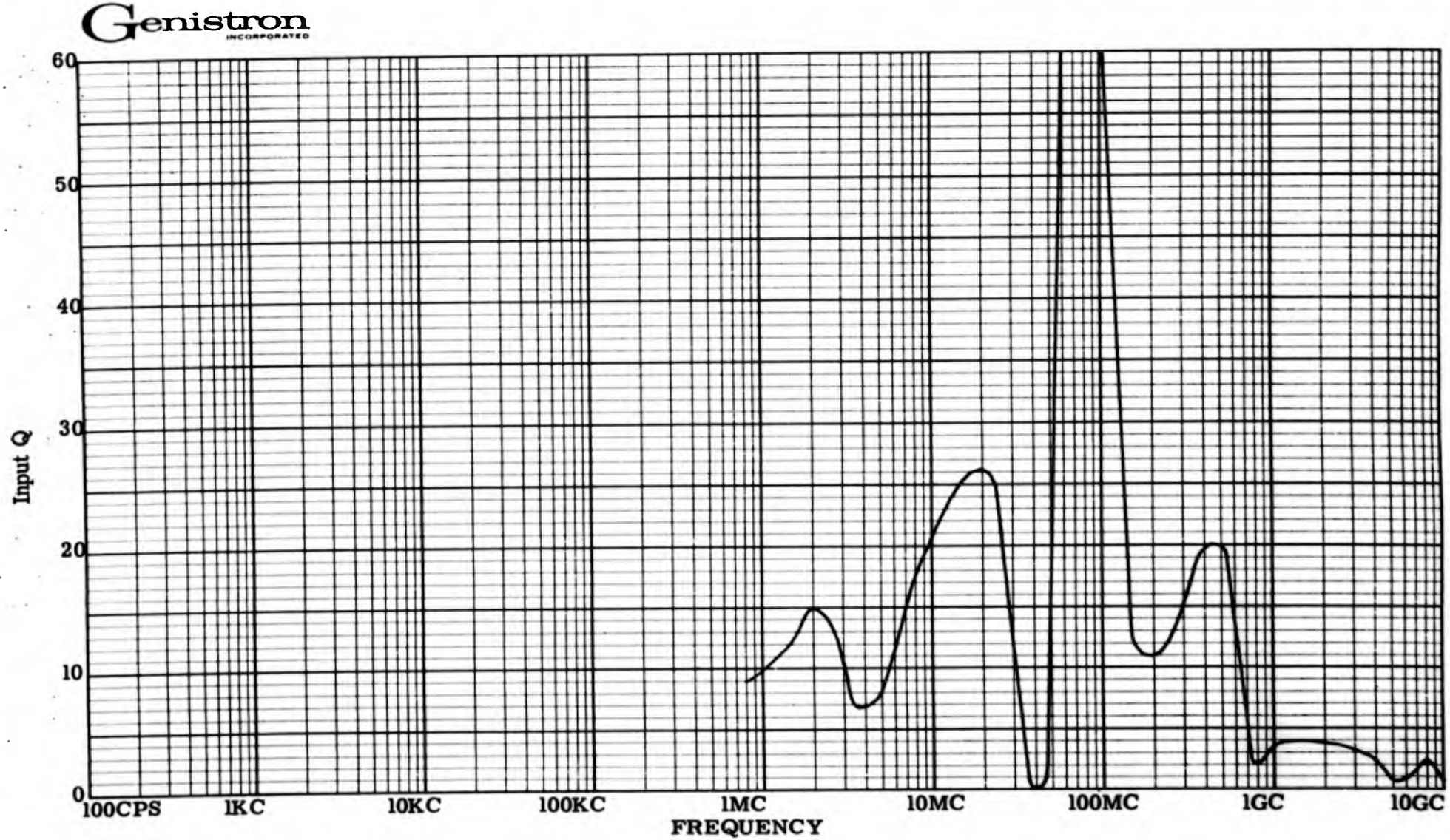

Figure 29: Input Q, lead-to-case, Serial #239.

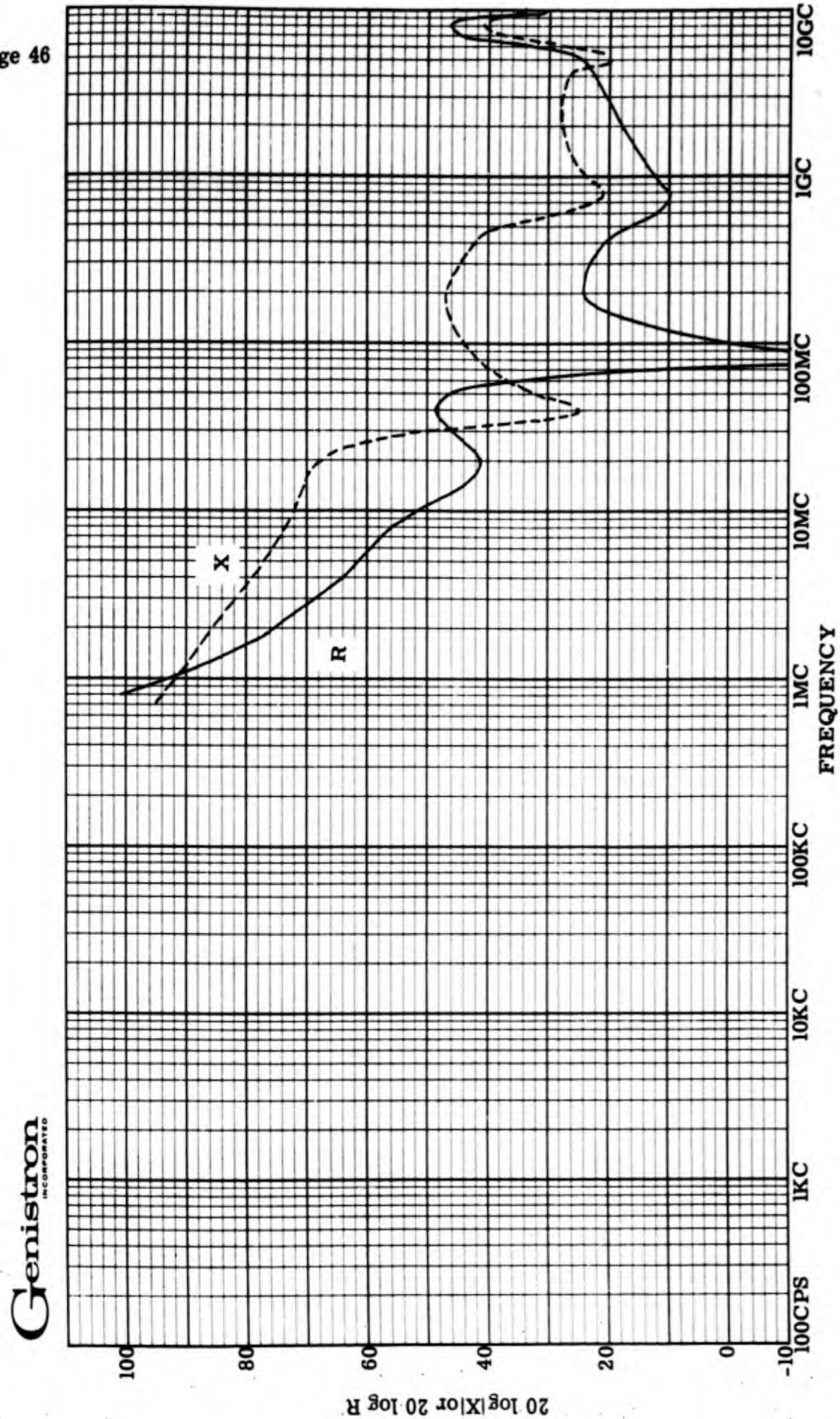

Figure 30: Input resistance and reactance, lead-to-lead, Serial #246.

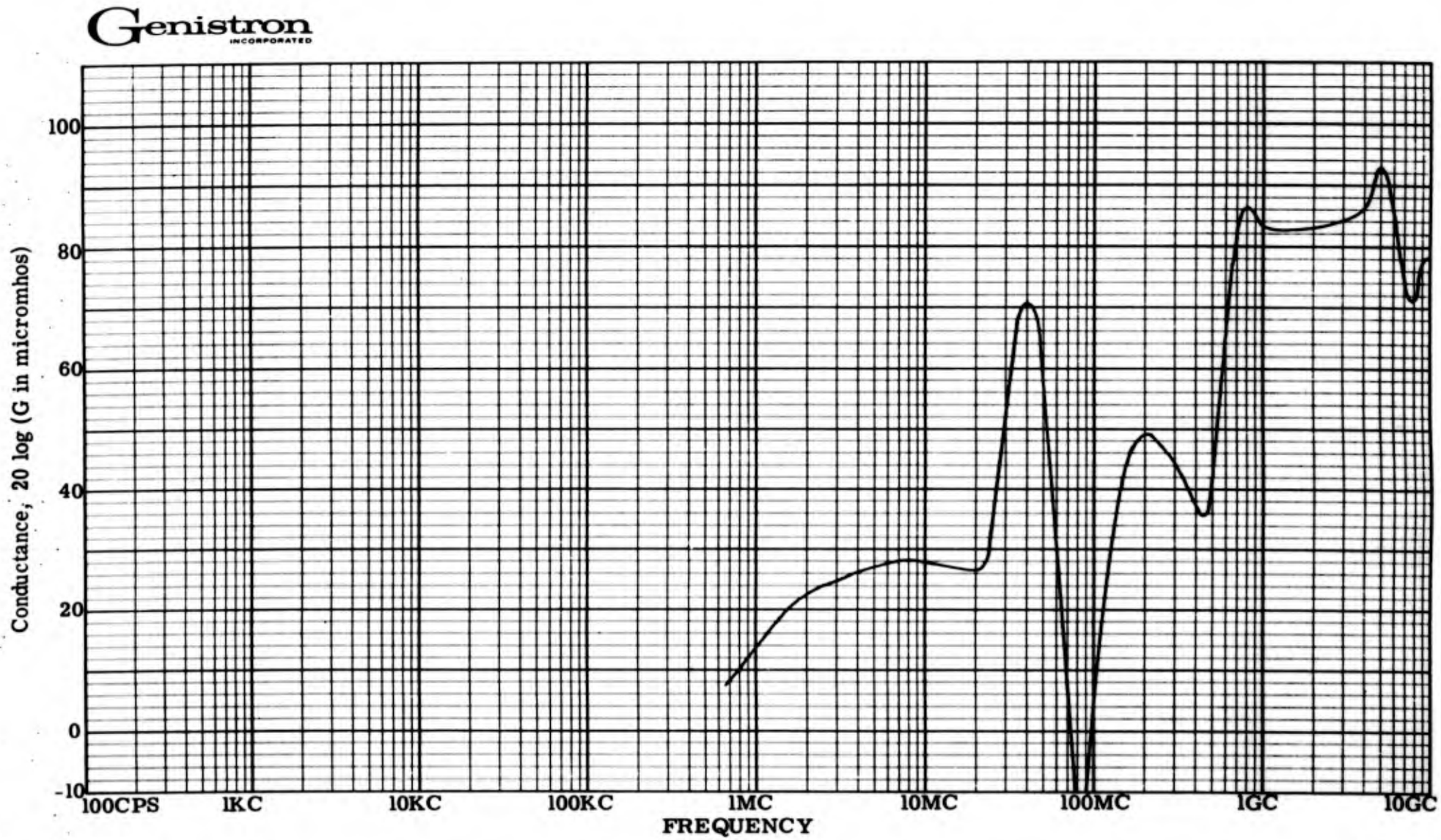

Figure 31: Input conductance, lead-to-lead, Serial #246.

Genistron INCORPORATED

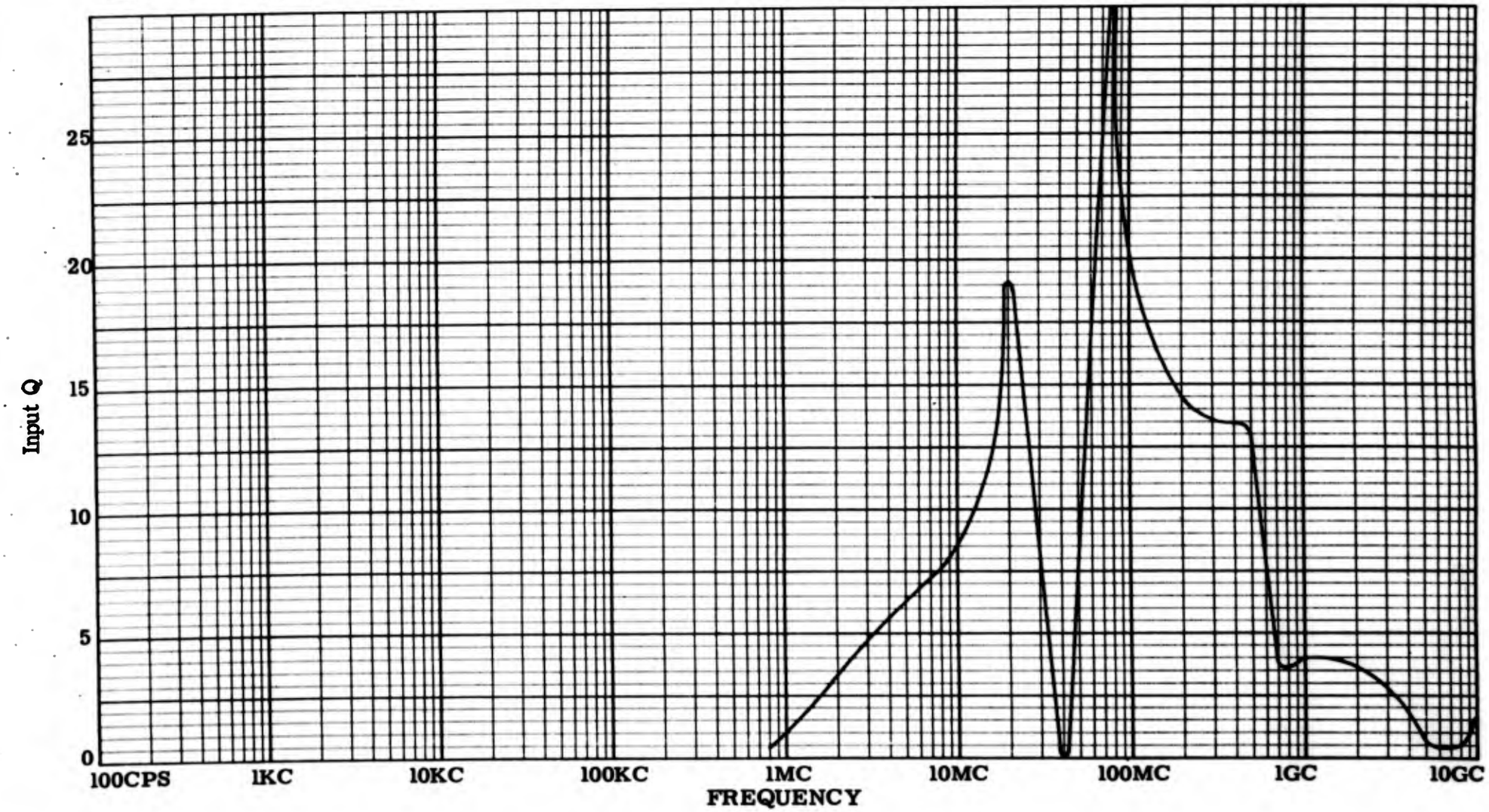

Figure 32: Input Q, lead-to-lead, Serial #246.

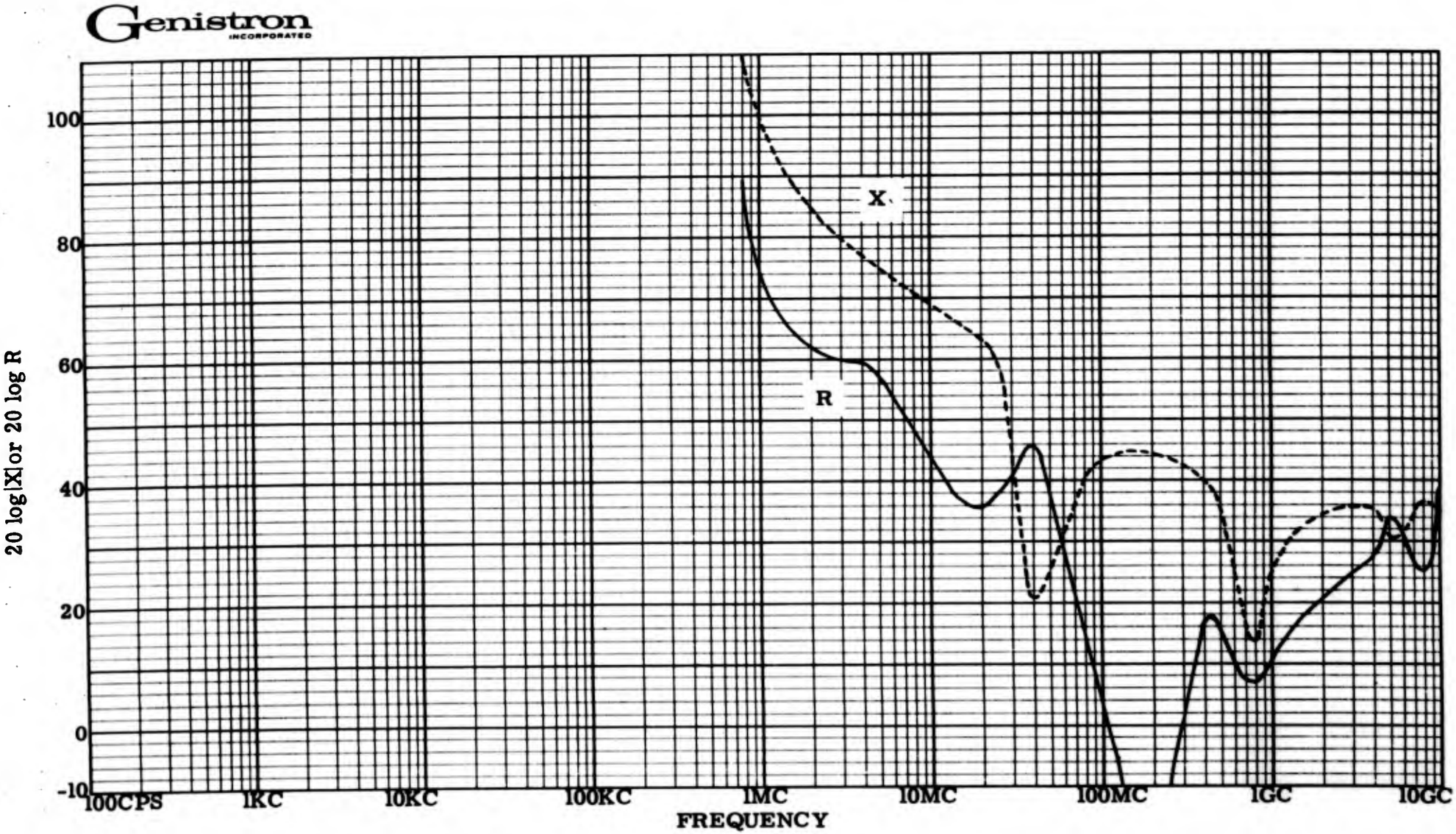

Figure 33: Input resistance and reactance, lead-to-case, Serial #246.

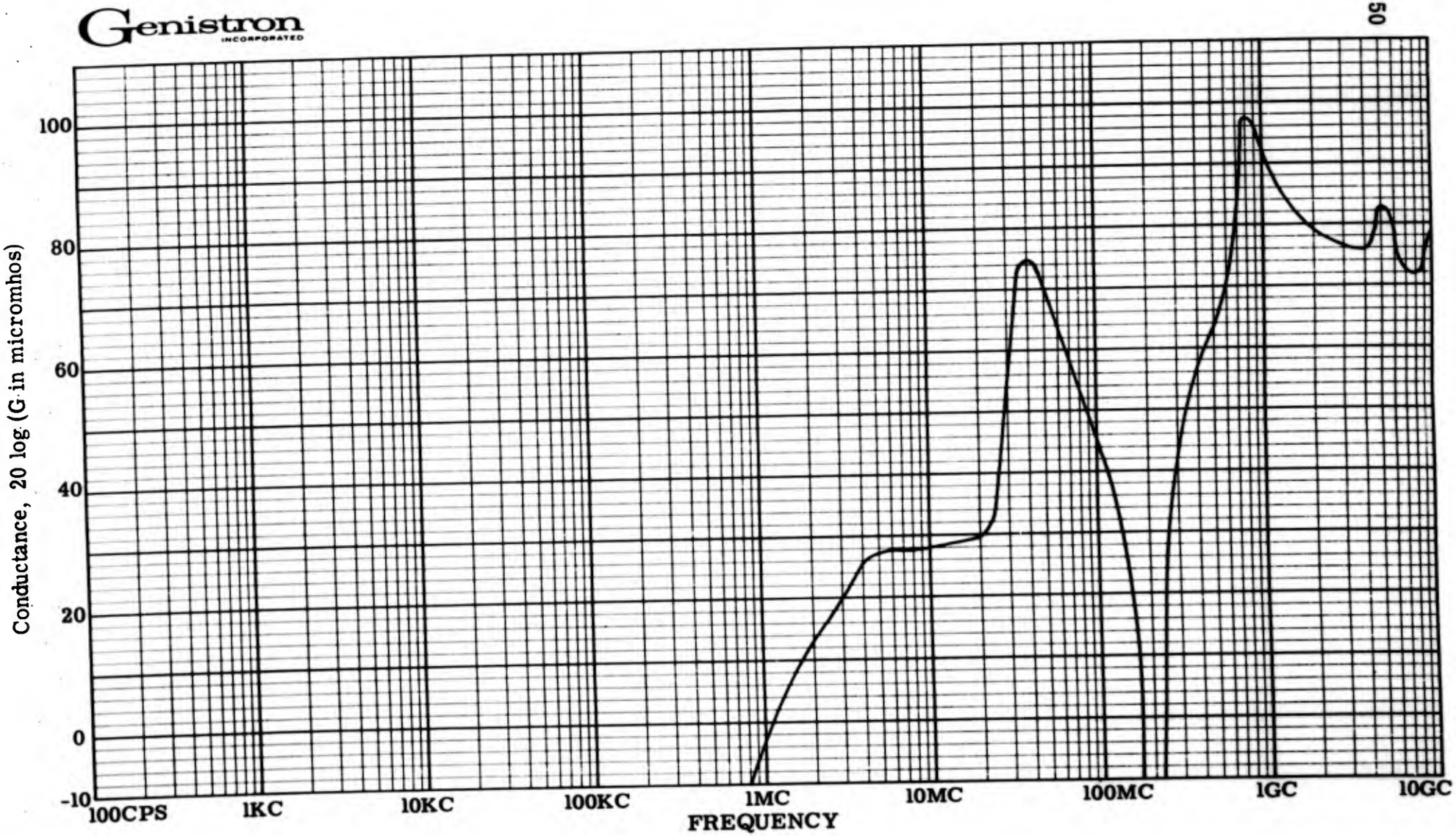

Figure 34: Input conductance, lead-to-case, Serial #246.

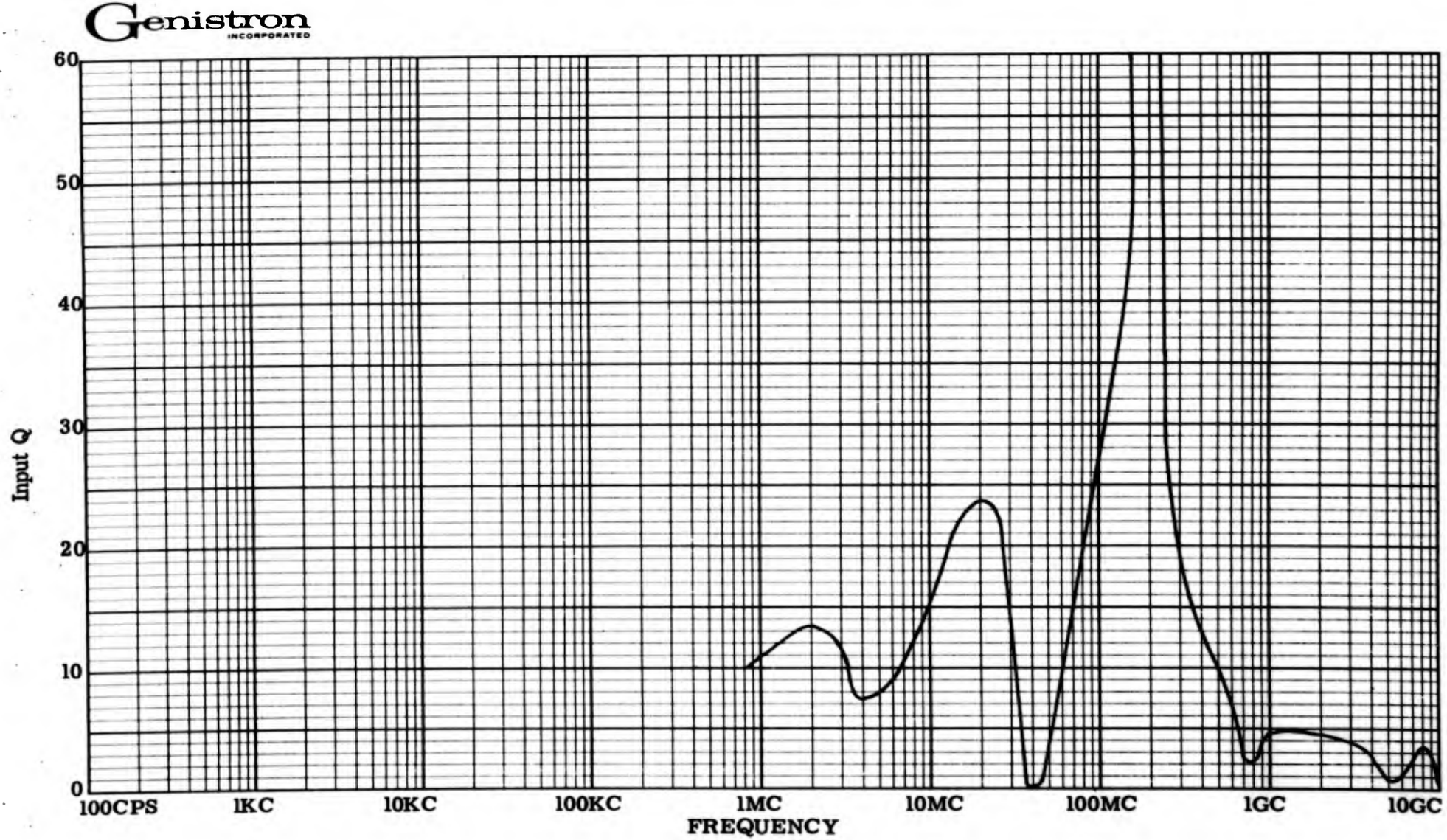

Figure 35: Input Q, lead-to-case, Serial #246.

Genistron
INCORPORATED

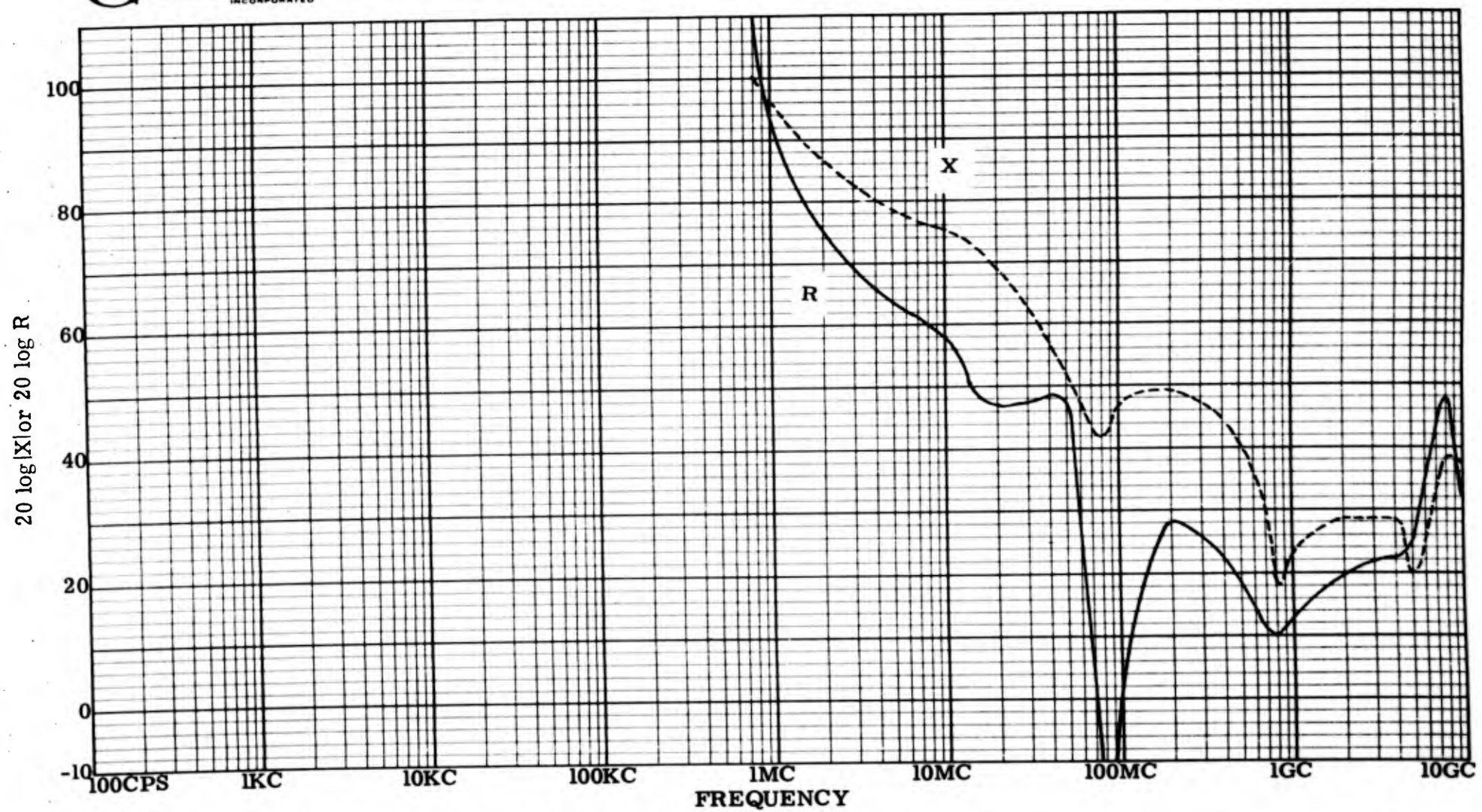

Figure 36: Input resistance and reactance, lead-to-lead, Serial #247.

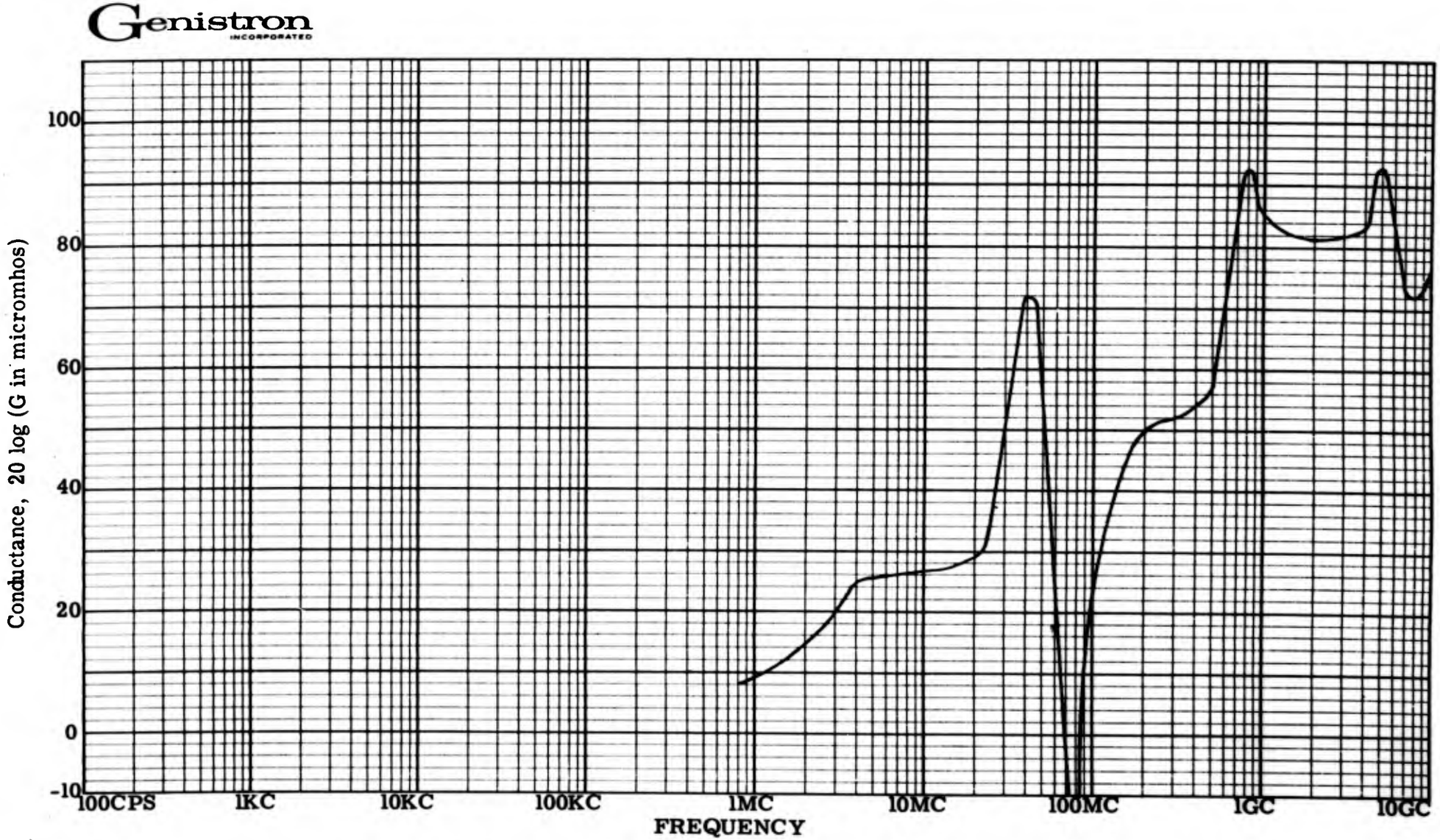

Figure 37: Input conductance, lead-to-lead, Serial #247.

Genistron INCORPORATED

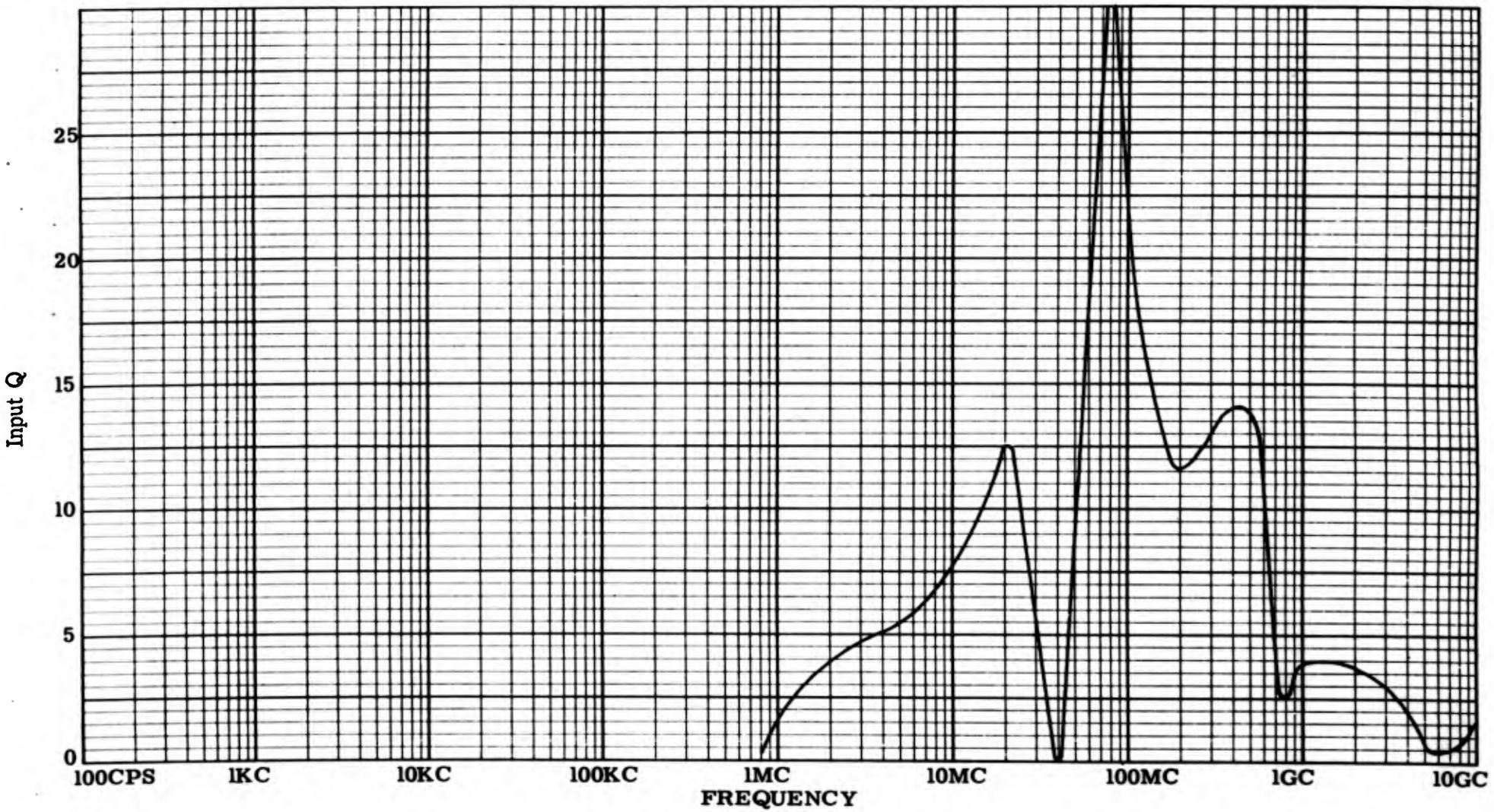

Figure 38: Input Q, lead-to-lead, Serial #247.

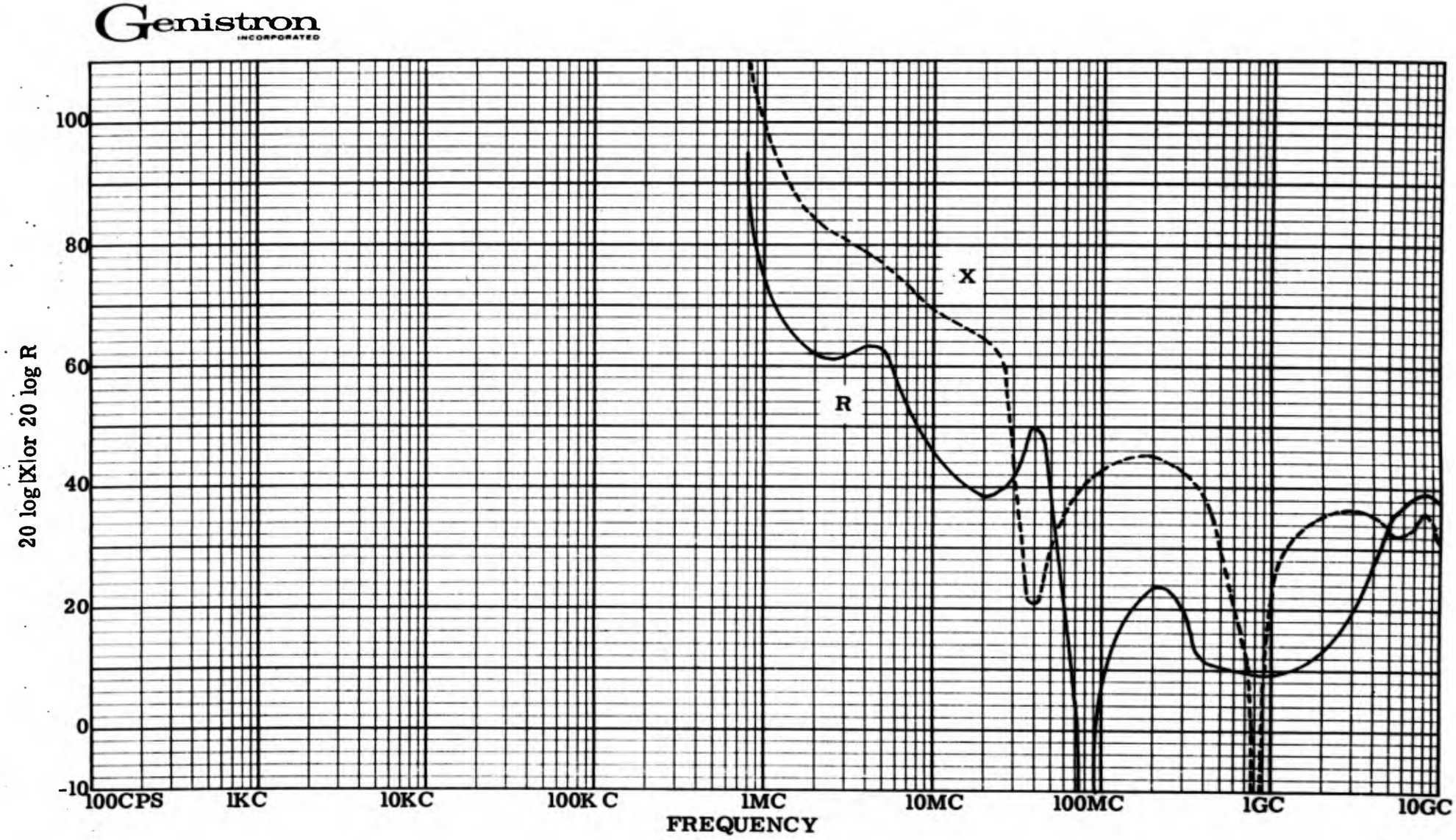

Figure 39: Input resistance and reactance, lead-to-case, Serial #247.

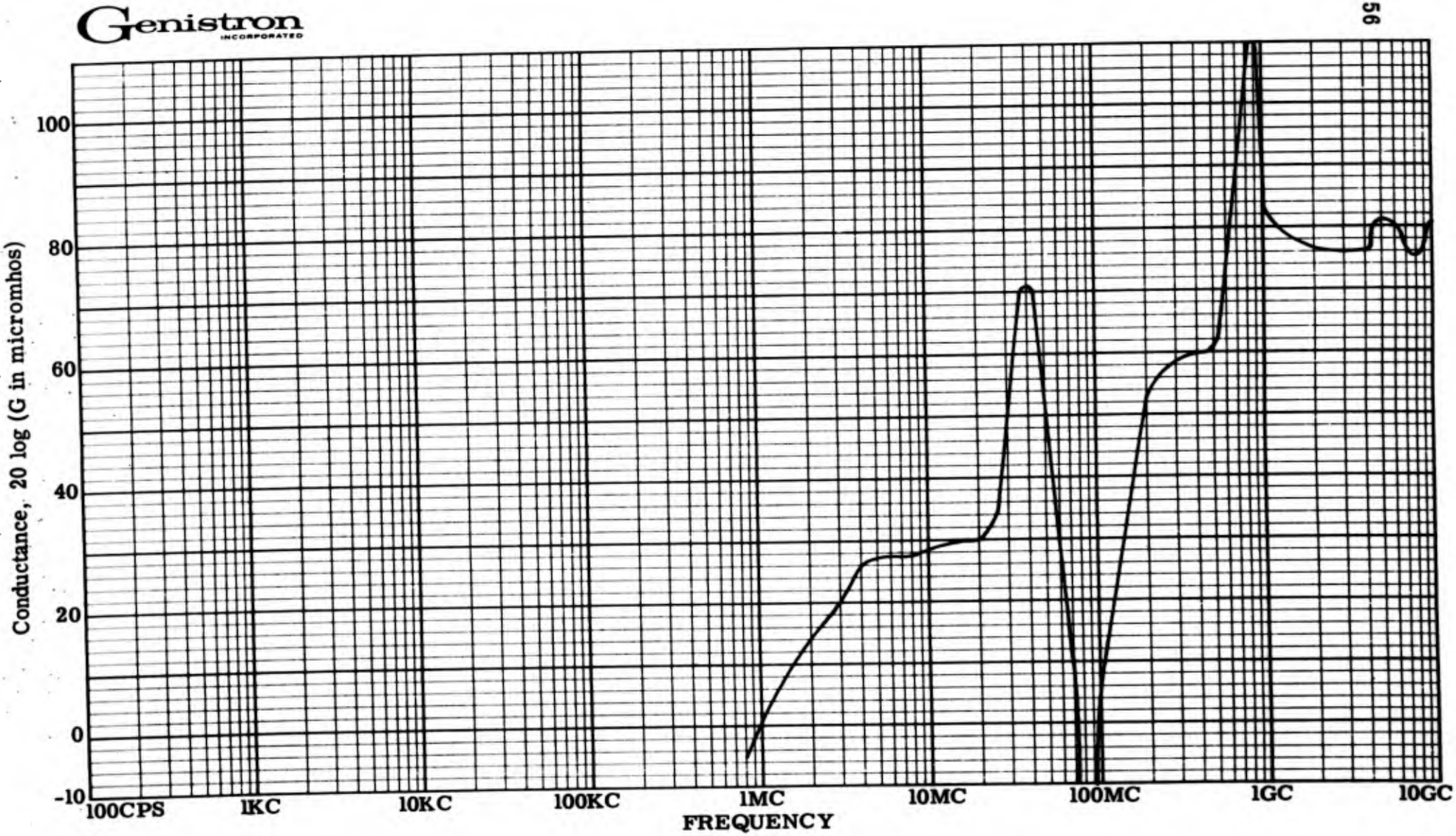

Figure 40: Input conductance, lead-to-case, Serial #247.

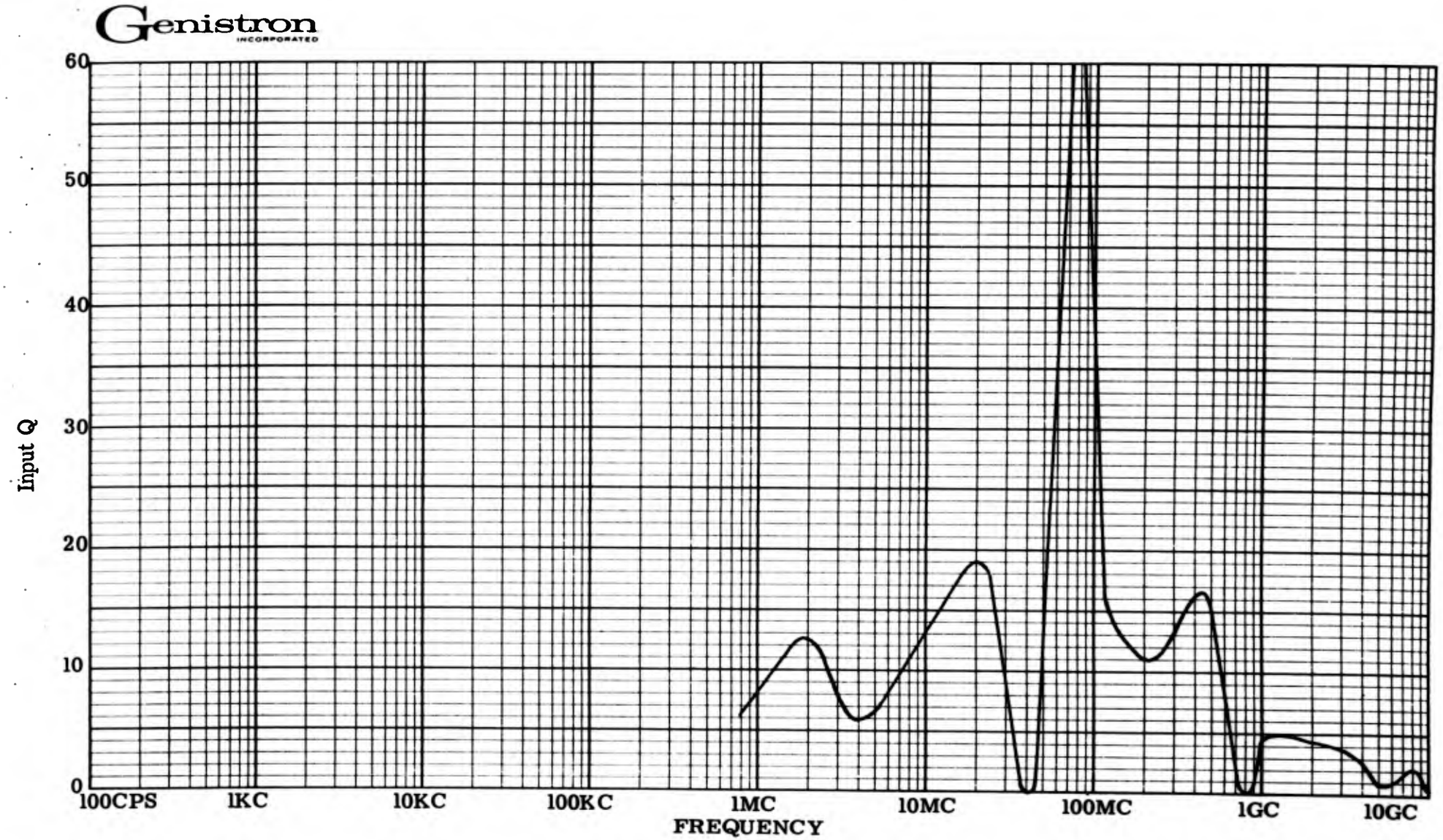

Figure 41: Input Q, lead-to-case, Serial #247.

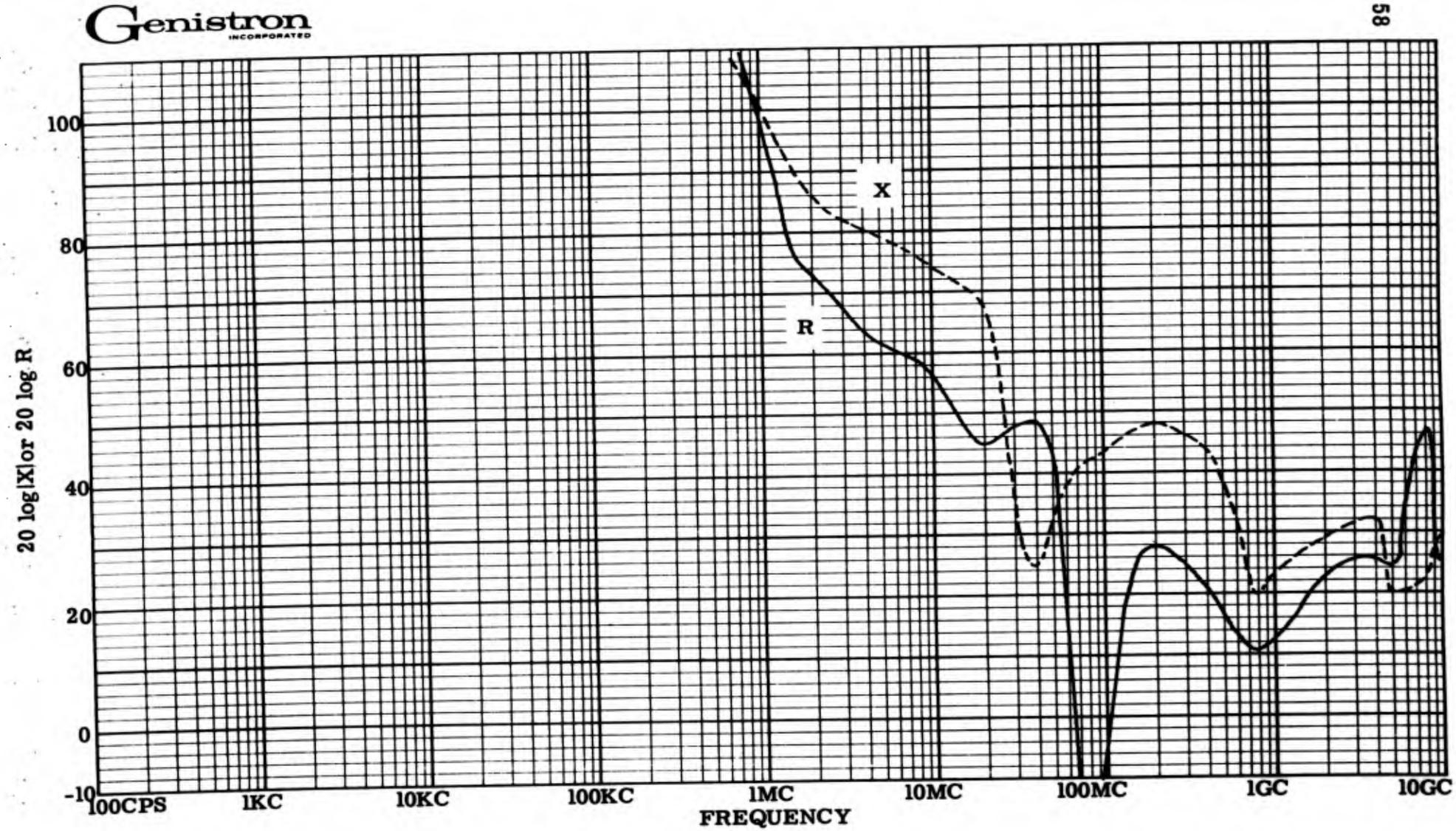

Figure 42: Input resistance and reactance, lead-to-lead, Serial #248.

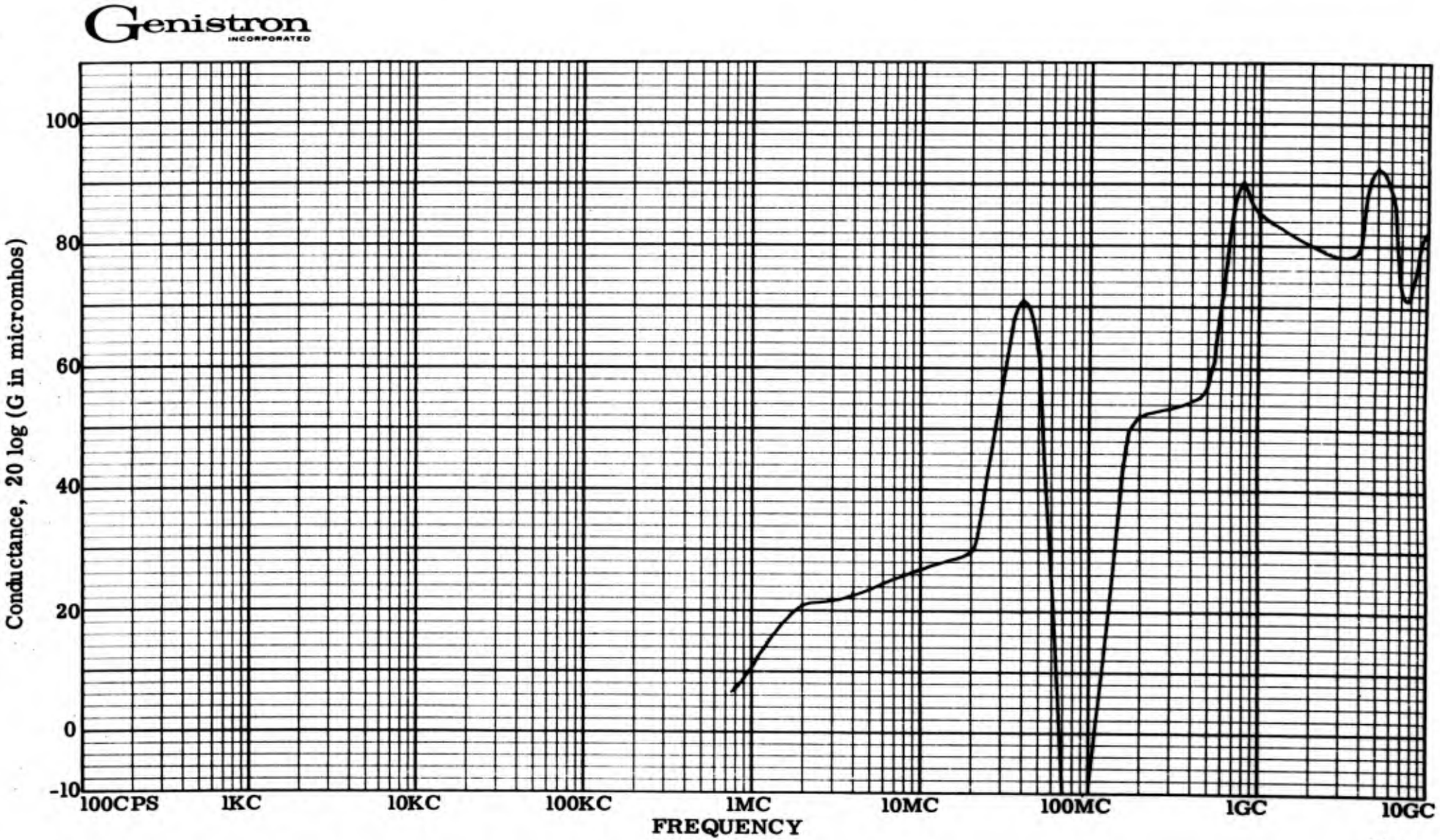

Figure 43: Input conductance, lead-to-lead, Serial #248.

Genistron
INCORPORATED

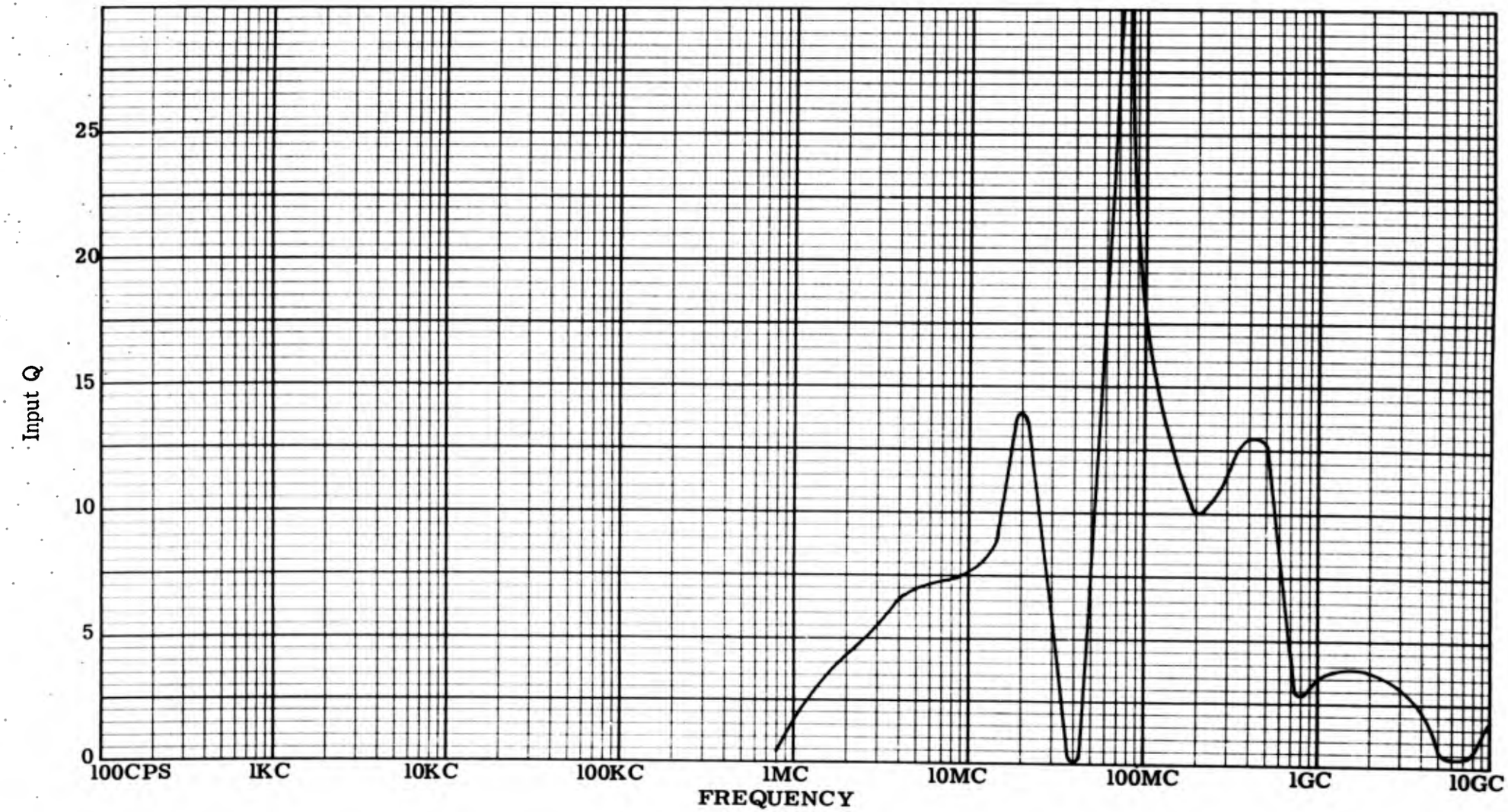

Figure 44: Input Q, lead-to-lead, Serial #248.

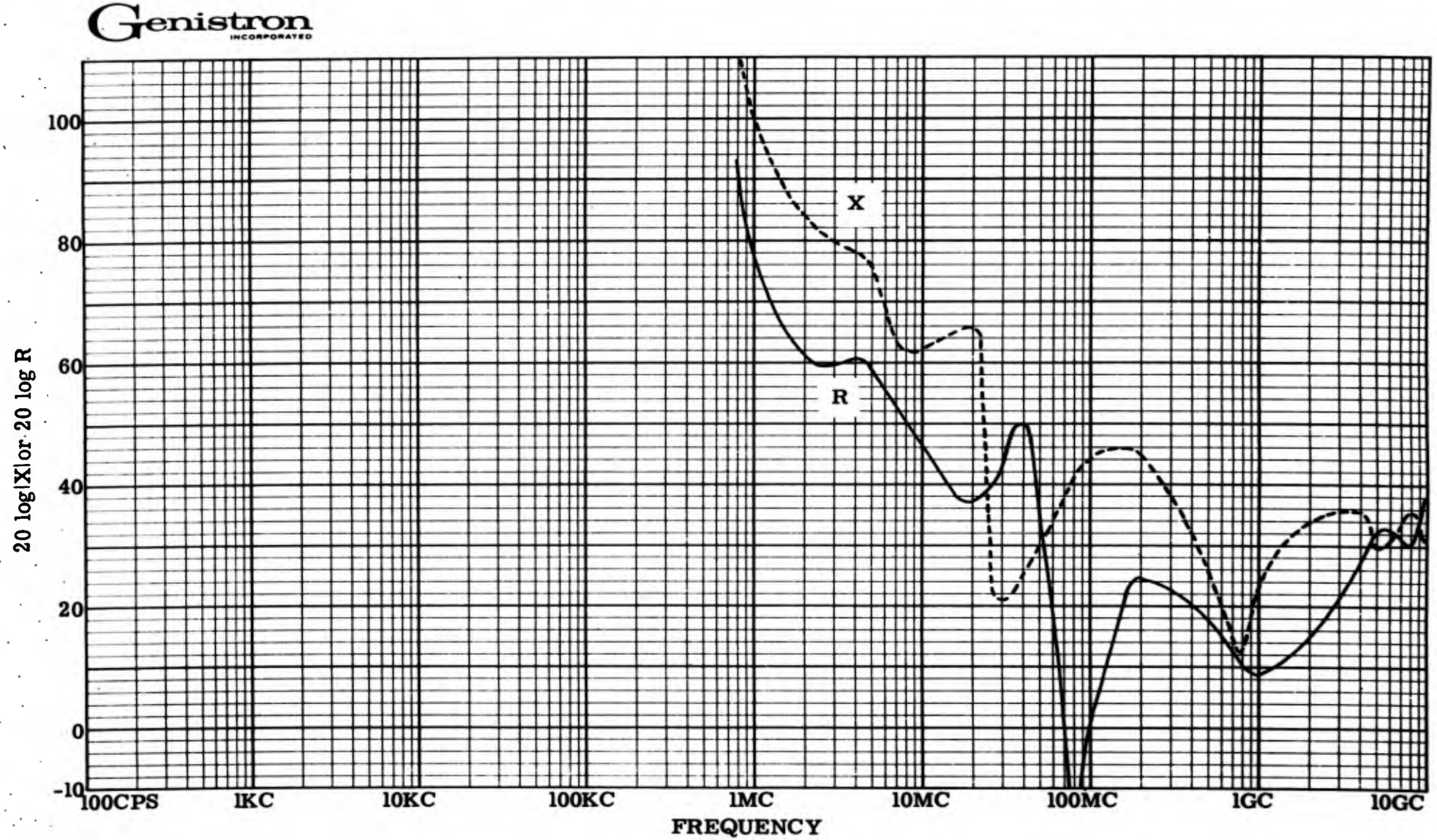

Figure 45: Input resistance and reactance, lead-to-case, Serial #248.

Genistron INCORPORATED

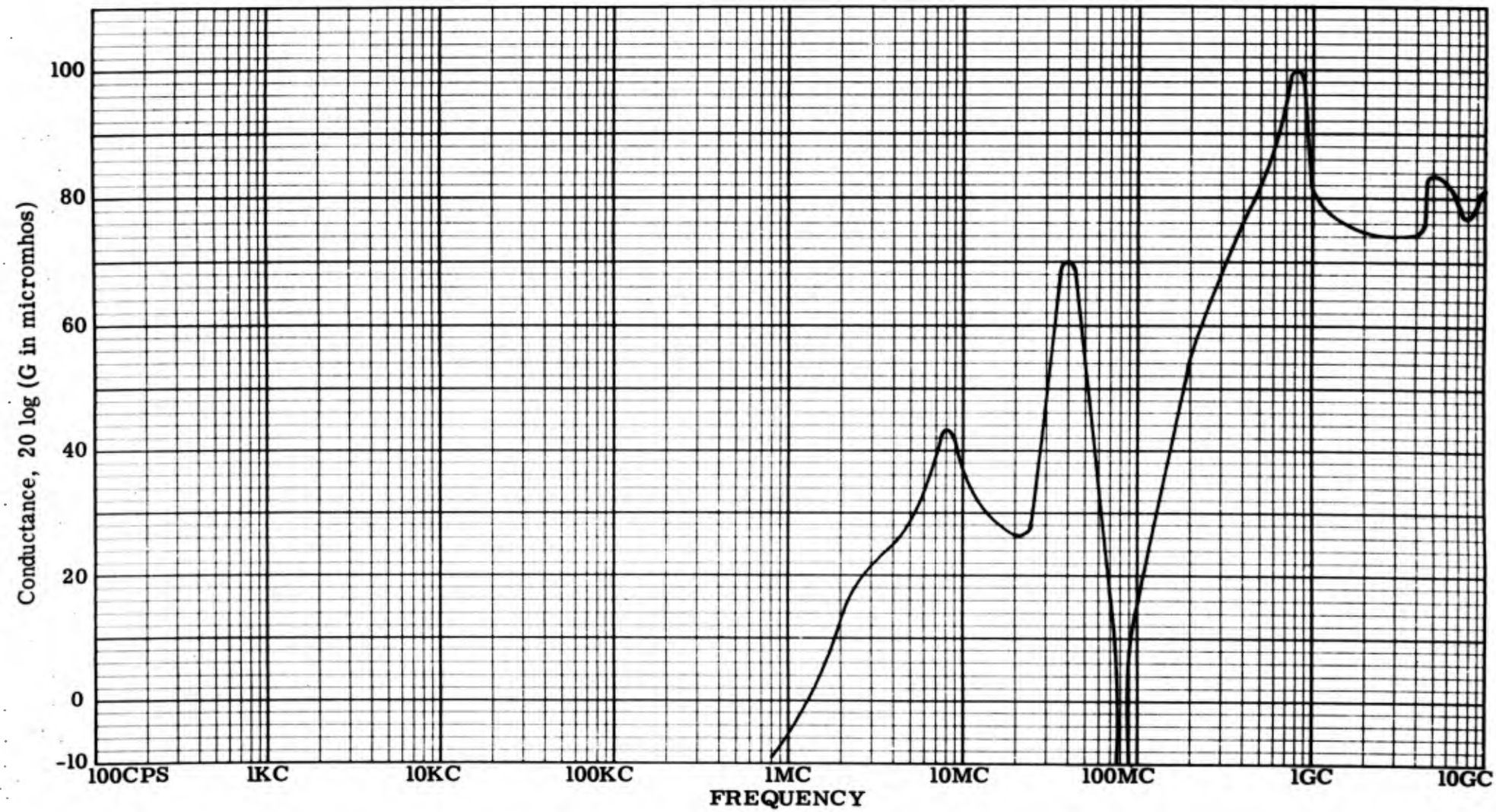

Figure 46: Input conductance, lead-to-case, Serial #248.

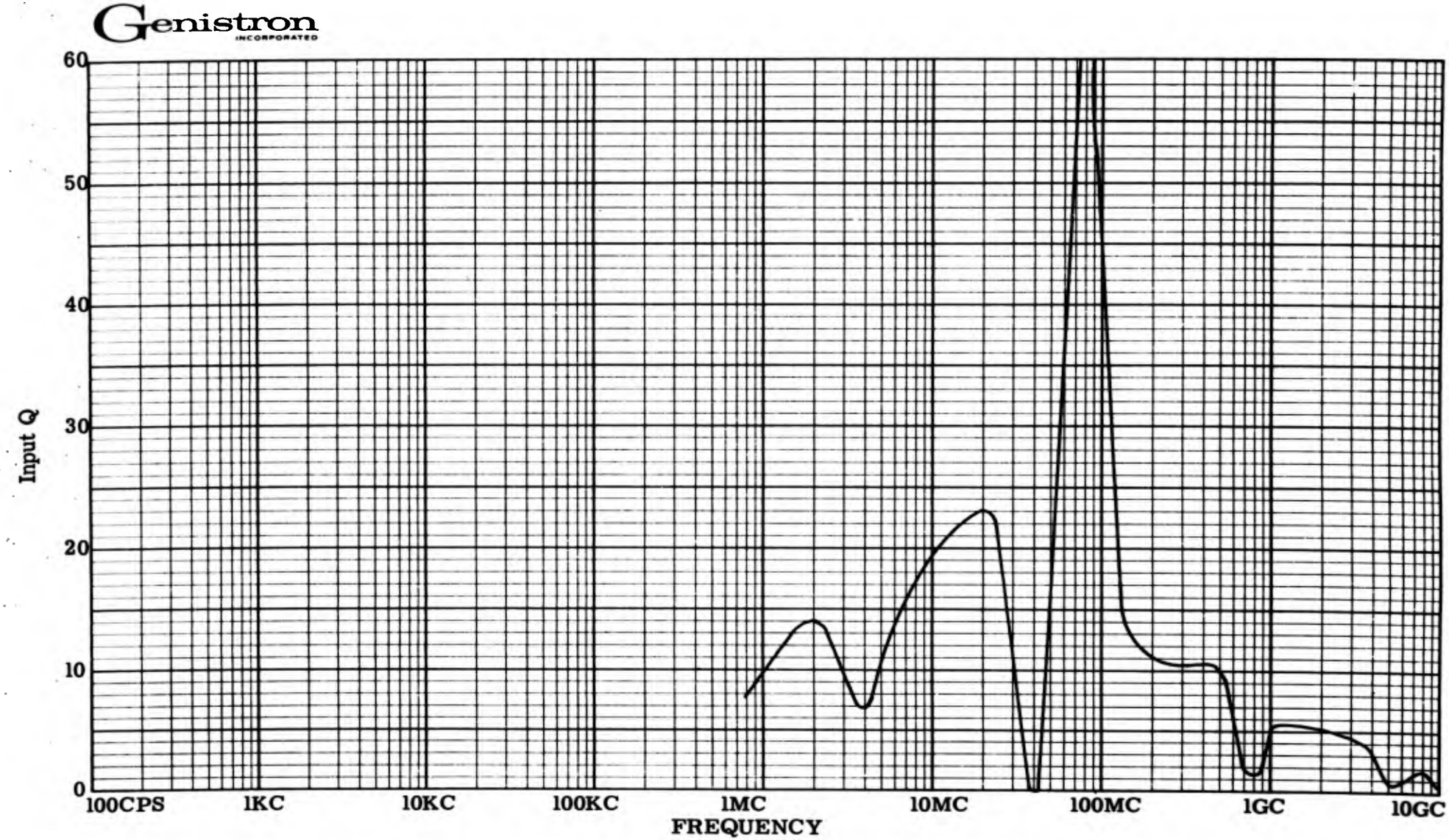

Figure 47: Input Q, lead-to-case, Serial #248.

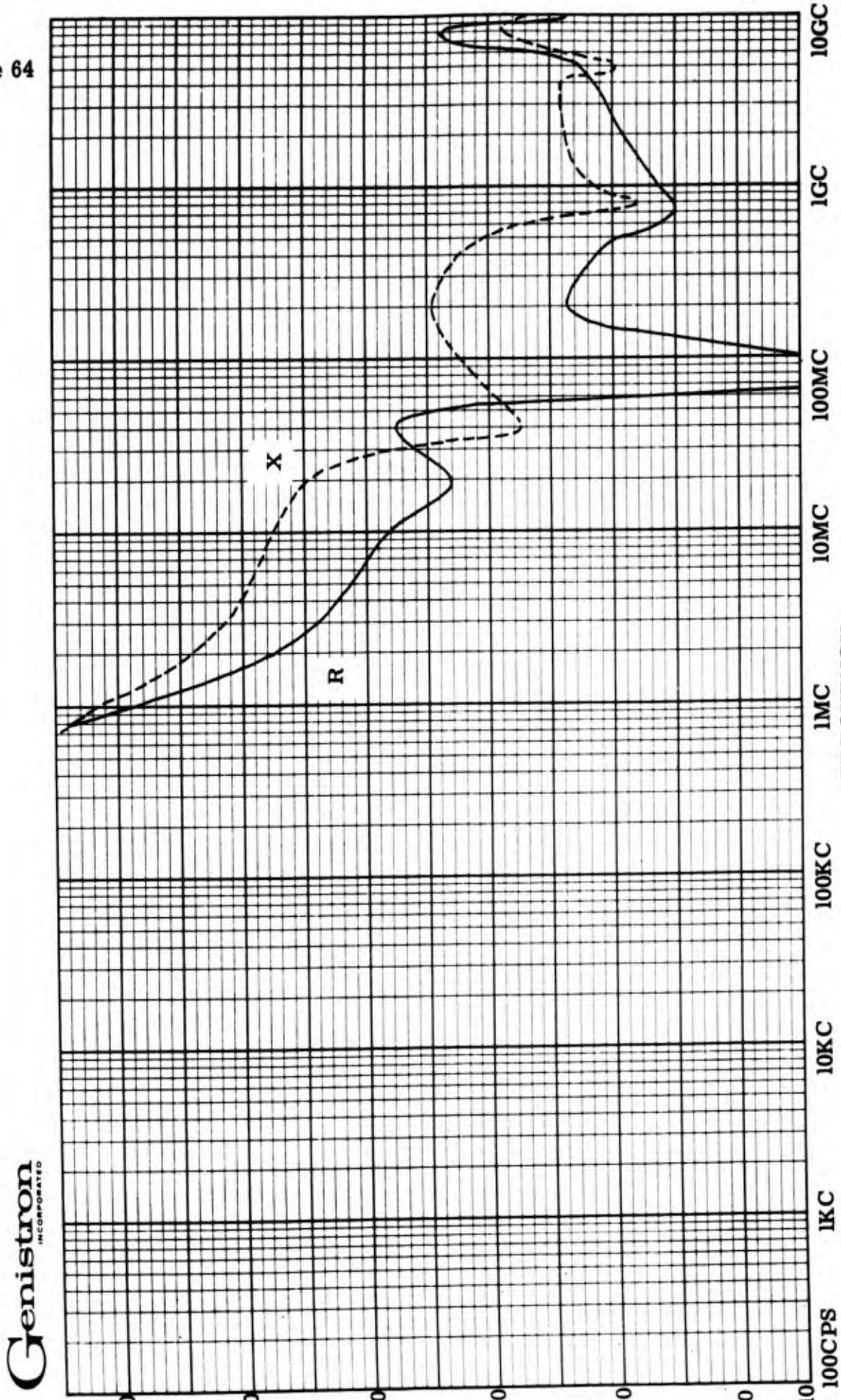

Figure 48: Input resistance and reactance, lead-to-lead, Serial #260.

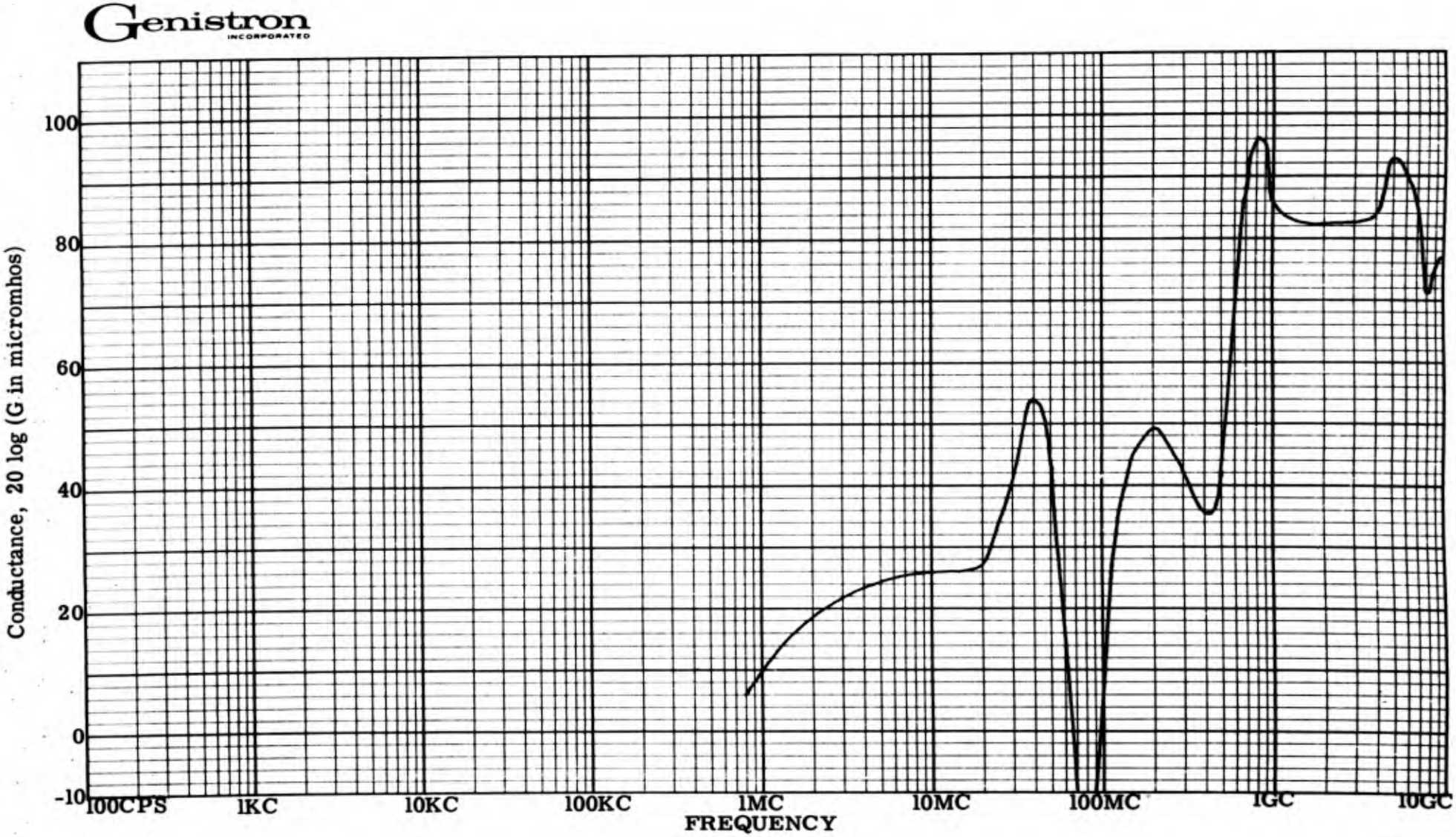

Figure 49: Input conductance, lead-to-lead, Serial #260.

Genistron INCORPORATED

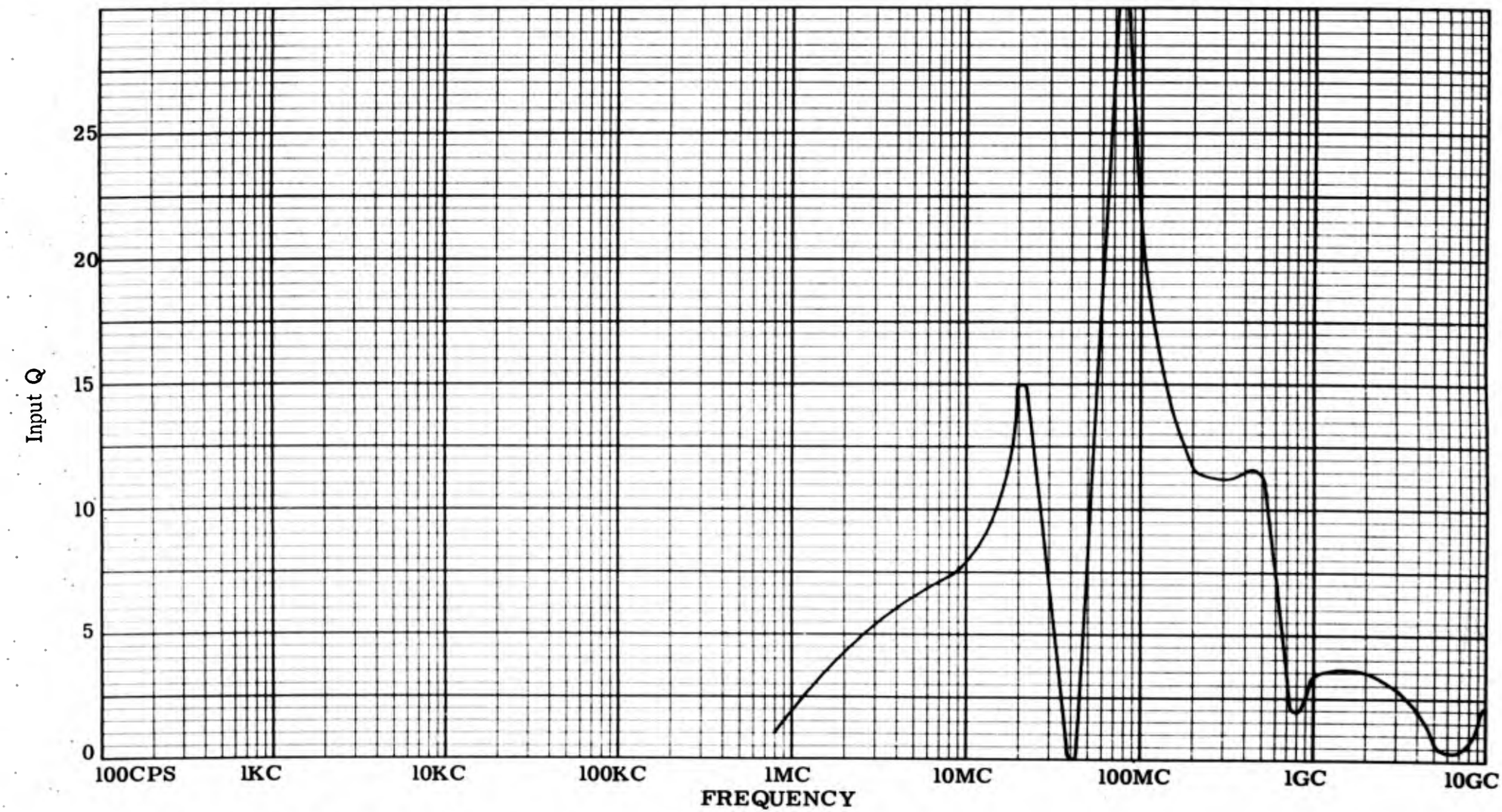

Figure 50: Input Q lead-to-lead, Serial #260.

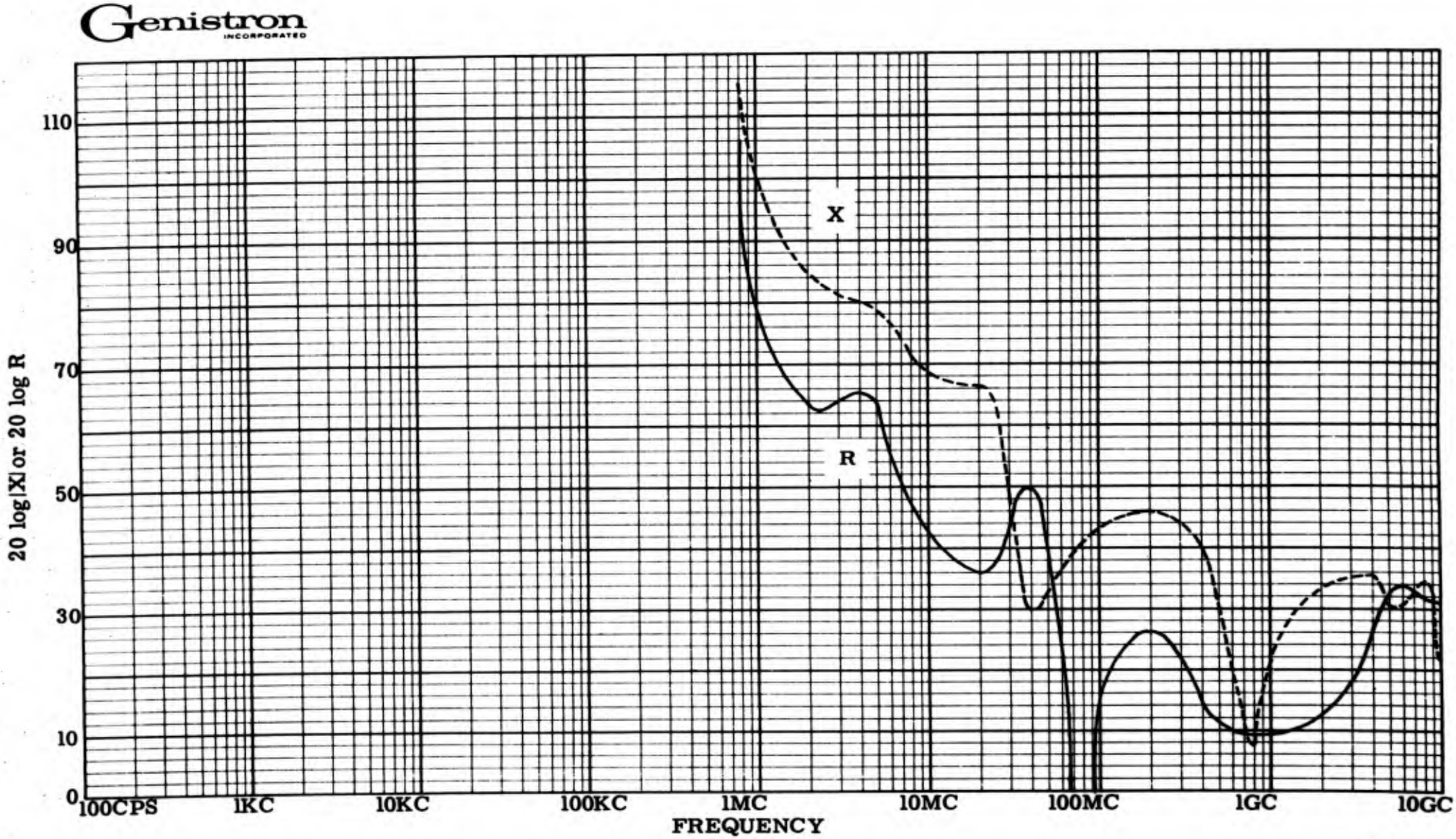

Figure 51: Input resistance and reactance, lead-to-case, Serial #260.

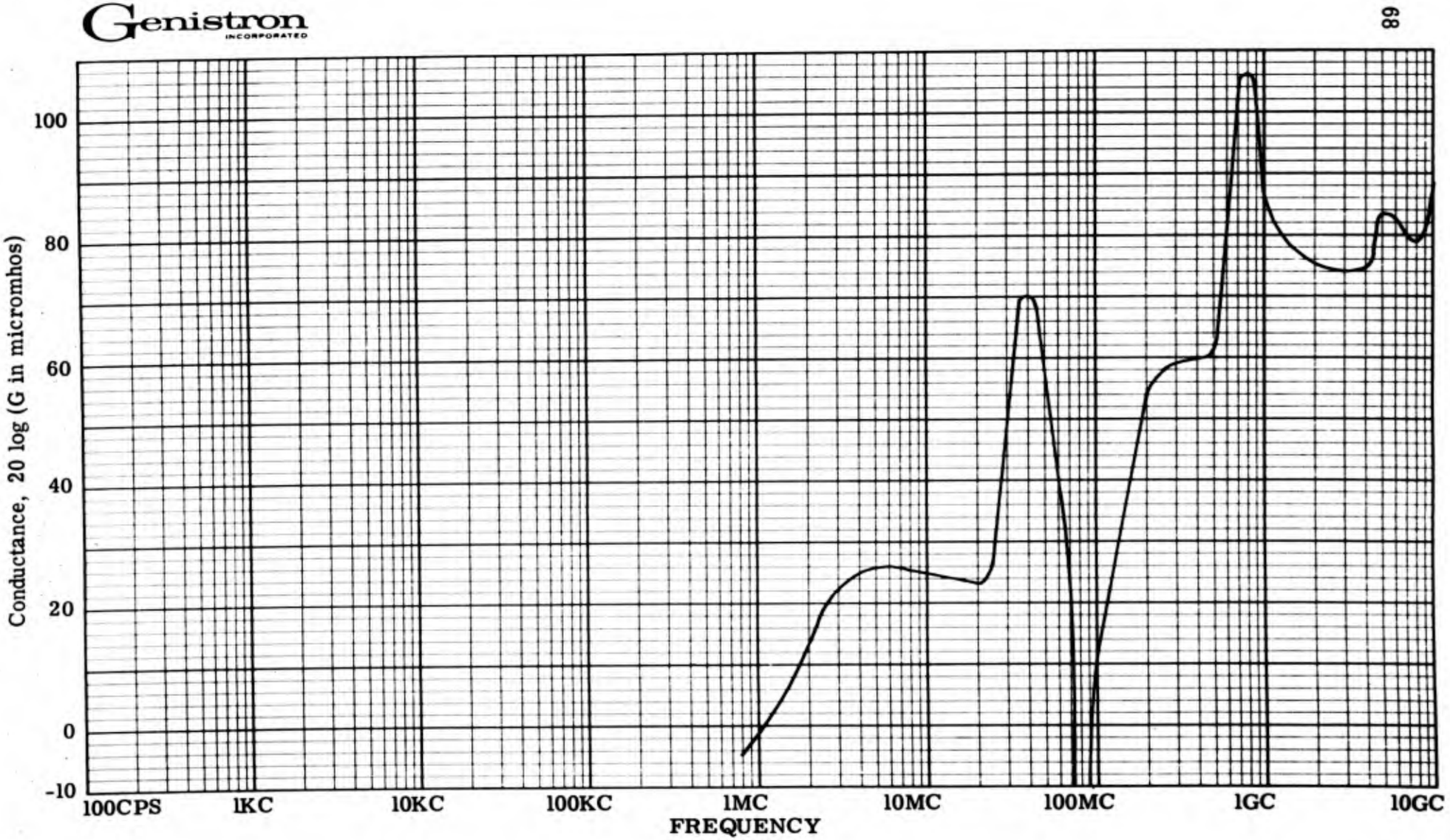

Figure 52: Input conductance, lead-to-case, Serial #260.

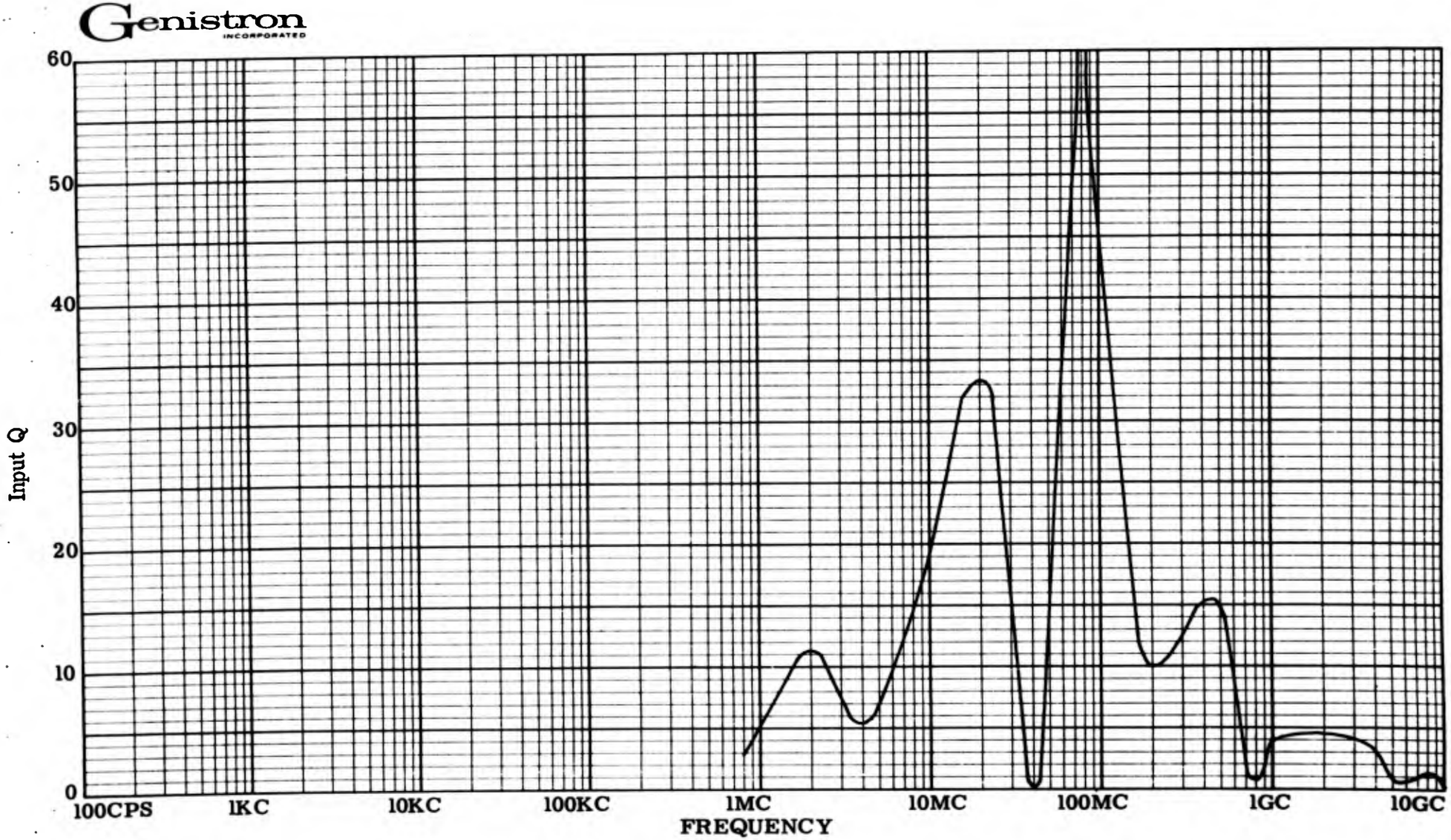

Figure 53: Input Q, lead-to-case, Serial #260.

Genistron
INCORPORATED

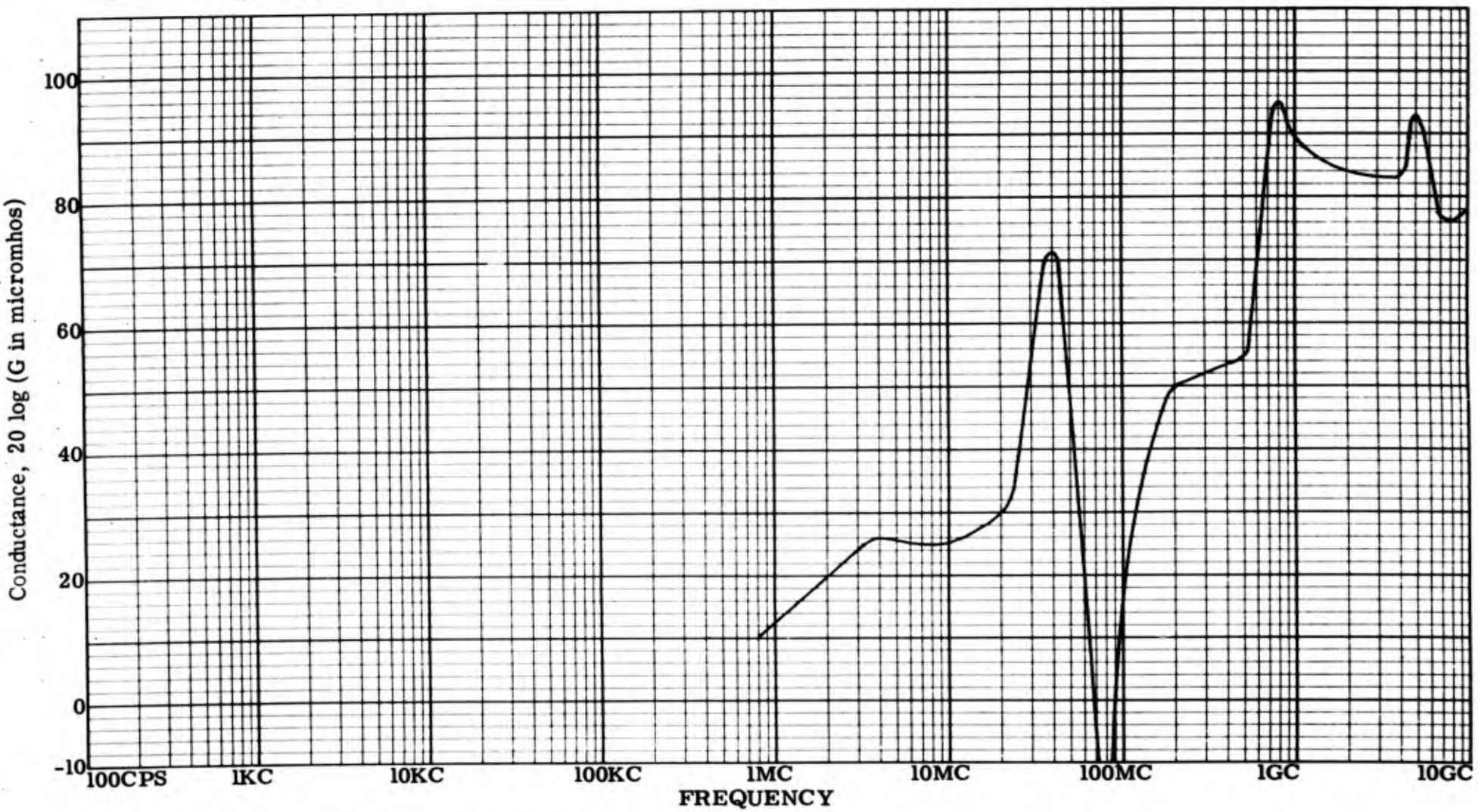

Figure 54: Input conductance, lead-to-lead, Serial #261.

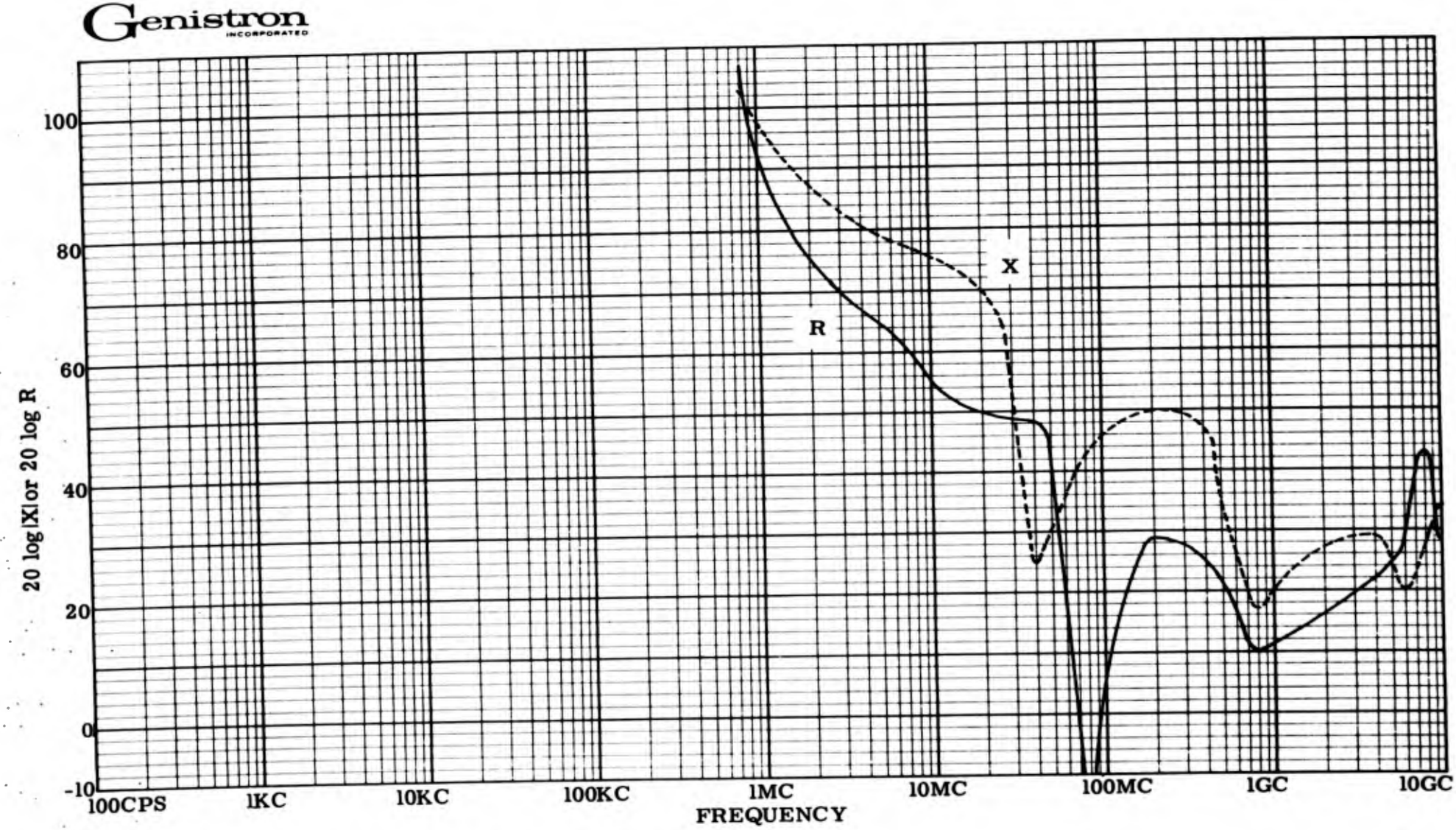

Figure 55: Input resistance and reactance, lead-to-lead, Serial #261.

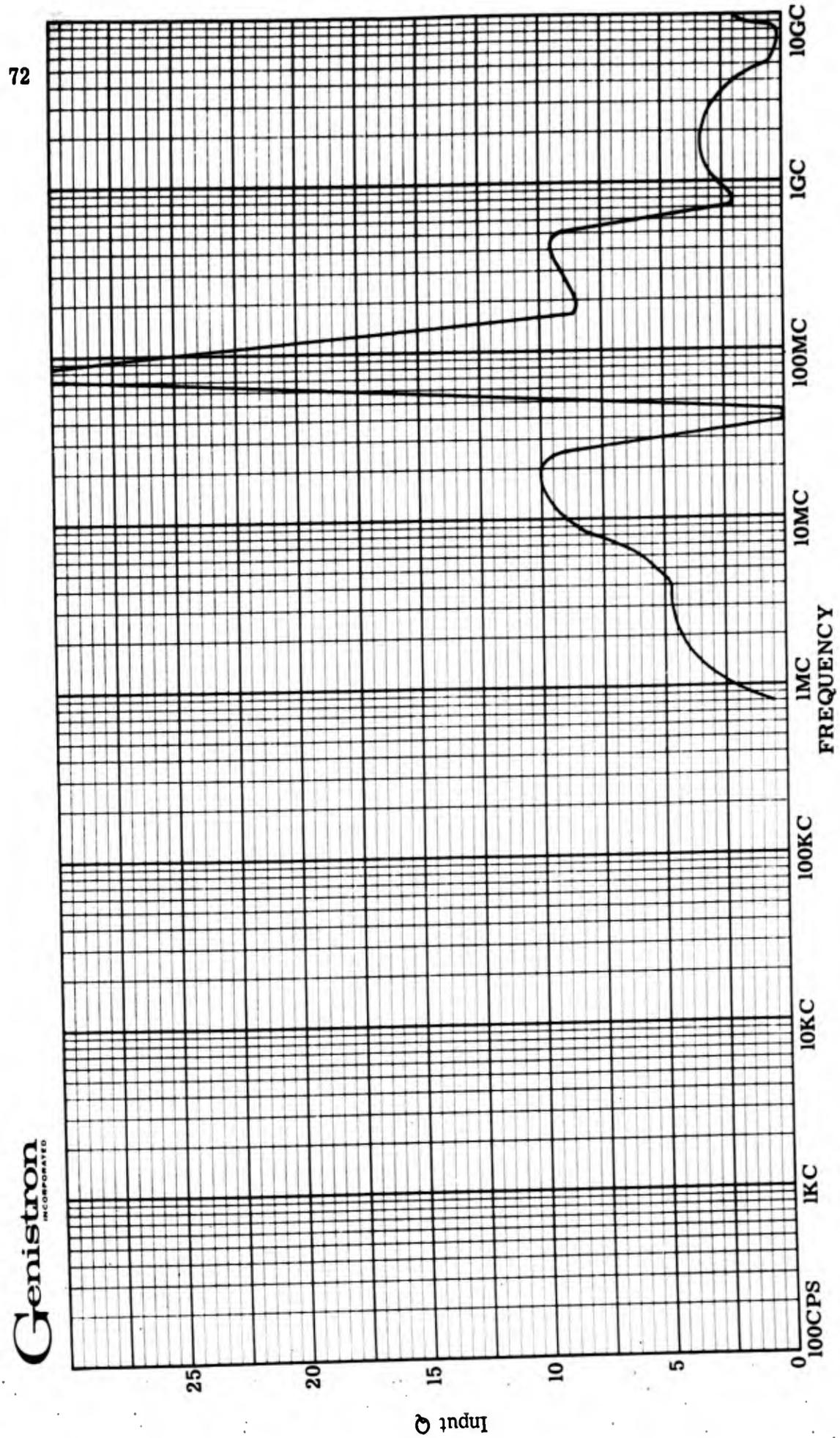

Figure 56: Input Q, lead-to-lead, Serial #261.

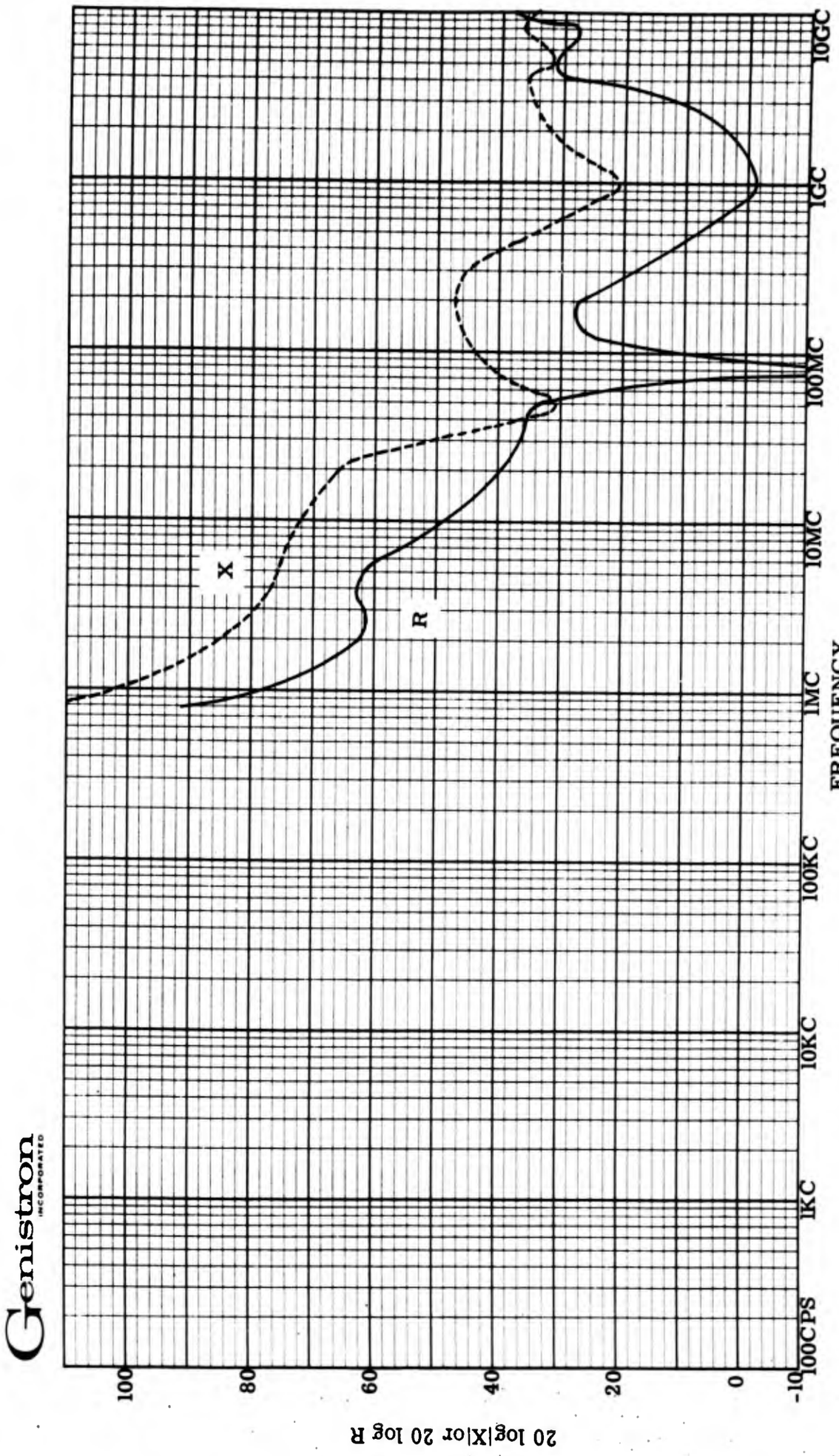

Figure 57: Input resistance and reactance, lead-to-case, Serial #261.

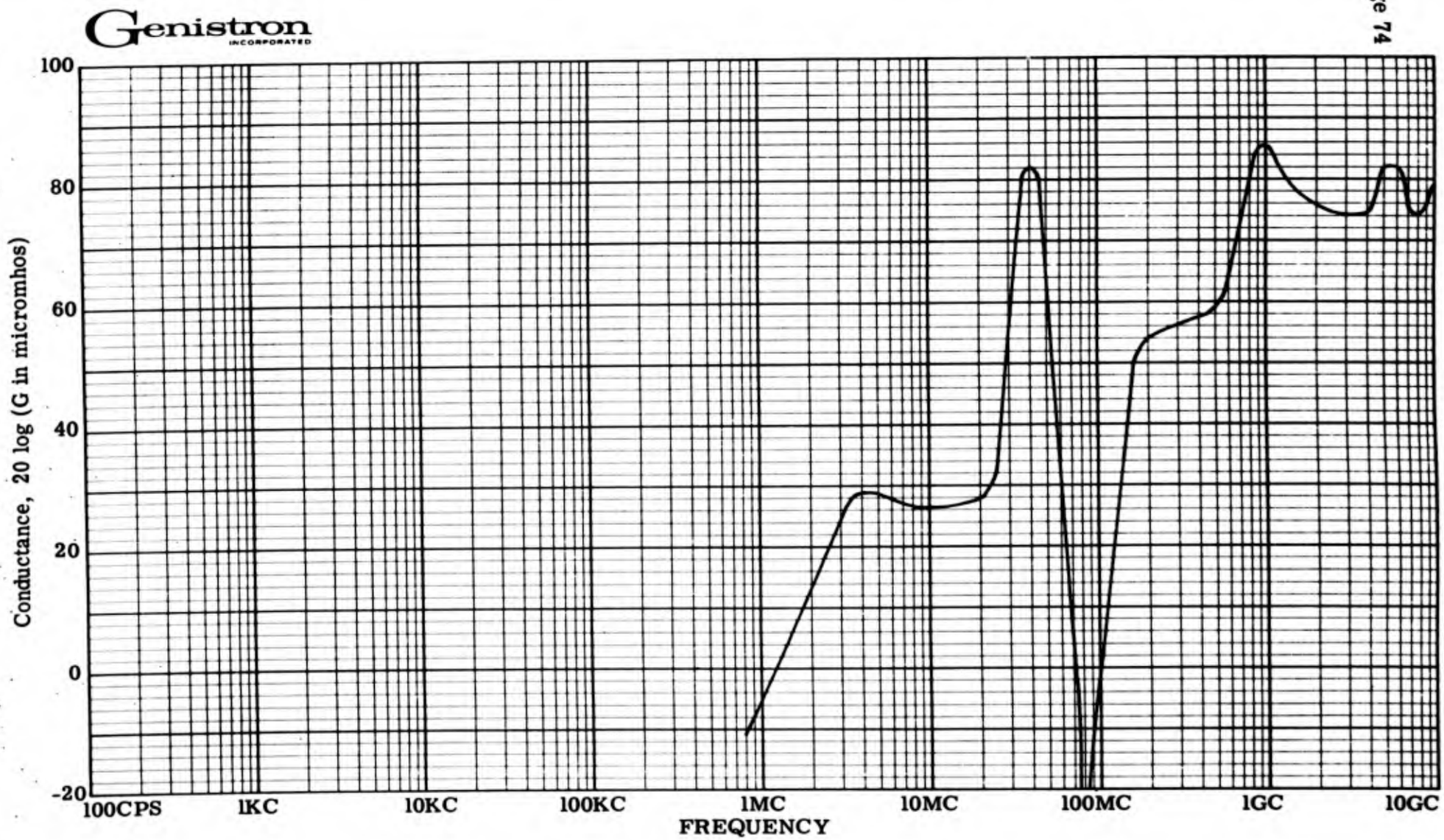

Figure 58: Input conductance, lead-to-case, Serial #261.

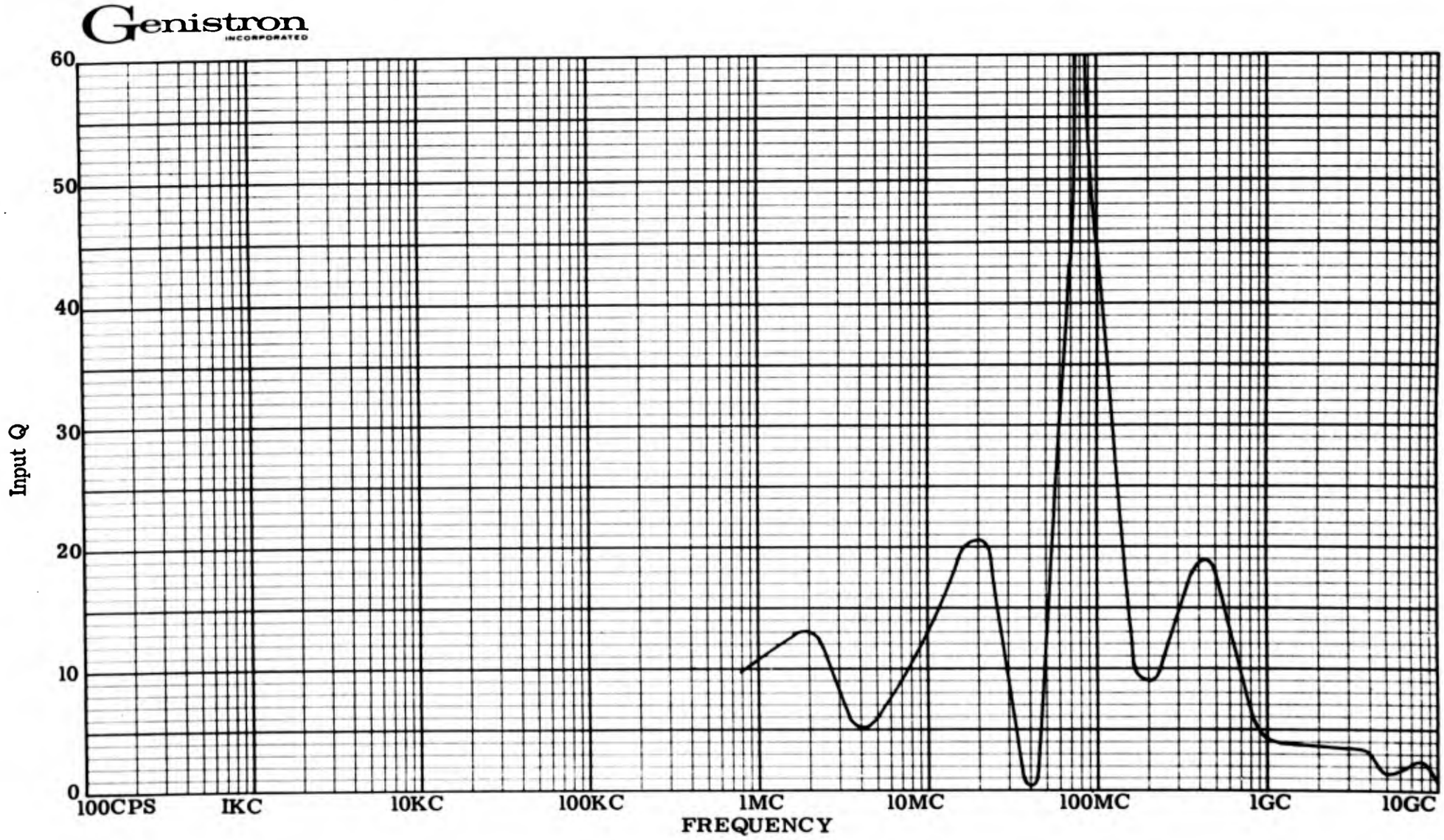

Figure 59: Input Q, lead-to-case, Serial #261.

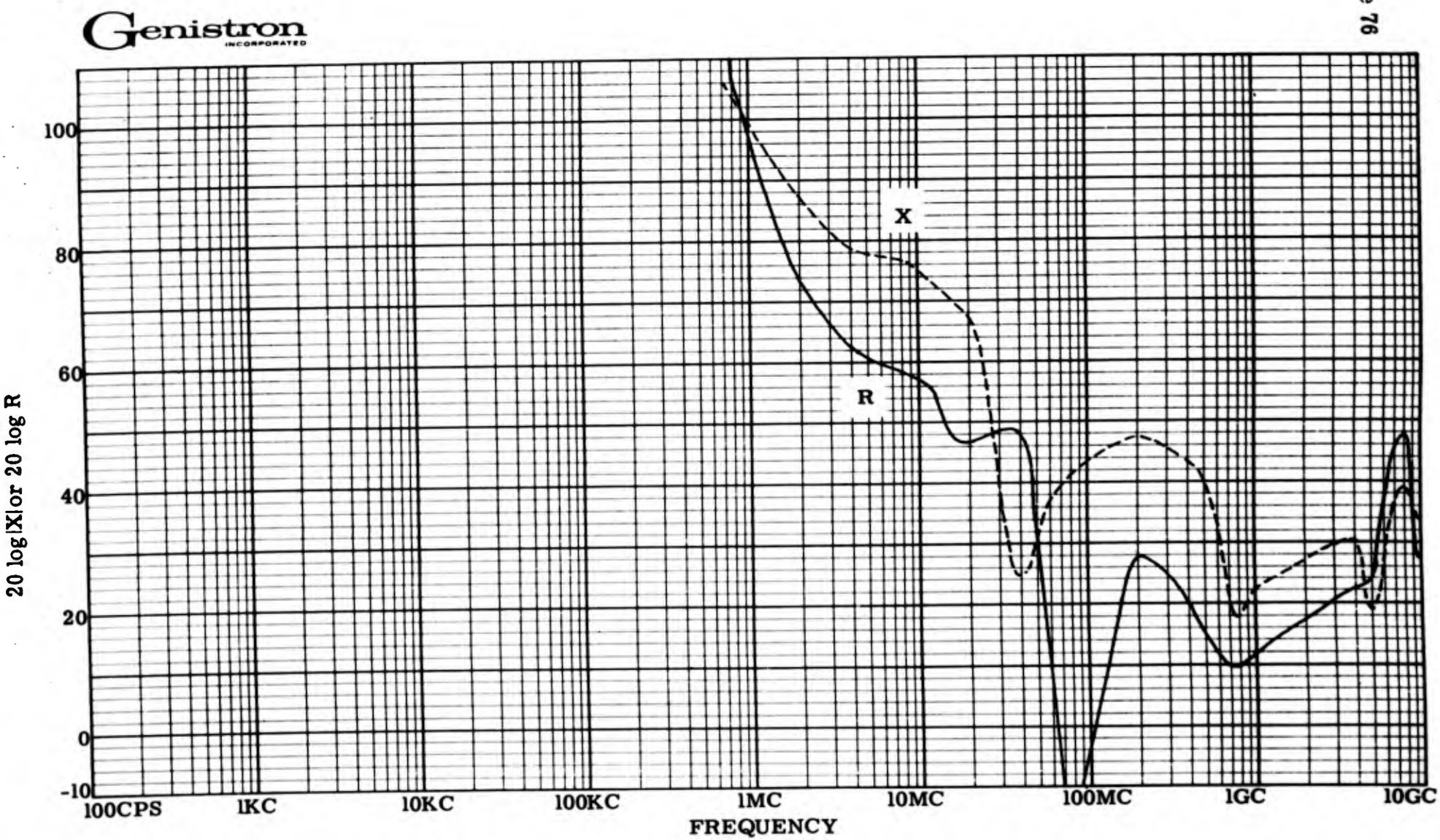

Figure 60: Input resistance and reactance, lead-to-lead, Serial #264.

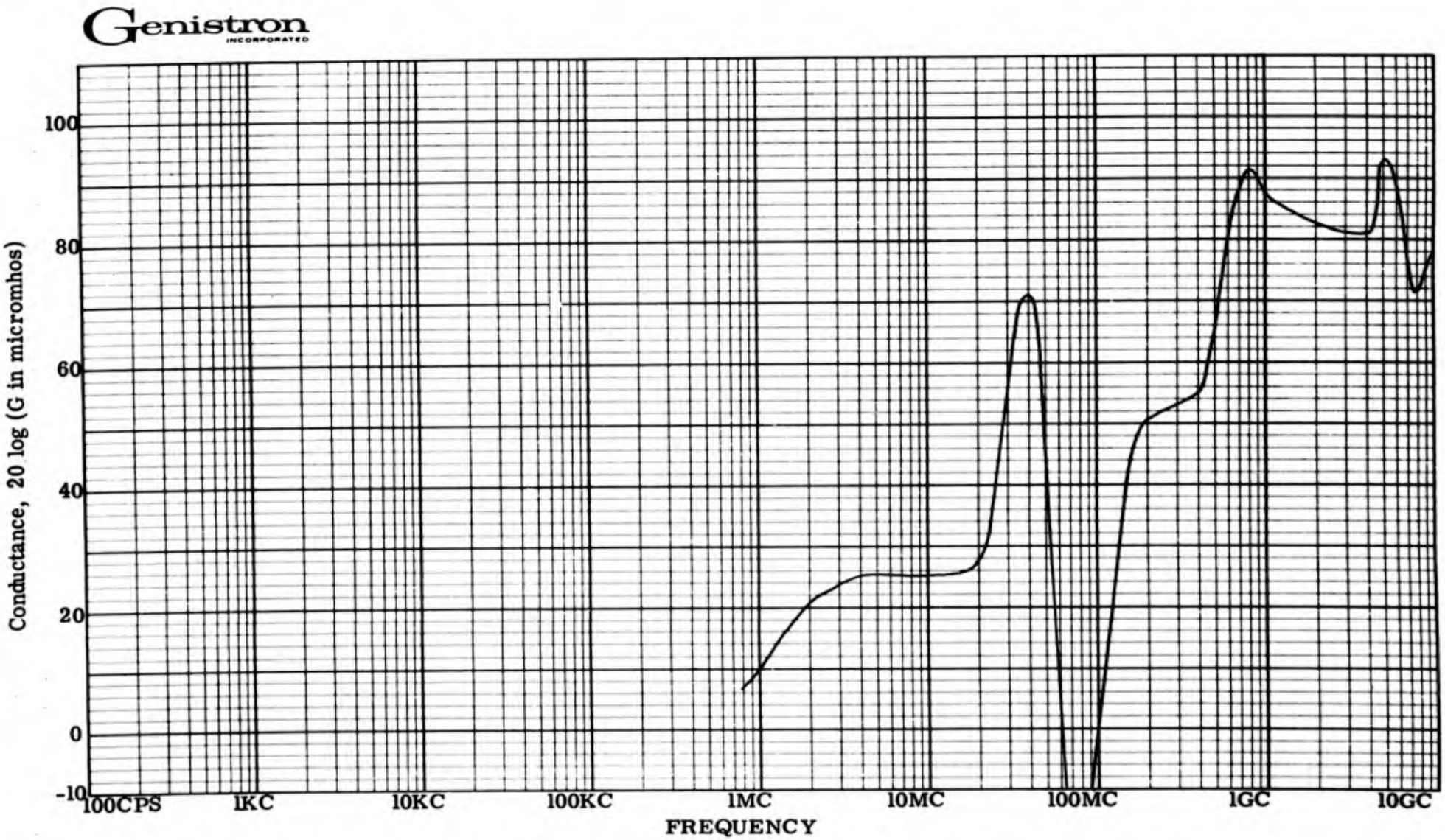

Figure 61: Input conductance, lead-to-lead, Serial #264.

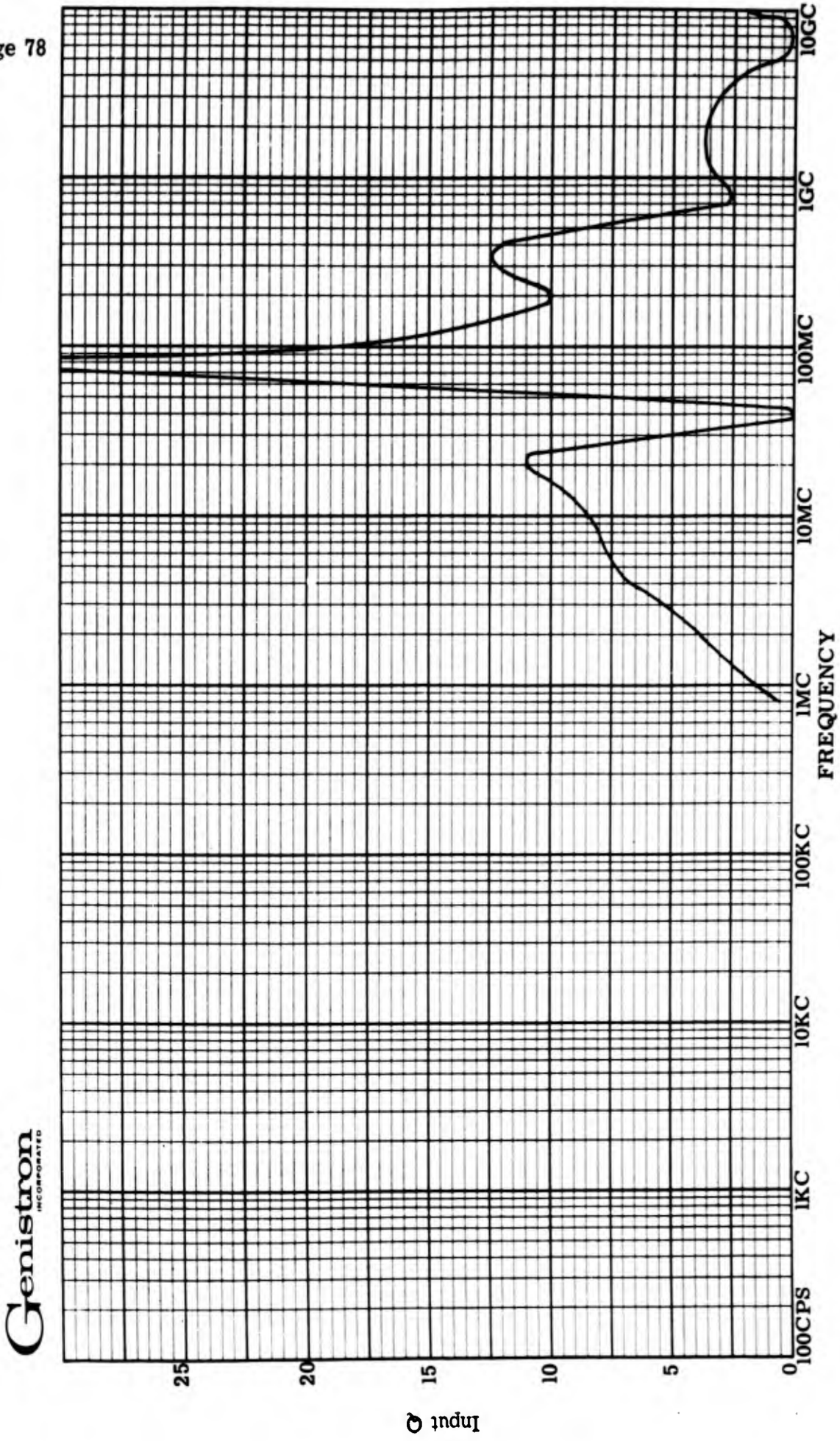

Figure 62: Input Q, lead-to-lead, Serial #264.

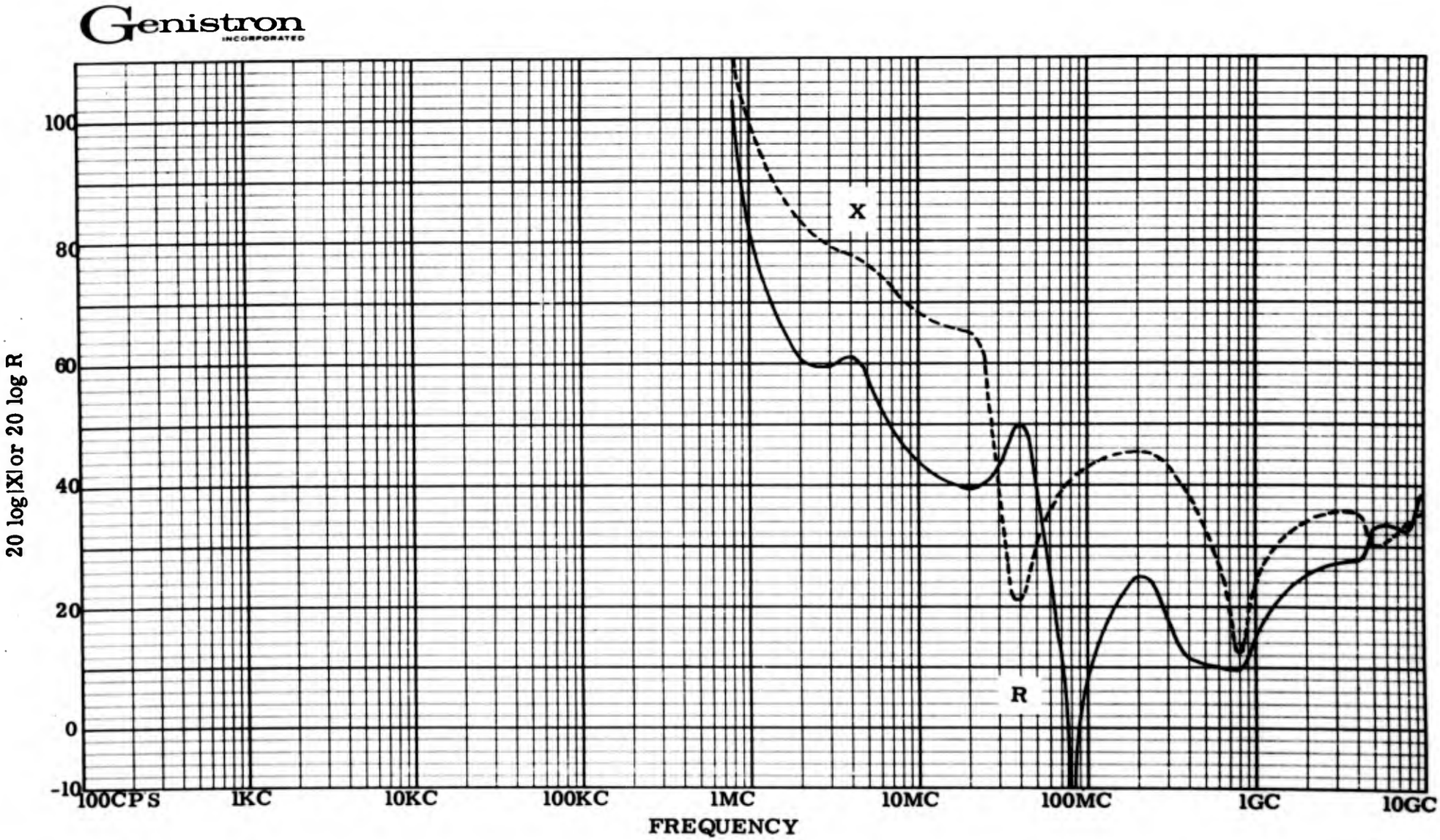

Figure 63: Input resistance and reactance, lead-to-case, Serial #264.

Genistron INCORPORATED

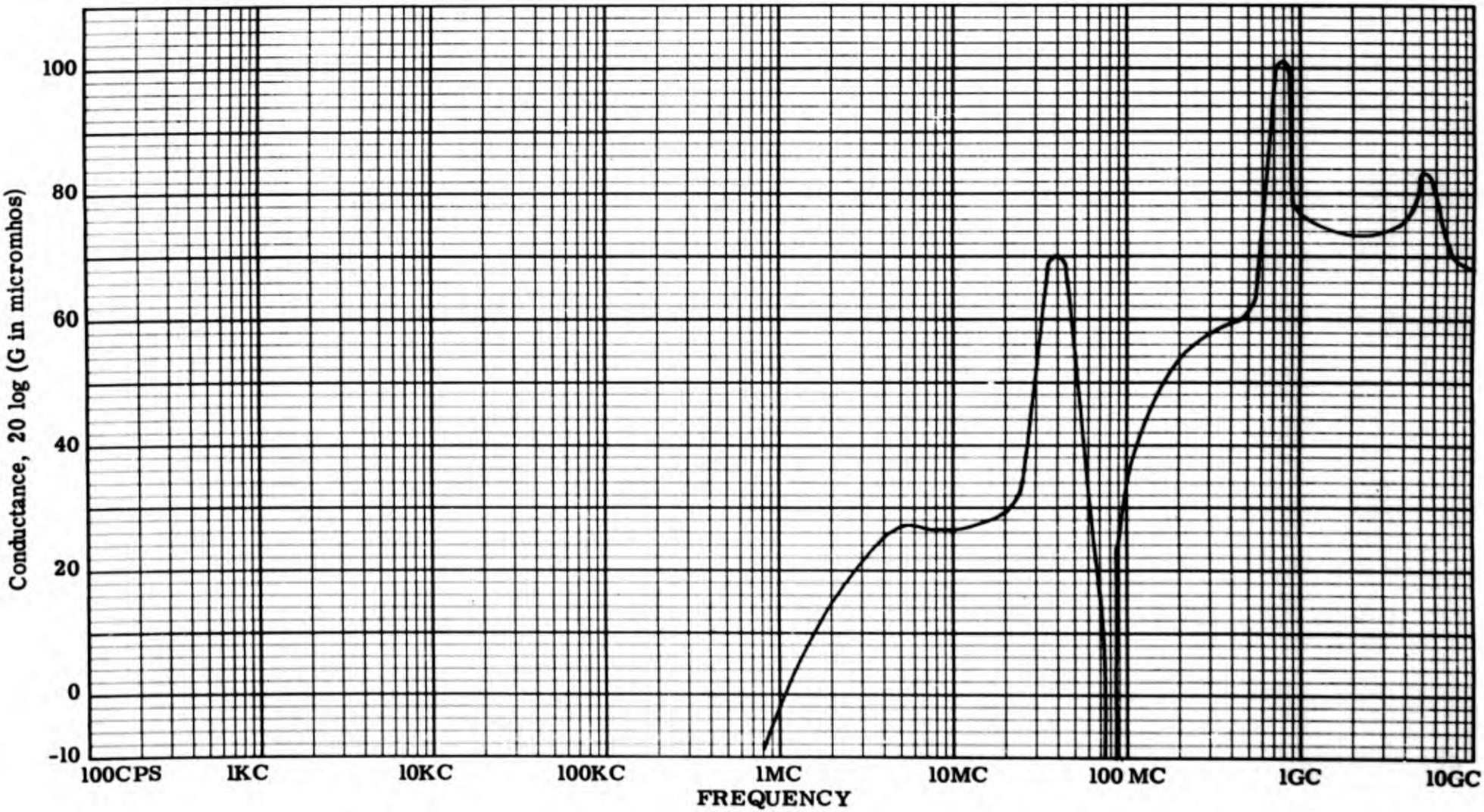

Figure 64: Input conductance, lead-to-case, Serial #264.

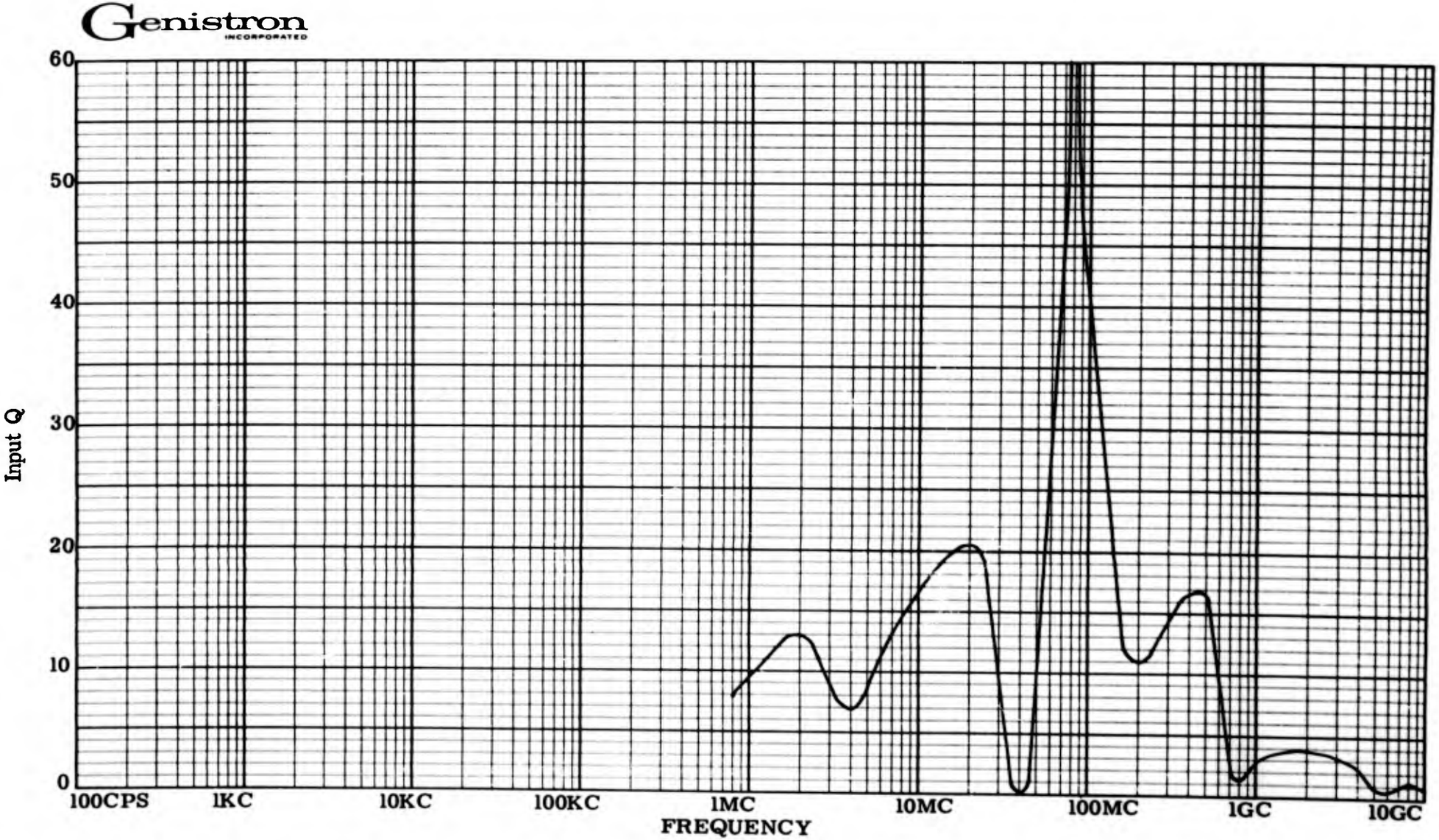

Figure 65: Input Q, lead-to-case, Serial #264.

Genistron INCORPORATED

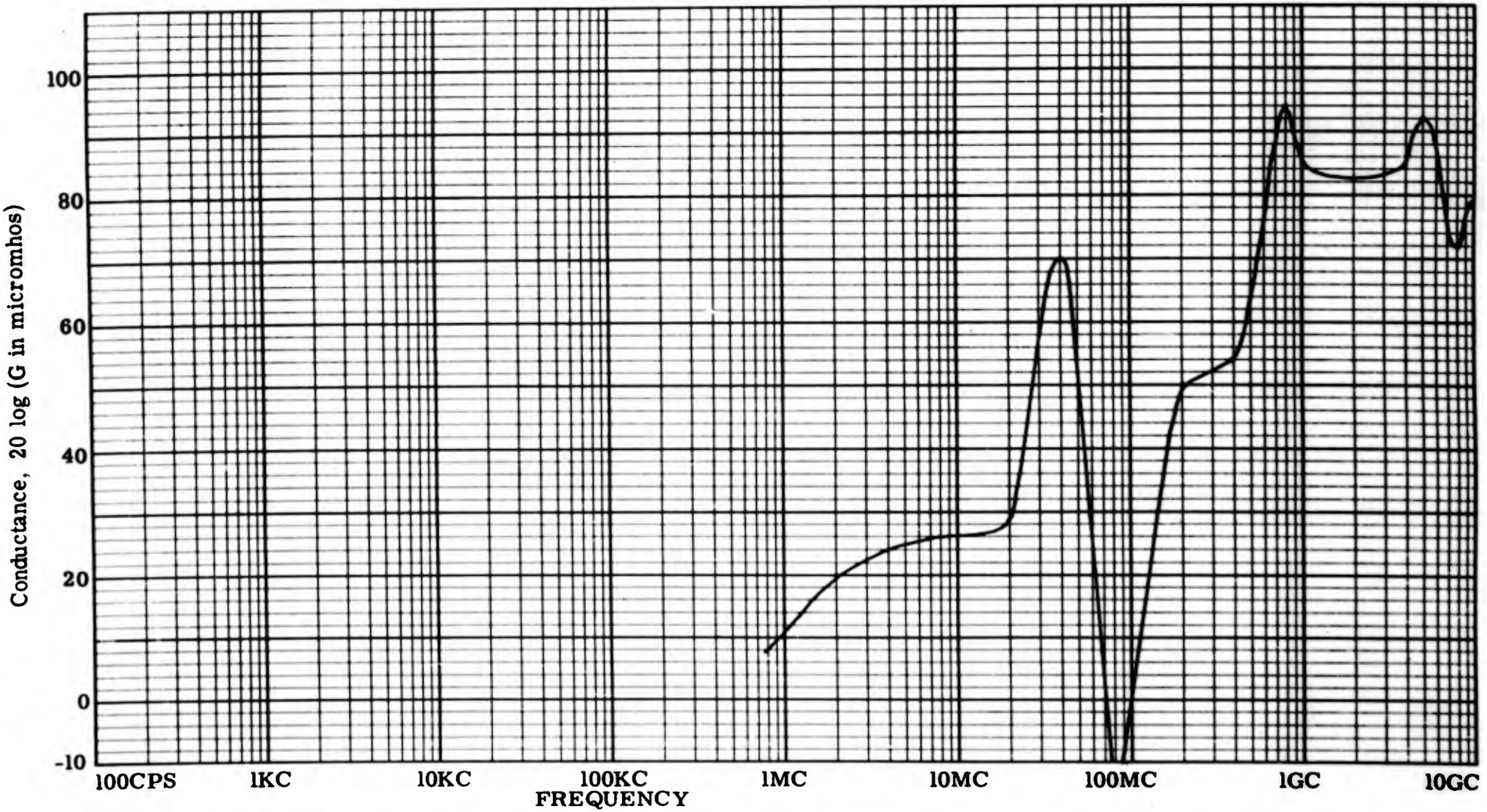

Figure 66: Average conductance, lead-to-lead.

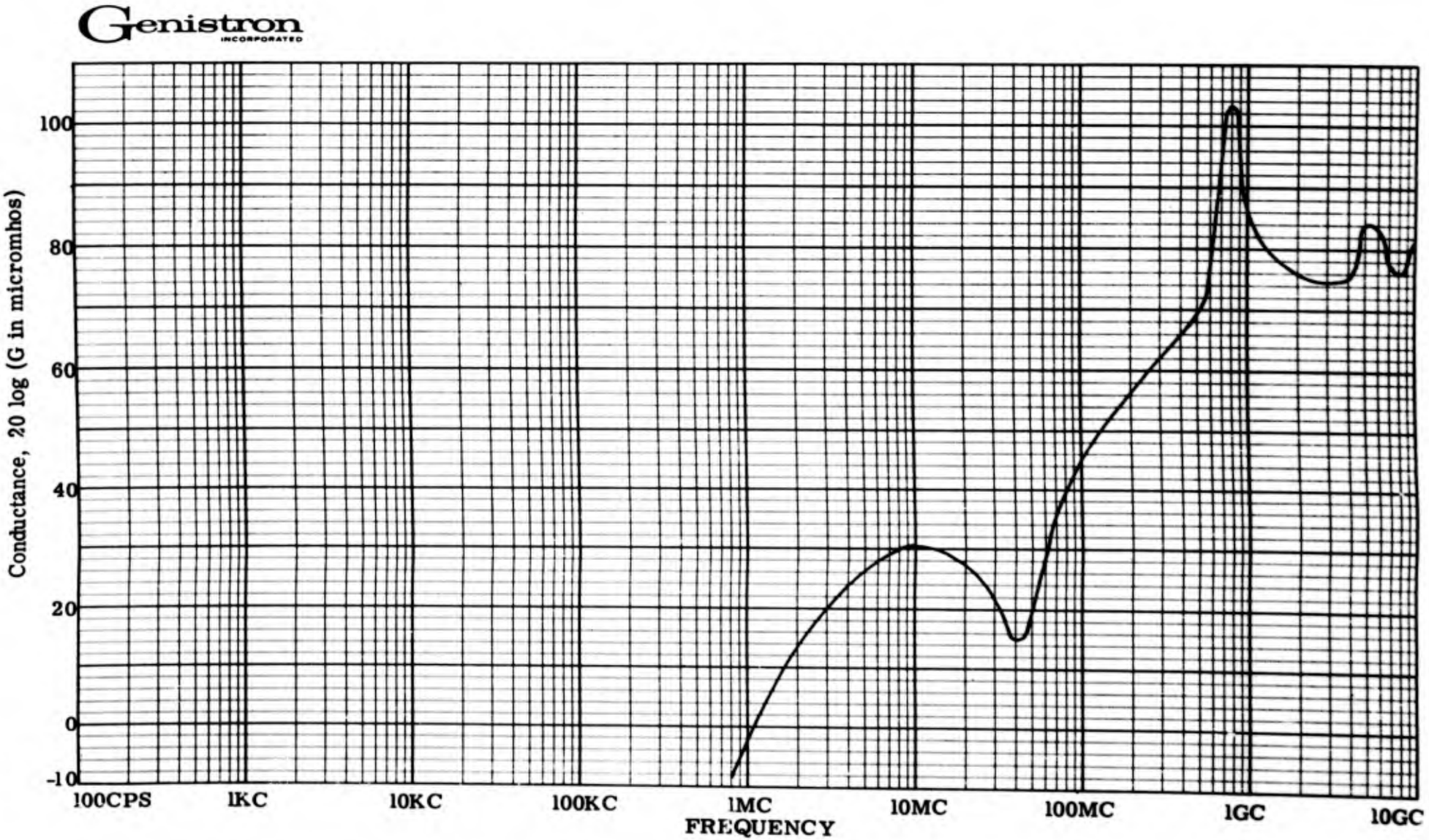

Figure 67: Average conductance, lead-to-case.

UNCLASSIFIED